2005

Structure of an initial n1ain sequence star of 1nixed opacity with negligible abundance of heavy ele1nents and studies of so1ne young clusters

Pramanik, Jogendra Nath

University of Rajshahi

Structure of an initial main sequence star of mixed opacity with negligible abundance of heavy elements and studies of some young clusters

Thesis submitted for the degree of Doctor of Philosophy
in the Rajshahi University

by

Jogendra Nath Pramanik, M.Sc. (Raj), M.Sc. (Shanghai)

March, 2005

Department of Mathematics
Rajshahi University
Rajshahi-6205
Bangladesh

Professor S. K. Bhattacharjee
Department of Mathematics
University of Rajshahi
Rajshahi - 6205. Bangladesh.

Phone: (off) 750041-49/4108
(Res) 0721-750223
E-mail: skbru@yahoo.com
Fax: 0088-0721-750064

Date 30.3.05

Certificate of Originality

This is to certify that Mr. Jogendra Nath Pramanik has worked on some aspects of stellar structure and evolution under my supervision for a Ph.D. degree. As far as I know this work is new and it has not been submitted anywhere else for the award of any degree.

I wish him success.

S. K. Bhattacharjee

(Prof. Shishir Kumar Bhattacharjee)
Supervisor

Abstract

In this thesis we have investigated some aspects of stellar structure and evolution. The thesis is divided into two sections. Section 1 deals with the structure of a star while section 2 deals with study of some young galactic clusters.

In chapters 1 and 2, in section 1, necessary theoretical aspects of stellar structure have been discussed. In chapter 3 we have determined the structure of a star of 2.5 solar mass in which the opacity is mixed, due to both electron scattering and free-free transition, and the abundance of heavy elements is negligible.

Section 2 A contains a brief outline of current views of star formation and investigation of three young galactic clusters, namely, NGC 1976, NGC 2264, and the Orion Nebula cluster following constant mass evolution of pre-main sequence stars. By analysing the observational data we have determined the mass functions, formation rates, and the mass-age correlation of stars in the clusters.

In section 2 B we have tested the theoretical prediction of an accretion model of star formation with observation of seven galactic clusters of young and intermediate ages, namely, NGC 1976, NGC 2264, NGC 6383, NGC 8611, NGC 6716, NGC 1245, and the Orion Nebula cluster. The predictions include the existence of a mass function, a formation rate of stars, and an explanation for the observed spread in the HR diagram of young clusters. To facilitate comparison we have deduced stellar masses of the first three clusters by polytropic method while for the remaining clusters we have used masses as deduced by other authors by using more reliable theoretical evolutionary tracks. NGC 2264 has been considered in both cases.

Acknowledgement

I would like to acknowledge, with gratitude, the help and guidance given to me, at all times, by my supervisor Professor Shishir Kumar Bhattacharjee.

I would also like to express thanks to the Chairman, Department of Mathematics, R.U. and to all of my colleagues in the department who have helped and cooperated with me in preparing the thesis. In particular, I am grateful to Mr. Gour Chandra Paul, Department of Mathematics. R.U. and Dr. Samsul Alam, RUET with whom I have had many valuable discussions.

I am thankful to Prof. Subrata Majumdar, Prof. M. Abdus Sattar, Dr. Nasima Akhtar and Mr. Kalyan Kumar Dey of the Department of Mathematics, R.U. for their constant encouragement throughout the period.

J.N. Pramanik.

(Jogendra Nath Pramanik)

CONTENTS

Section 1. A Stellar Model of Mixed Opacity and Negligible Abundance of Heavy Elements

Chapter 1: Fundamental Equations of Stellar Structure

Chapter 2: Method of Solution of Structure Equations

Chapter 3: Calculation of the Stellar Model

Section 2. Young Stellar Clusters

A. Studies of three Young Clusters with Constant Mass Evolution

Chapter 1: Star Formation

Chapter 2: The Young Clusters NGC 2264, NGC 1976 and the Orion Nebula Cluster

Chapter 3: Some Properties of the Clusters

B. Observational Tests of an Accretion Model of Star Formation in Galactic clusters

Chapter 1. An Accretion Model of Star Formation

Chapter 2: Pre Main Sequence Evolution of Accreting Stars

Chapter 3: Observational Tests of the Theoretical Predictions

List of Figures

List of tables

SECTION 1

A STELLAR MODEL OF MIXED OPACITY AND NEGLIGIBLE ABUNDANCE OF HEAVY ELEMENTS

A Stellar Model

Chapter 1: Fundamental Equations of Stellar Structure

i. Introduction

Stars are hot, massive and luminous celestial objects. Observed masses of stars range from $0.01M_{\odot}$ to $100M_{\odot}$ where $M_{\odot}$ is the solar mass. Stars with masses greater than $100M_{\odot}$ may also exist. But their lifetime is very short, being of the order of 10^6 years. Harm & Schwarzschild (1955) has shown that the maximum possible mass of a stable normal star is $60M_{\odot}$. There is a bit uncertainty in the minimum mass of a star. It is believed that stars with mass less than $0.01M_{\odot}$ can also exist. But they will never be main sequence stars. Because their interior will not be hot enough to burn hydrogen (Kumar, 1963). They will shrink directly to the white dwarf state. The main constituent of a star is hydrogen. The composition of star is usually determined by the abundances X, Y and Z, of hydrogen, helium and other heavier elements, in ionized form, respectively such that

$$X + Y + Z = 1$$

This means that one gram of stellar material contains X gram of hydrogen, Y gram of helium and Z gram of heavy elements. For the sun, for example,

$$X = 0.73, \qquad Y = 0.25, \qquad Z = 0.02.$$

The only measurable quantity of a star is its luminosity, which obviously depends on the physical conditions prevailing in its interior. The distribution of the thermodynamic variables such as pressure (P), temperature (T), and density

(ρ) inside a star determines its interior physical condition, in other words, its structure. The basic problem in determining the structure of a star is to obtain a set of differential equations defining the structure with necessary boundary conditions and solve them for given mass (M), radius (R) and luminosity (L), and also to derive information about the chemical composition, the energy source and the transport of energy from the centre to the surface of the star.

ii. Energy Production in Stars

A normal main sequence star derives energy from its nuclear source. That a star can derive energy from thermonuclear reaction is understood from the following example,

$$4\ {}_1H^1 = {}_2He^4 + 2\beta^+ + 2\nu + \gamma \qquad (1)$$

That means four hydrogen atoms combine to give one helium atom with the production of two positrons (β^+), two neutrinos (ν), and radiation (γ).

Now, the mass of four hydrogen atoms is greater than the mass of a helium atom. Therefore, there is mass loss in the reaction (1). This mass is converted to energy by Einstein's principle of mass-energy equivalence. If we neglect the energy taken away by two positrons and two neutrinos then by the conservation principle, γ represents the total energy available.

Of course it is not just the conversion of the hydrogen into helium that produces energy. Transmutation of heavier elements by nucleosynthesis in different evolutionary phases also liberates energy. We are however concerned with the reaction (1) only. This reaction does not take place in one stage. It is generally

completed through different steps either by (a) Proton-Proton (pp) chain or by (b) Carbon-Nitrogen (CN) cycle (see Erika Bohm Vitense 1992).

(a) Proton- Proton (pp) chain

Proton-proton reaction produces transmutation of hydrogen into helium. The easiest nuclear reaction is the reaction between a deuteron and a proton. The deuteron and proton can directly form a stable helium nucleus with mass 3. This reaction can happen with the temperature around 2 million degrees.

Once two protons have combined to form a deuteron, ${}_1H^2$, further reactions quickly follow. At low temperature the following reactions happen, called PPI chain:

PPI: $${}_1H^1 + {}_1H^1 \rightarrow {}_1H^2 + \beta^+ + \nu$$

$${}_1H^2 + {}_1H^1 \rightarrow {}_2He^3 + \gamma$$

and then

$${}_2He^3 + {}_2He^3 \rightarrow {}_2He^4 + 2{}_1H^1$$

where ν indicates the emission of a neutrino, and γ indicates the emission of γ ray. Positron β^1 combines with an electron and disappears in the form of radiation.

The reaction chain can also end in the following ways, called PPII and PPIII chain:

PPII: $${}_2He^3 + {}_2He^4 \rightarrow {}_4Be^7 + \gamma$$

$$_4Be^7 + e^- \rightarrow {}_3Li^7 + \nu$$

$$_3Li^7 + {}_1H^1 \rightarrow 2\ {}_2He^4$$

PPIII:

$$_4Be^7 + {}_1H^1 \rightarrow {}_5B^8 + \gamma$$

$$_5B^8 \rightarrow {}_4Be^8 + \beta^+ + \nu$$

$$_4Be^8 \rightarrow 2\ {}_2He^4$$

The relative importance of the PPI and PPII chains depends on the relative importance of the reactions of He^3 with He^3 in PPI as compared to the relations He^3 with He^4 in PPII. For $T > 1.4x10^7\ K$, He^3 prefers to react with He^4. For lower T the PPI chain is more important.

If we assume that the reactions go to completion, the rate of production of energy per unit mass per unit mass can be calculated to be given by the equation

$$\varepsilon_{pp} = 2.5\times10^6 \times \rho X^2 \times \left(\frac{10^6}{T}\right)^{3/2} \times e^{-33.8\left(\frac{10^6}{T}\right)^{1/3}} \qquad (2)$$

which approximates to the simple power law form

$$\varepsilon_{pp} = \varepsilon_1 \times \rho X^2 \times \left(\frac{T}{10^6}\right)^{16} \qquad (3)$$

(b) Carbon-Nitrogen(CN) cycle

In temperature above $2x10^7$ K, CN cycle dominates. For higher temperatures reactions involving nuclei with somewhat higher nuclear charge(Z_i)

can become important if the reaction cross sections are especially large, as in resonance reactions. Resonance relations occur when the kinetic energy of the captured nucleon coincides with an excited energy level of the combined nucleus; this makes the formation of the combined nucleus very easy.

In the Carbon cycle the following reactions constitute the main cycle.

$$_6C^{12} + {}_1H^1 \rightarrow {}_7N^{13} + \gamma$$

$$_7N^{13} \rightarrow {}_6C^{13} + \beta^+ + \nu$$

$$_6C^{13} + H^1 \rightarrow {}_7N^{14} + \gamma$$

$$_7N^{14} + {}_1H^1 \rightarrow {}_8O^{15} + \gamma$$

$$_8O^{15} \rightarrow {}_7N^{15} + \beta^+ + \nu$$

$$_7N^{15} + {}_1H^1 \rightarrow {}_6C^{12} + {}_2He^4$$

As in the pp chain different endings are possible. N^{15} can also react in the following way:

$$N^{15} + H^1 \rightarrow O^{16} + \gamma$$

$$O^{16} + H^1 \rightarrow F^{17} + \gamma$$

$$F^{17} \rightarrow O^{17} + \beta^+ + \nu$$

$$O^{17} + H^{1} \rightarrow N^{14} + He^{4}$$

N^{14} then enters into the main cycle and increase the production of He^{4}. The main importance of this bi-cycle is a change in the O^{16} and O^{17} abundance.

The rate of energy release per gram is

$$\varepsilon_{pp} = 9.5\times10^{28} \times \rho X X_{CN} \times \left(\frac{10^{6}}{T}\right)^{2/3} \times e^{-152.3\left(\frac{10^{6}}{T}\right)^{1/3}} \quad (4)$$

which approximates to power law form

$$\varepsilon_{CN} = \varepsilon_{0} \times \rho X X_{CN} \times \left(\frac{T}{10^{6}}\right)^{16} \quad (5)$$

To relate the carbon-nitrogen abundance to the abundance of all the heavier elements, Z, we frequently use the relation

$$X_{CN} = \frac{1}{3} Z \quad (6)$$

iii. Energy Transport in Stellar Interior

We know that the thermal equilibrium in different regions of the stellar interior is maintained by a balance of the flux of radiation between these various parts. The magnitude of this flux essentially depends on the temperature gradient prevailing in the interior and the opacity of the material through which the energy is being carried out. Among three energy transportation mechanisms conduction,

convection, and radiation, the radiation is important for the transfer of energy from central to surface layers, conduction is important in the condition of degeneracy (in white dwarfs and in cores of red giant), and the convection is important in some limited zones where transport by radiation falls short of the required amount to be carried out in order to maintain the thermal equilibrium around these specified zones (cores of massive hot star).

(a) Radiative Energy Transport

The principal means of energy transport in stars is by photons or radiation. The photons travel a "mean free path" before being absorbed or scattered by other particles. The mean free path in stellar interiors is very small of the order of about 1 cm, so the radiation is almost isotropic. It is the slight departure from isotropy which causes a net flux of energy. The problem is to relate the flux of energy carried by radiation to the thermodynamic variables (ρ, P, T).

The standard equation of radiative transfer of energy is given by (e.g. Chandrasekhar, 1950)

$$\underline{K} \cdot grad(I(\underline{r}, \underline{K})) = \frac{J\rho}{4\pi} - \kappa \rho I \qquad (7)$$

where $I(\underline{r}, \underline{K})$ is the integrated specific intensity of the radiation field at any point $\underline{r}$ in the direction $\underline{K}$, J is the emission coefficient which is the amount of energy emitted by a body per unit mass per unit time per unit solid angle, ρ is the density of the medium, I is the intensity of radiation over all frequencies, κ is the opacity or the mass absorption coefficient. Opacity is the resistance of the gas to the flow of energy. It is caused by many different atomic processes involving many elements and many stages of ionization. The accurate calculation of stellar opacity taking all these processes into account is a very difficult task. The three atomic

processes which contribute most to the opacity are (a) Bound-Free transition, (b) Free-Free transition, and (c) Electron scattering.

In bound-free(B-F) transition an atom absorbs a photon and sets a bound electron free. A quantum of energy which is at least equal to the binding energy of the electron is responsible for this. Any surplus energy imparts kinetic energy to the electron. Any energy greater than the binding energy may be absorbed, and so continuous absorption takes place in bound-free transition. Opacity in this B-F transition is approximated by the following expression

$$\kappa_{bf} = 4.34 \times 10^{25}\ Z\ (1+X)\,\rho T^{-3.5}\ \ cm^2/gm$$

In free-free(F-F) transition electron passing an atom absorbs a photon and moves to another more excited free orbit. In this process also continuous absorption take place. In this case the opacity is approximately given by

$$\kappa_{ff} = 3.68 \times 10^{22}\ (X+Y)\ (1+X)\,\rho T^{-3.5}\ \ cm^2/gm$$

Solitary electron can also interact with radiation by changing the direction and frequency of the incident beam of radiation. Opacity due to this scattering is independent of temperature and it is approximated by the following expression

$$\kappa_e = 0.2\ (1+X)\ \ cm^2/gm$$

In high temperature and low density condition electron scattering is the dominant opacity source. In high density and low temperature condition, the other two opacity sources collectively called Kramer's opacity, are dominant. However in the cool surface layer of stars negative hydrogen ions are the major contributions to the opacity. In recent years, just a number of opacity tables based

on detail computation have been published. In analytical work it is convenient to have an interpolation formula of the form

$$\kappa = \kappa_0 \rho^{\alpha} T^{\beta} \quad cm^2 / gm$$

where κ_0 is a constant whose value depends on the composition of stellar material and α and β are parameters whose values are adjusted so that the formula fits the opacity table.

In the stellar interior the radiation field is almost isotropic. Therefore, we write

$$I(\underline{r}, \underline{K}) = I_0(\underline{r}) + I_1(\underline{r}, \underline{K})$$

where I_0 isotropic part, and I_1 is the small departure with $I_1 << I_0$.

The transfer equation (7) can be written as

$$\underline{K} \cdot \underline{n} \frac{\partial I}{\partial n} = \frac{J\rho}{4\pi} - \kappa \rho I \tag{8}$$

Multiplying both side by $(\underline{K} \cdot \underline{n})\, d\omega$ and integrating we have

$$\int (\underline{K} \cdot \underline{n})^2 \frac{\partial I}{\partial n} d\omega = \int \frac{J\rho}{4\pi} (\underline{K} \cdot \underline{n}) d\omega - \int \kappa \rho I (\underline{K} \cdot \underline{n}) d\omega \tag{9}$$

where $\underline{n}$ is the normal and $d\omega$ is the solid angle.

Now $$\int (\underline{K} \cdot \underline{n})^2 \frac{\partial I}{\partial n} d\omega = \int \cos^2 \theta \frac{\partial (I_0 + I_1)}{\partial n} d\omega$$

$$\approx \int \cos^2\theta \frac{\partial(I_0)}{\partial n} d\omega$$

$$= \frac{\partial(I_0)}{\partial n} \int_0^{2\pi} \int_0^{\pi} \cos^2\theta \sin\theta \, d\theta \, d\phi = \frac{4\pi}{3} \frac{\partial(I_0)}{\partial n} \qquad (10)$$

$$\int \frac{J\rho}{4\pi} (\underline{K} \cdot \underline{n}) d\omega = \frac{J\rho}{4\pi} \int \cos\theta \, d\omega$$

$$= \frac{J\rho}{4\pi} \int_0^{2\pi} \int_0^{\pi} \sin\theta \cos\theta \, d\theta \, d\phi = 0 \qquad (11)$$

and

$$\int \kappa \rho (\underline{K} \cdot \underline{n}) I \, d\omega = \kappa \rho \int I \cos\theta \, d\omega = \kappa \rho F_n \qquad (12)$$

From equations (9), (10), (11), and (12) we have

$$F_n = -\frac{4\pi}{3\kappa\rho} \frac{\partial(I_0)}{\partial n} \qquad (13)$$

$$\underline{F} = -\frac{4\pi}{3\kappa\rho} \nabla I_0 \qquad (14)$$

But integrating transfer equation over all solid angle gives

$$\int (\underline{K} \cdot \underline{n}) \frac{\partial I}{\partial n} d\omega = \int \left(\frac{J\rho}{4\pi} - \kappa\rho I\right) d\omega \qquad (15)$$

Now $$\int (\underline{K} \cdot \underline{n}) \frac{\partial I}{\partial n} d\omega = \int \cos\theta \frac{\partial}{\partial n} (I_0 + I_1) d\omega$$

$$= \frac{\partial I_0}{\partial n} \int \cos\theta \, d\omega = 0 \qquad (16)$$

and

$$\int \left(\frac{J\rho}{4\pi} - \kappa\rho I\right)d\omega = \int \frac{J\rho}{4\pi}d\omega - \int \kappa\rho(I_0 + I_1)d\omega$$

$$\approx J\rho - 4\pi\kappa\rho I_0 \tag{17}$$

Therefore, from equations (15), (16), and (17), we have

$$I_0 = \frac{J}{4\pi\kappa} \tag{18}$$

Therefore, $$\underset{\sim}{F} = -\frac{4\pi}{3\kappa\rho}\nabla\left(\frac{J}{4\pi\kappa}\right) = -\frac{1}{3\kappa\rho}\nabla\left(\frac{J}{\kappa}\right) \tag{19}$$

For a medium in thermodynamic equilibrium by Kirchhoff's law we have

$$\frac{J}{\kappa} = acT^4$$

where a is the radiation density constant related to the Stefan Boltzmann's constant σ by

$$\sigma = \frac{ac}{4}$$

Therefore, equation (19) becomes

$$\underset{\sim}{F} = -\frac{1}{3\kappa\rho}\nabla\left(acT^4\right) = -\frac{4acT^3}{3\kappa\rho}\nabla T$$

Therefore, the flux of energy crossing a spherical surface of radius r is

$$L_r = 4\pi r^2 F_r = -\frac{16\pi ac}{3\kappa\rho} r^2 T^3 \frac{dT}{dr}$$

and then

$$\frac{dT}{dr} = -\frac{3}{4ac}\frac{\kappa\rho}{T^3}\frac{L_r}{4\pi r^2} \qquad (20)$$

This is the temperature gradient for radiative energy transport.

(b) Convective Energy Transport

Suppose that in a certain layer of a given star radiative equilibrium holds. If this equilibrium is stable against perturbation then no convective mass motion can persist and convective energy transport does not occur. If however the radiative equilibrium is found to be unstable mass motion can occur.

Take a small volume element within a star and displace this element upward by a distance *dr*. Let the element expand adiabatically until the pressure inside is in balanced with the of the surrounding. Release the element and use whether it starts moving downwards to its original position or continues to move upwards.

Let ρ_1^* and P_1^* be the density and pressure inside the blob in its original position, the corresponding quantities outside being ρ_1 and P_1. In its displaced position, let ρ_2^* and P_2^* be the density and pressure inside the blob while corresponding quantities outside be ρ_2 and P_2.

Before the perturbation

$$\rho_1^* = \rho_1 \quad and \quad P_1^* = P_1$$

After the perturbation

$$\rho_2^* = \rho_1^*\left(\frac{P_2^*}{P_1^*}\right)^{1/\gamma} \quad and \quad P_2^* = P_2$$

where γ is the ratio of specific heats C_p / C_v and has the value 5/3 for highly ionized gas. The layer may be stable if $\rho_2^* > \rho_2$. Therefore mass motion will occur if $\rho_2^* > \rho_2$. Now we have from the above equations

$$\rho_2^* = \rho_1 \left(\frac{P_2}{P_1}\right)^{1/\gamma}$$

The equilibrium is stable or unstable according as $\rho_1 \left(\frac{P_2}{P_1}\right)^{1/\gamma} > or < \rho_2$.

Let $P_1 = P(r)$ *and* $\rho_1 = \rho(r)$

$P_2 = P(r+dr)$ *and* $\rho_1 = \rho(r+dr)$

From stable-unstable condition we have $\left(\frac{P_2}{P_1}\right)^{1/\gamma} > or < \frac{\rho_2}{\rho_1}$.

Which implies $\left(\frac{P(r+dr)}{P(r)}\right)^{1/\gamma} > or < \frac{\rho(r+dr)}{\rho(r)}$

Or $\left(1+\frac{1}{P}\frac{dP)}{dr}dr\right)^{1/\gamma} > or < \left(1+\frac{1}{\rho}\frac{d\rho}{dr}dr\right)$

Expanding left side of the above inequalities in Taylor series and neglecting higher order terms we have

$$\left(1+\frac{1}{\gamma P}\frac{dP}{dr}dr\right) > or < \left(1+\frac{1}{\rho}\frac{d\rho}{dr}dr\right)$$

or $$\frac{1}{\gamma P}\frac{dP}{dr} > or < \frac{1}{\rho}\frac{d\rho}{dr} \tag{21}$$

We know that $P = \frac{K}{\mu H}\rho T$, then by differentiating we have

$$\frac{1}{P}\frac{dP}{dr} = \frac{1}{\rho}\frac{d\rho}{dr} + \frac{1}{T}\frac{dT}{dr} \tag{22}$$

For stability condition we have from equation (21) and (22)

$$\frac{1}{\gamma P}\frac{dP}{dr} > \frac{1}{P}\frac{dP}{dr} - \frac{1}{T}\frac{dT}{dr}$$

that is $$-\left(1-\frac{1}{\gamma}\right)\frac{dP}{dr} > -\frac{P}{T}\frac{dT}{dr}$$

Therefore mass motion will occur when

$$-\left(1-\frac{1}{\gamma}\right)\frac{dP}{dr} < -\frac{P}{T}\frac{dT}{dr} \tag{23}$$

Schwarzschild (1958) has shown that the temperature gradient for the convection is well represented by

$$\frac{dT}{dr} = \left(1-\frac{1}{\gamma}\right)\frac{T}{P}\frac{dP}{dr} \tag{24}$$

iv. Equation of Structures and the Over all Problem

Hydrostatic equilibrium means that all the forces acting on any small volume within the star must compensate each other exactly, since a non vanishing net force would cause motions and hence change the structure. In a spherically symmetric star, the outward pressure force – dP must balance the inward gravitational force

$$\frac{G M(r) \rho(r) dr}{r^2}.$$

Therefore, for equilibrium we have

$$-dP = \frac{G M(r) \rho(r) dr}{r^2}$$

that is
$$\frac{dP}{dr} = -\frac{G M(r) \rho(r)}{r^2} \qquad (25)$$

where $M(r)$ is the mass inside radius r, $\rho(r)$ is the density at r.

We consider a spherically symmetric distribution of matter and assume that $\rho(r)$ is the density of material at distance r from the centre. Then the mass of a thin spherical shell of thickness dr at distance r is

$$dM(r) = 4\pi r^2 \rho(r) dr$$

that is
$$\frac{dM(r)}{dr} = 4\pi r^2 \rho(r) \qquad (26)$$

Similarly if $\varepsilon(r)$ is the energy generated by unit mass of stellar material at distance r from the centre, the energy generated by a thin spherical shell bounded by r and $r + dr$ is
$$dL(r) = 4\pi r^2 \rho(r) \varepsilon(r) dr$$

that is $$\frac{dL(r)}{dr} = 4\pi r^2 \rho(r) \varepsilon(r) \qquad (27)$$

Equations (26) and (27) give the conservation of mass and energy inside the star.

The structure of a star is determined, on the one hand, by the requirements of mass conservation, energy conservation, equilibrium of forces, and by the mode of energy transport. On the other hand, the structure of the star depends on the chemical composition, which may vary in course of time either due to nuclear reactions in the deep interior, or due to mixing in convective layers of the star. If the star is taken to be non-magnetic, non-rotating, and spherically symmetric, all physical quantities are functions of one single spatial variable (Lagrangian co-ordinate), and of time t. But it is convenient to use the radius r directly as an independent variable. Considering the stellar atmosphere and stellar interior, Reiter (1994) cast the equations of stellar evolution in Eulerian picture by the complete set of following equations

$$\frac{\partial M_r}{\partial r} = \begin{cases} 4\pi r^2 \rho & 0 \le r \le R \\ 0 & R < r \le R + \Delta R \end{cases}$$

$$\frac{\partial L_r}{\partial r} = \begin{cases} (\xi + \xi_g) \dfrac{\partial M_r}{\partial r} & 0 \le r \le R \\ 0 & R < r \le R + \Delta R \end{cases}$$

$$\frac{\partial T_r}{\partial r} = \begin{cases} \nabla \dfrac{T}{P} \dfrac{\partial P}{\partial r} & 0 \le r \le R \\ -\dfrac{3}{16} \kappa \rho \dfrac{T_e^4}{T^3} \left(1 + \dfrac{\partial q}{\partial \tau}\right) & R < r \le R + \Delta R \end{cases}$$

$$\frac{\partial P}{\partial r} = \begin{cases} -\dfrac{G M_r \rho}{r^2} & 0 \le r \le R \\ -g\rho & R < r \le R + \Delta R \end{cases}$$

$$\frac{\partial \tau}{\partial r} = \begin{cases} 0 & 0 \le r \le R \\ -\kappa \rho & R < r \le R + \Delta R \end{cases}$$

$$\frac{\partial X_i}{\partial t} = \begin{cases} \Omega_i + \left(\dfrac{\partial M_r}{\partial r}\right)^{-1} \dfrac{\partial X_i}{\partial r} \dfrac{\partial M_r}{\partial t} & 0 \le r \le R \\ 0 & R < r \le R + \Delta R \end{cases}$$

where the parameters have conventional meaning as in Reiter et al(1994).

However, if the chemical composition remains fixed in time, and no atmosphere is considered then the partial differential equations defining the stellar structure reduces to the following set of ordinary differential equations (Rothe 1930).

$$\frac{dP}{dr} = \frac{G M(r) \rho(r)}{r^2}, \qquad \text{hydrostatic equation} \tag{28}$$

$$\frac{dM(r)}{dr} = 4\pi r^2 \rho(r), \qquad \text{conservation of mass} \tag{29}$$

$$\frac{dL(r)}{dr} = 4\pi r^2 \rho(r) \varepsilon(r), \qquad \text{conservation of energy} \tag{30}$$

$$\frac{dT}{dr} = -\frac{3}{4ac}\frac{\kappa\rho}{T^3}\frac{L(r)}{4\pi r^2}, \text{ radiative temperature gradient} \qquad (31)$$

$$\frac{dT}{dr} = \left(1-\frac{1}{\gamma}\right)\frac{T}{P}\frac{dP}{dr}, \qquad \text{convective temperature gradient} \qquad (32)$$

These equations pose the overall problem for the theory of stellar interior.

In addition to the above differential equations which characterize general conditions, we have three explicit relations which characterize more specifically the behavior of the interior of the star. These are equation of state, the equation for the absorption coefficient, and the equation for the energy generation by nuclear processes, which we represent by the following formal equations

$$P = P(\rho, T, X, Y) \qquad (33)$$

$$\kappa = \kappa(\rho, T, X, Y) \qquad (34)$$

$$\varepsilon = \varepsilon(\rho, T, X, Y) \qquad (35)$$

All these gas characteristic relations directly depend on the hydrogen abundance X and the helium abundance Y. Equations (28) to (32) must all be fulfilled in every layer of the star. We have the following boundary conditions also.

Boundary Condition:

Considering a sphere of infinitesimal radius r at the centre, we find that

$$M(r) = \frac{4}{3}\pi r^3 \rho,$$

and $$L(r) = \frac{4}{3}\pi r^3 \rho\varepsilon = M(r)\varepsilon,$$

since we may treat ρ and ε sensibly constant in this sphere. Hence as $r \to 0$,

$$M(r) \to 0 \quad \text{and} \quad L(r) \to 0, \tag{36}$$

for ρ and ε remain finite as $r \to 0$. It is clear that the condition $L(r) = 0$ at $r = 0$ is a consequence of the condition $M(r) = 0$ at $r = 0$.

This gives us only one independent boundary condition at the centre, namely,

$$M(r) = 0 \quad \text{at} \quad r = 0. \tag{37}$$

It is clear that

$$M(r) = M \quad \text{and} \quad L(r) = L \tag{38}$$

at the surface, i.e., at $r = R$.

In addition, we can derive suitable conditions for pressure and temperature of a star at its surface. The surface temperatures of stars are, in general, of order of a few thousand degrees while their central temperatures are of order of a few million degrees, so that the surface temperatures may approximately be taken as zero. The mass of the atmosphere of a star is just a minute fraction of its total mass, therefore we may take the pressure on its surface as approximately equal to zero. Thus we have two more conditions at the surface, namely,

$$T = 0, \quad P = 0 \quad \text{at } r = R \tag{39}$$

which are referred to as the "zero boundary condition". For stars whose outermost layers are in radiative equilibrium, these conditions provide a good approximation to the actual boundary conditions.

We can, however, deduce more accurate surface conditions from the consideration of the atmospheric condition. We may take

$$T = T_e \qquad \text{at} \qquad r = R \tag{40}$$

more reasonably. Since the radius of the star is determined from the equation

$$L = 4\pi R^2 \frac{ac}{4} T_e^4,$$

condition (40) is not independent of condition (38), namely,

$$L(r) = L \qquad \text{at} \qquad r = R.$$

The hydrostatic equilibrium of the atmosphere of a star is governed by the equation

$$\frac{dP}{dr} = -\rho g = GM\frac{\rho}{r^2},$$

since the mass within radius r may be taken to be the total mass without involving any appreciable error. Therefore, the pressure at the surface is given by

$$P(R) = GM \int_R^\infty \frac{\rho\, dr}{r^2} \tag{41}$$

The optical thickness τ of the atmosphere is given by

$$\tau = \int_R^\infty \kappa \rho\, dr \tag{42}$$

If the opacity of the atmosphere is too little, i.e., if τ is too small, the radiation from the surface will be too large; on the other hand, if the atmosphere is too opaque, i.e., if τ is too large, the radiation from the surface will be too little.

This consideration imposes a certain condition on τ . From the approximate relation between temperature and optical depth,

$$T^4 = \frac{1}{2}T_e^4\left(1+\frac{3}{2}\tau\right)$$

For the atmosphere, we may take

$$\tau = \frac{2}{3} \tag{43}$$

Now since ρ falls rapidly as r increases, the main contribution to (41) comes from the photosphere so that we may approximately write (41) as

$$P(R) \approx \frac{GM}{R^2}\int_R^\infty \rho\, dr \tag{44}$$

From the similar consideration, we may write (42) in the following form

$$\tau \approx \kappa(R)\int_R^\infty \rho\, dr \tag{45}$$

From (44) and (45) we get

$$P(R)\,\kappa(R) \approx \frac{GM}{R^2}\,\tau \tag{46}$$

$$\approx \frac{2}{3}\frac{GM}{R^2}\,\tau, \tag{47}$$

in the view of (43). Thus knowing the value of τ and $\kappa(R)$ from the study of atmospheres, we can estimate $P(R)$. If we compare (47) with the result of the accurate computations of the stellar atmospheres, we find that it is not in error by more than a factor of 3/2 for most of the stars. We can, therefore, obtain the condition

$$P = P(R) \approx \frac{2}{3}\frac{GM}{R^2}\frac{1}{\kappa(R)} \qquad \text{at} \qquad r = R \tag{48}$$

as a condition alternative to (39).

Thus our basic problem consists of four simultaneous, total, non-linear first order differential equations for four variables (P, M, L, and T), all are the functions of the fifth variable r. These four differential equations, together with the four boundary conditions above (equations (36) to (39)) represent a typical, well defined boundary value problem. According to Vogt-Russell theorem (see Bhatnagar et al. 1963) if the pressure P, the opacity κ, and the rate of energy generation ε are functions of the local values of density ρ, temperature T, and the chemical composition only, then the structure of a star is uniquely determined by its mass and chemical composition.

$$P = P(R) \approx \frac{2}{3}\frac{GM}{R^2}\frac{1}{\kappa(R)} \qquad \text{at} \qquad r = R \tag{48}$$

as a condition alternative to (39).

Thus our basic problem consists of four simultaneous, total, non-linear first order differential equations for four variables (P, M, L, and T), all are the functions of the fifth variable r. These four differential equations, together with the four boundary conditions above (equations (36) to (39)) represent a typical, well defined boundary value problem. According to Vogt-Russell theorem (see Bhatnagar et al. 1963) if the pressure P, the opacity κ, and the rate of energy generation ε are functions of the local values of density ρ, temperature T, and the chemical composition only, then the structure of a star is uniquely determined by its mass and chemical composition.

v. References

Bhatnagar P., Menzel D.H., and Sen H., 1963, Stellar Interiors, Chapman & Hall

Chandrasekhar S., 1950, Radiative Transfer, Oxford University Press.

Erika B.V, Introduction to Stellar Astrophysics, Volume 3: Stellar Structure and Evolution, Cambridge University Press, 1992

Harm R. and Schwarzchild M., 1955, ApJ. Suppl. Series, 1, 319

Kumar S.S., 1963, ApJ, 137, 1121

Reiter J., Bulirsch R., Pfleiderer J., 1994, Astron. Nachr., 3, 205-234

Rothe E., 1930, Math. Ann. 102, 650-670

Schwarzschild M., 1958, Structure and Evolution of Stars, Chicago Univ. Press, Dover.

Chapter 2: Method of Solution of Structure Equations

i. Numerical Method

Although in principle it is easy to solve the said boundary value problem yet it is a difficult task. Since all the structure equations are not analytic no analytical solution is possible. Approximate numerical solution is the only possible solution of the differential equations. Since there are two boundary conditions at the centre and other two at the surface, numerical integration of the differential equations are not straightforward. It would be convenient if all the four boundary conditions were at the centre or at the surface. To get an approximate solution selection of numerical method is very much important.

The stellar evolution codes in use today can be classified into three categories according to their approach for solving the stellar structure equations.

Finite difference method

The stellar structure equations are approximated, over the full range of integration, by (low-order) finite difference formula at a number of discrete mesh points. The resulting system of algebraic equations, together with the boundary conditions, are solved iteratively by Newton's method to give approximations to the dependent variable simultaneously at all the discrete knots. Since Newton's method is iterative in its nature appropriate guesses of the independent variables at the mesh points need to be provided. The method has been first introduced by Henyey et al. (1959). Variants of it have been developed by, Iben (1965), Kippenhahn et al.(1967), Paczynski (1969, 1970) and Christensen-Dalsgaard (1982).

Collocation Method

The unknown functions involved in the stellar structure equations are approximated, in the range of integration, by piecewise-defined (low-order) polynomials. The unknown coefficients of these polynomials are determined by forcing the polynomials to satisfy the differential equations at an adhoc prescribed set of collocation points, together with the given boundary conditions. Whilst the collocation method is widely used in numerical analysis for solving BVPs, it has been introduced only recently by Morel et al. (1990) for solving the stellar structure problem.

Shooting Method

In this approach, which is also known as fitting method or integration method, the BVP is solved by actually converting it into a series of IVPs. Principally, the IVPs may be solved by any numerical integration. But if the true initial values are unknown they have to be estimated. The guesses are justified iteratively by Newton's method such that the trajectories become continuous at *"fitting points"* inside the range of integration, and all boundary conditions are finally fulfilled. The earliest codes for numerically solving the stellar-structure equations were based on the shooting technique (e.g., Cowling 1936; Haselgrove and Hoyle 1956; Schwarzschild 1958). Whilst these early codes used only one fitting point, improved version of the shooting method may employ up to a few hundred fitting points. Stellar-evolution codes based on a multiple shooting technique were developed by, Peterson (1967), Wilson (1981), Bahcall and Ulrich (1988) and Reiter et al. (1994).

For general purpose of stellar-evolution calculations the Henyey method has found the most widespread application. The main reason is that this method is more stable; small local errors do not propagate to other mesh points and do not

affect the over-all solution of the BVP too much (de Loore and Doom 1992). For similar reason collocation method is also stable. Although shooting method becomes extremely unstable where time steps have to be used, yet it gives more better result without any use of time step.

ii. Polytropic Method

A quasistatical change in which the specific heat remains constant is called a polytropic change, i.e., $\frac{dQ}{dT} = c$, a constant, where Q is the heat and T is the temperature.

Now, from the first law of thermodynamics

$$dQ = dU + PdV$$

Therefore, for a polytropic change we have

$$c\,dT = dU + PdV$$

$$= c_v\,dT + \frac{RT}{V}dV$$

$$= c_v\,dT + \left(c_p - c_v\right)\frac{T}{V}dV$$

or, $$\frac{dT}{T} + \frac{c_p - c_v}{c_v - c}\frac{dV}{V} = 0$$

or, $$\frac{dT}{T} + \frac{1}{n}\frac{dV}{V} = 0 \qquad (49)$$

where $n = \dfrac{c_v - c}{c_p - c_v}$ and all other variables have conventional meanings.

From logarithmic differentiation of

$$PV = (c_p - c_v)T$$

we get $$\frac{dP}{P} + \frac{dV}{V} = \frac{dT}{T} \tag{50}$$

Eliminating $\dfrac{dT}{T}$ from (49) and (50) and replacing V in terms of ρ we have

$$\frac{dP}{P} = \left(1 + \frac{1}{n}\right)\frac{d\rho}{\rho}$$

i.e., $$P = K\,\rho^{1+\frac{1}{n}} \tag{51}$$

where K is a constant and n is called the polytropic index.

Replacing P and $M(r)$ in terms of ρ from equations (25) and (26) the equation of hydrostatic equilibrium gives

$$\frac{1}{r^2}\frac{d}{dr}\left[K(n+1)r^2\frac{d\rho^{\frac{1}{n}}}{dr}\right] = -4\pi G\,\rho \tag{52}$$

Solution of this equation gives the density in terms of r. If we introduce the scaled variables θ and ξ defined by

$$\rho = \rho_c \theta^n \tag{53}$$

$$r = \left[\frac{K(n+1)}{4\pi G} \rho_c^{\frac{1}{n}-1} \right]^{\frac{1}{2}} \xi , \tag{54}$$

where ρ_c is the central density, then equation (52) reduces to

$$\frac{1}{\xi^2} \frac{d}{d\xi} \left(\xi^2 \frac{d\theta}{d\xi} \right) = -\theta^n \tag{55}$$

which is known as the Lane-Emden equation.

For any value of n this equation can be solved for θ in terms of ξ by series expansion and numerical integration, the necessary boundary conditions being

$$\theta = 1 \quad and \quad \frac{d\theta}{d\xi} = 0 \quad at \quad \xi = 0.$$

The general solution of the equation(55) is given by

$$\theta = 1 - \frac{1}{6}\xi^2 + \frac{n}{120}\xi^4 - \frac{n(8n-5)}{42x360}\xi^6 + \ldots\ldots\ldots \tag{56}$$

The mass relation

The radius of the polytrope is

$$R = a\xi_1$$

where
$$a = \left[\frac{K(n+1)}{4\pi G}\,\rho_c^{\frac{1}{n}-1}\right]^{\frac{1}{2}}, \tag{57}$$

and ξ_1 is the value of ξ at $\theta = 0$. Therefore, the total mass of the configuration is

$$m = \int_0^{a\xi_1} 4\pi r^2 \rho\, dr$$

$$= 4\pi a^3 \rho_c \int_0^{\xi_1} \xi^2 \theta^n\, d\xi, \tag{58}$$

which with the help of equation (55) gives

$$m = -4\pi a^3 \rho_c \int_0^{\xi_1} \frac{d}{d\xi}\left(\xi^2 \frac{d\theta}{d\xi}\right) d\xi$$

$$= -4\pi a^3 \rho_c \left(\xi^2 \frac{d\theta}{d\xi}\right)_{\xi_1} \tag{59}$$

The central density

Let $\bar{\rho}$ be the mean density of the polytrope. Then

$$\bar{\rho} = \frac{3m}{4\pi R^3} = \frac{3m}{4\pi a^3 \xi_1^3}$$

Substituting for m from equation (59) gives

$$\overline{\rho} = -3\rho_c \left(\frac{1}{\xi} \frac{d\theta}{d\xi} \right)_{\xi_1} \tag{60}$$

or

$$\rho_c = -\frac{m}{4\pi R^3} \left(\frac{\xi}{\frac{d\theta}{d\xi}} \right)_{\xi_1} \tag{61}$$

The central pressure

For a complete polytrope we have

$$P_c = K \rho_c^{1+\frac{1}{n}}$$

Substituting for K and ρ_c from equations (57) and (61) gives

$$P_c = a_n \frac{Gm^2}{R^4} \tag{62}$$

where

$$a_n = \left[\frac{1}{4\pi (n+1) \left(\frac{d\theta}{d\xi} \right)^2} \right]_{\xi_1}$$

The central temperature

The equation for state for perfect gas in which radiation pressure is neglected is

$$P = \frac{k}{\mu H} \rho T$$

where k is a Boltzmann constant, μ the mean molecular weight and H the mass of proton. Therefore, the central temperature is

$$T_c = \frac{\mu H}{k}\left(\frac{P_c}{\rho_c}\right) \tag{63}$$

Substituting for ρ_c and P_c from equations (61) and (62) we have

$$T_c = b_n \frac{G m}{R} \tag{64}$$

where $$b_n = \left[\frac{1}{(n+1)\xi \frac{d\theta}{d\xi}}\right]_{\xi_1} \frac{\mu}{k}$$

For given values of n the coefficients a_n and b_n are known numerical constant (e. g. Chandrasekhar, 1939).

The potential energy

The gravitational potential energy of a spherical mass m and radius R is

$$\Omega = -\int \frac{G m_r \, dm_r}{r}$$

$$= -\frac{G m^2}{2R} - \int_0^R \frac{1}{2}\frac{G m_r^2}{r^2} dr \tag{65}$$

Now from equation (25) and (51) we have

$$\frac{d}{dr}\left\{(n+1)\frac{P}{\rho}\right\} = -\frac{G m_r}{r^2}$$

Therefore, equation (65) gives

$$\Omega = -\frac{G m^2}{2R} + \frac{1}{2}(n+1)\int_0^R \frac{d}{dr}\left(\frac{P}{\rho}\right) m_r \, dr$$

$$= -\frac{G m^2}{2R} + \frac{1}{2}(n+1)\left\{\left[m_r \frac{P}{\rho}\right]_0^R - \int_0^R 4\pi r^2 P \, dr\right\}$$

$$= -\frac{G m^2}{2R} - \frac{1}{2}(n+1)\int_0^R 4\pi r^2 P \, dr \qquad (66)$$

where we have used the boundary conditions that $m_r = 0$ at $r = 0$ and $P = 0$ at $R = 0$.

But $$\int_0^R 4\pi r^2 P \, dr = \left[\frac{4}{3}\pi r^3 P\right]_0^R - \int_0^R \frac{4}{3}\pi r^3 \, dP$$

$$= \frac{1}{3}\int \frac{G m_r \, dm_r}{r}, \qquad \text{by equation (25)}$$

Hence, from the equation (66) we have

$$\Omega = -\frac{G m^2}{2R} + \frac{1}{6}(n+1)\,\Omega$$

that is,

$$\Omega = -\frac{3}{5-n}\frac{Gm^2}{R} \tag{67}$$

The total energy

From equations (25) and (26) we have already obtained

$$4\pi r^3 dP = -\frac{G m_r\, dm_r}{r}$$

If integrate this equation over the whole star, then

$$3\int_{P_c}^{P_s} v\,dP = -\int_0^{m_s} \frac{G m_r\, dm_r}{r} = \Omega \tag{68}$$

where v is the volume contained within radius r and the dummies c and s are used to denote the volumes of the parameters at the centre and the surface respectively. Equation (68) thus gives

$$\Omega = 3\left[Pv\right]_c^s - 3\int_0^{v_s} P\,dv$$

Since $dm = \rho\,dv$ and $\left[Pv\right]_c = 0$ we have

$$3\int \frac{P}{\rho}dm + \Omega = 0, \tag{69}$$

where again we have assumed $P_s = 0$. Equation (69) is usually known as the Viral Theorem. Using the equation of state of an ideal gas with negligible radiation pressure equation (69) gives

$$\Omega = -3\int \left(c_p - c_v\right) T\, dm$$

$$= -3(\gamma - 1)\int c_v\, T\, dm,$$

where γ is the ratio of specific heats c_p and c_v. Now,

$$\int c_v\, T\, dm = U,$$ the total internal energy of the system.

Therefore, $$3(\gamma - 1)\, U + \Omega = 0 \qquad (70)$$

If we neglect the magnetic and ionization effects then the total energy of the polytrope is

$$E = U + \Omega$$

which with equations (67) and (70) gives

$$E = -\frac{(3\gamma - 4)}{(\gamma - 1)(5 - n)}\frac{Gm^2}{R} \qquad (71)$$

iii. References

Bahcall J.N., and Ulrich R.K., 1988, Rev. Mod. Phys., 60, 297

Chandrasekhar S., 1939, An Introduction to the Study of the Stellar Structure, Chicago University Press.

Christensen-Dalsgaard J., 1982, MNRAS, 199, 735

Cowling T.G., 1936, MNRAS, 96, 42

De Loore C.W.H., and Doom C., 1992, Structure and Evolution of Single and Binary Stars, Kluwer, Dordrecht.

Haselgrove C.B., and Hoyle F., 1956, MNRAS, 116, 515

Henyey L.G., Wilets L., Bohm K.H., LeLevier R. Levee, R.D., 1959, Ap.J, 129, 628

Iben I. Jr., 1965, Ap.J, 142,1447

Kippenhahn R., Weigert A., Hofmeister E., 1967, In Methods in Computational Physics, ed. B. Alder, S. Fernbach and M. Rotenberg, Academic Press, New York, Vol. 7, 129

Morel P., Provost J., Berthomieu G., 1990, Solar Phys., 128, 7

Paczynski B., 1969, Acta Astron., 19, 1

Paczynski B., 1970, Acta Astron., 20, 47

Peterson J.O., 1967, Copenhagen University Internal Report, Unpulished.

Reiter J., Bulirsch R., Pfleiderer, J., 1994, Astron. Nachr., 3, 205-234

Schwarzschild M., 1958, Structure and Evolution of Stars, Chicago Univ. Press, Dover.

Wilson R.E., 1981, Astr. Ap., 99, 43

Chapter 3: Calculation of the Stellar Model

i. The Model Star

We consider a star of mass $2.5M_{\odot}$ with chemical composition $X = 0.90$, $Y = 0.09$, and $Z = 0.01$, in which ideal gas laws hold. Since for stars of masses $\geq 2M_{\odot}$ the energy generation is principally due to CN cycle, the energy generation law is taken as

$$\varepsilon_{CN} = \varepsilon_0 \times \rho X X_{CN} \times \left(\frac{T}{10^6}\right)^{16} \tag{72}$$

where $X_{CN} = \frac{Z}{3}$, and $\varepsilon_0 \approx 10^{-17}$.

For most main sequence stars opacity is caused by bound-free and free-free transitions while for very hot stars it is due to electron scattering. For upper main sequence stars in the intermediate regime the opacity is likely to be mixed. Stellar models of mixed opacity have been calculated by Harm and Schwarzschild (1955), Kushwaha (1957), Morton (1959), and S. S. Huang (1960). In these calculations opacity has been taken due to both electron scattering and Kramer's opacity combined by straight addition. However, Reiz (1954) proposed an expression for mixed opacity where free-free transition and electron scattering are of the same order. In our problem, we have chosen the mixed opacity proposed by Reiz given by

$$\kappa = \kappa_0 \left(\frac{\rho}{T^{3.5}}\right)^{1/2}, \tag{73}$$

where $\kappa_0 = 1.6x10^{11}(1+X)$, (74)

The structure of the model star is then given by equations (28 - 32) together with (72), (73), and $P = \frac{\Re}{\mu}\rho T$, the equation of state for an ideal gas.

ii. Integration of the Equations

The mathematical problem of solving the equations of structure is much simplified by of structure introducing the dimensionless variables p, t, q, l, and x defined by

$$P(r) = \frac{GM^2}{4\pi R^4} p, \qquad T(r) = \frac{\mu}{\Re}\frac{GM}{R} t,$$

$$M(r) = qM, \qquad L(r) = lL, \qquad \text{and} \qquad r = xR.$$

Under the above transformation the equations (28 - 32) with the help of (72), (73), and the equation of state for ideal gas, reduce to

$$\frac{dp}{dx} = -\frac{q\,p}{t\,x^2} \tag{75}$$

$$\frac{dq}{dx} = \frac{p\,x^2}{t} \tag{76}$$

$$\frac{dt}{dx} = -C\frac{p^{1.5}\,l}{x^2\,t^{6.25}}, \text{ radiative layers} \tag{77}$$

$$\frac{dt}{dx} = \frac{2}{5}\frac{t}{p}\frac{dp}{dx}, \qquad \text{convective layers} \tag{78}$$

$$\frac{dl}{dx} = Dx^2 p^2 t^{14} \tag{79}$$

where $$C = \frac{3\kappa_0}{128\pi^{2.5} ac}\left(\frac{\Re}{\mu G}\right)^{5.75} LR^{0.25} M^{-4.25}, \tag{80}$$

$$D = \frac{\varepsilon_0 XX_{CN}}{4\pi}\left(\frac{\mu G}{\Re}\right)^{16} \frac{M^{18}}{LR^{19}}, \tag{81}$$

with all symbols having conventional meanings.

In our calculations we shall use approximate 'zero boundary conditions'. These are now given by

$p = 0 = t, q = 1$ at $x = 1$ and $l = 0$ at $x = 0$.

In the numerical solutions of the structure equations, Henyey's (1959) method is very popular where all the structure equations are transformed into equations with mass as independent variable instead of radius. He used the finite difference method. Besides Henyey's method, Schwarzschild method is the best known for numerical solution of structure equations. We have however used the matching method given by Cowling (1936).

Since the model star is likely to have a small convective core with a radiative envelope, in principle we have two solutions, one in the envelope and one in the core. These two solutions must match at the interface.

Polytropic Core Solution

In the convective core the non dimensional equations are

$$\frac{dp}{dx} = -\frac{q\,p}{t\,x^2} \tag{75}$$

$$\frac{dq}{dx} = \frac{p x^2}{t} \tag{76}$$

$$\frac{dp}{dx} = \frac{5}{2}\frac{p}{t}\frac{dt}{dx}, \quad or \quad P = E t^{5/2}, \tag{78}$$

Eliminating q from equation (75) and (76) we have

$$\frac{d}{dx}\left(\frac{x^2}{p}\frac{t}{dx}\frac{dp}{dx}\right) = -\frac{dq}{dx} = \frac{p x^2}{t}$$

Substituting for $\frac{t}{p}\frac{dp}{dx}$ from equation (78) we have

$$\frac{5}{2}\frac{d}{dx}\left(x^2\frac{dt}{dx}\right) = -\frac{p x^2}{t} \tag{82}$$

Now introduce the polytropic variables η and θ, defined by

$$p = p_c \theta^{5/2}, \quad t = t_c \theta, \quad \text{and} \quad x = \left(\frac{5}{2}\frac{t_c^2}{p_c}\right)^{1/2} \eta$$

where p_c and t_c are the central pressure and temperature in non-dimensional form.

Under the above substitutions we have from equation (82)

$$\frac{1}{\eta^2}\frac{d}{d\eta}\left(\eta^2\frac{d\theta}{d\eta}\right) = -\theta^{3/2} \tag{83}$$

where $\theta = 1$, $\frac{d\theta}{d\eta} = 0$ at $\eta = 0$.

Equation (83) is the well known Lane-Emden equation with index 3/2. We know the general solution of the Lane-Emden equation with index n is

$$\theta = 1 - \frac{1}{6}\eta^2 + \frac{n}{120}\eta^4 - \frac{n(8n-5)}{42x360}\eta^6 + \ldots\ldots\ldots \tag{84}$$

Therefore solution of equation (83) is

$$\theta = 1 - \frac{1}{6}\eta^2 + \frac{1}{80}\eta^4 - \frac{1}{1440}\eta^6 + \ldots\ldots\ldots$$

For small η this is a rapidly converging series.

We take $$\theta = 1 - \frac{1}{6}\eta^2 + \frac{1}{80}\eta^4 \tag{85}$$

Introducing Schwarzschild homology variables defined by

$$U = +\frac{r}{M(r)}\frac{dM(r)}{dr} = \frac{x}{q}\frac{dq}{dx} = \frac{px^3}{qt} \tag{86}$$

$$V = -\frac{r}{P}\frac{dP}{dr} = -\frac{x}{p}\frac{dp}{dx} = \frac{q}{tx} \tag{87}$$

$$n+1 = \frac{T}{P}\frac{dP}{dT} = \frac{t}{p}\frac{dp}{dt} = \frac{qt^{6.25}}{Cp^{1.5}} \tag{88}$$

The advantage of these variables is that they are scale independent, multiplying r or $M(r)$ by a constant doesn't change U since they occur on both the numerator and denominator.

For the convective core we have

$$U = \frac{x}{q}\frac{dq}{dx} = -\frac{px^2}{t^2\frac{dp}{dx}} = -\frac{\eta\theta^{3/2}}{\frac{d\theta}{d\eta}} \cong 3 - \frac{3\eta^2}{10} + \ldots\ldots\ldots\ldots \quad (89)$$

$$V = \frac{x}{p}\frac{dp}{dx} = -\frac{\eta}{\theta^{5/2}}\frac{d\theta^{5/2}}{d\eta} \cong \frac{5\eta^2}{6}\left(1 + \frac{\eta^2}{60} + \ldots\ldots\right) \quad (90)$$

So as to good approximation

$$U = 3 - \frac{18}{50}V + \ldots\ldots\ldots\ldots, \quad (91)$$

This gives the core solution in the U-V plane.

Envelope solution and the matching point

The envelope of the model star is in radiative equilibrium. Its structure is determined by equations (75) - (77). The equation (77) contains an unknown parameter C. We thus have an one-parameter family of solutions, our aim is to determine the correct value of C and obtain the envelope solution for that value of the parameter. In order to do this we have to solve the envelope solutions for different trial values of C and find for which value of C the solution just matches the core solution at the interface. However the solution is not straightforward. Because of the existence of singularity at the surface, integration can not be started right from the surface ($x = 1$). To avoid this difficulty we have to look for series expansion of the variables about the singular point.

The envelope solutions we have calculated numerically, however since the equations are singular at the surface, $p = t = 0$, we have chosen the series expansion of the variables near the singular point in the following way.

Let $\frac{1}{x} - 1 = \xi$, i.e., $x = \frac{1}{1+\xi}$ (92)

Then the equations (75) - (77) reduces to

$$\frac{dp}{d\xi} = \frac{q\,p}{t} \tag{93}$$

$$\frac{dt}{d\xi} = C\frac{p^{1.5}}{t^{6.25}} \tag{94}$$

$$\frac{dq}{d\xi} = -\frac{p}{t(1+\xi)^4} \tag{95}$$

Here the singular point is $\xi = 0$ since $x = 1 \Rightarrow \xi = 0$. Now the series expansion of the variables about $\xi = 0$ can easily be done. By Fuchs theorem (e.g. Rajput & Yog Prakash, 1977) a convergent development of the solution in a power series about the singular point having a finite number of terms is possible. We, therefore, take

$$t = \xi^u \left(c_0 + c_1 \xi + \ldots\ldots + c_n \xi^n \right) \tag{96}$$

$$p = \xi^v \left(d_0 + d_1 \xi + \ldots\ldots + d_n \xi^n \right) \tag{97}$$

$$q = 1 + g_1 \xi + g_2 \xi^2 + \ldots\ldots + g_n \xi^n \tag{98}$$

In equation (98) we have used the condition that

$$q = 1 \quad at \quad \xi = 0.$$

Substituting for p, q, and t in equation (93) we have

$$\xi^{u}\left(c_0 + c_1\xi + \ldots\ldots + c_n\xi^{n}\right)\left(d_0\, v\xi^{v-1} + d_1(v+1)\xi^{v} + \ldots + d_n(v+n)\xi^{n+v-1}\right)$$

$$= \left(1 + g_1\xi + g_2\,\xi^2 + \ldots\ldots + g_n\xi^{n}\right)\left(d_0\,\xi^{v} + d_1\,\xi^{v+1} + \ldots + d_n\,\xi^{v+n}\right)$$

or $$c_0 d_0 v\xi^{u+v-1} + \left(d_0 c_1\, v + c_0 d_1\,(v+1)\right)\xi^{u+v} + \ldots\ldots \textit{higher order of } \xi$$

$$= d_0\xi^{v} + \left(d_1 + d_0 g_1\right)\xi^{v+1} + \ldots\ldots\ldots \textit{higher order of } \xi$$

Since the two polynomials are equal we must have

$$u+v-1 = v, \quad u+v = v+1, \quad \textit{etc.} \tag{99}$$

and

$$c_0\, d_0\, v = d_0\ , \tag{100}$$

From equation (99) and (100), we have

$$u = 1 \quad \text{and } c_0 v = 1 \tag{101}$$

With $u = 1$, t becomes

$$t = \left(c_0\,\xi + c_1\,\xi^2 + \ldots\ldots + c_n\,\xi^{n+1}\right)$$

Equation (94) then gives

$$\left(c_0\,\xi + c_1\,\xi^2 + \ldots\ldots \textit{to n terms}\right)^{6.25}\left(c_0 + 2c_1\,\xi + \ldots\ldots \textit{to n terms}\right)$$

$$= C\left(d_0\,\xi^{v} + d_1\,\xi^{v+1} + \ldots\ldots \textit{to n terms}\right)^{1.5}$$

or $$\left[c_0^{7.25}\,\xi^{6.25} + \left(2c_1\,c_0^{6.25} + 6.25\,c_0^{6.25}\,c_1\right)\xi^{7.25} + \ldots\ldots \textit{higher power of } \xi\right]$$

$$= C\left[d_0^{1.5}\,\xi^{1.5v5} + \left(1.5\,d_0^{0.5}\,d_1\right)\xi^{0.5v+v+1} + \text{.....higher power of } \xi\right]$$

Again equating powers and coefficients we have

$$1.5v = 6.25 \quad \text{and} \quad c_0^{7.25} = C\,d_0^{1.5} \tag{102}$$

So from equations (101) and (102) we get

$$u = 1,\quad v = 4.17,\quad c_0 = \frac{1}{4.17} \quad \text{and} \quad d_0 = \frac{1}{C^{0.67}}\left(\frac{1}{4.17}\right)^{4.83}$$

Therefore, in the first approximation we have about $\xi = 0$, i.e., $x = 1$

$$\left.\begin{aligned} p &\approx \left(\frac{1}{4.17}\right)^{4.83}\frac{1}{C^{0.67}}\xi^{4.17} = \left(\frac{1}{4.17}\right)^{4.83}\frac{1}{C^{0.67}}\left(\frac{1}{x}-1\right)^{4.17} \\ t &\approx \frac{1}{4.17}\xi = \frac{1}{4.17}\left(\frac{1}{x}-1\right) \\ \text{and}\quad q &\approx 1 \end{aligned}\right\} \tag{103}$$

These relations determine the values of the parameters at any point near the surface. With these values as the boundary values the envelope equations can easily be solved numerically for given value of C. C is an unknown constant whose value for a star of given mass depends on its luminosity and radius. As is evident from equation (80) C is very small. For solar type stars C is of the order of 10^{-5}. We shall treat C as a free parameter and consider a number of values close to 10^{-5}.

We take a point $x = 0.99$ very near to the surface. Then from equation (103) the values of the parameters at that point are found to be

$$p_0 = 3.18e-10 \qquad t_0 = 2.42e-3 \qquad q_0 = 1$$

Taking these values as the boundary values we have integrated the equations for the radiative envelope numerically inwards up to where

$$n+1 = \frac{t}{p}\frac{dp}{dt} = 5/2 = 2.5,$$

appropriate for convection, by the fourth order Runge-Kutta method for a number of trial values of C. Some of these calculations, namely for C = $1.5\text{x}10^{-5}$, $2.0\text{x}10^{-5}$, $2.08\text{x}10^{-5}$, $3.5\text{x}10^{-5}$, etc, together with the convective track, equation (91), are drawn in the U-V plane (Fig 1). At the junction between the convective core and the radiative envelope both (U,V) and their derivatives must be continuous. So the curve for the correct radiative solution must touch the convective curve at the interface. From Fig 1 it is found that this happens for $C = 2.08 \times 10^{-5}$. This is, therefore, the correct value of C for our model star. For this value of C the matching point is at $x_f = 0.203$. The radiative solution for the envelope $0.203 \leq x < 1$ for $C = 2.08x10^{-5}$ is given in table 1.

Table 1 : Radiative structure of the model star M=2.5, X=0.90, Y=0.09, Z=0.01 (Solar Unit).

x=r/R	p	t	q=Mr/M	logρ	Lr/L
1.000	0.00E+00	0.00E+00	1.00E+00		1.000
0.990	5.44E-09	2.40E-03	1.00E+00	-6.001	1.000
0.900	9.42E-05	2.44E-02	1.00E+00	-2.770	1.000
0.800	3.20E-03	5.66E-02	9.98E-01	-1.604	1.000
0.700	3.20E-02	9.84E-02	9.90E-01	-0.844	1.000
0.600	2.03E-01	1.54E-01	9.61E-01	-0.236	1.000
0.500	1.02E+00	2.28E-01	8.85E-01	0.294	1.000
0.400	4.33E+00	3.30E-01	7.28E-01	0.761	1.000
0.300	1.51E+01	4.67E-01	4.73E-01	1.153	1.000
0.203	3.78E+01	6.38E-01	2.01E-01	1.416	1.000

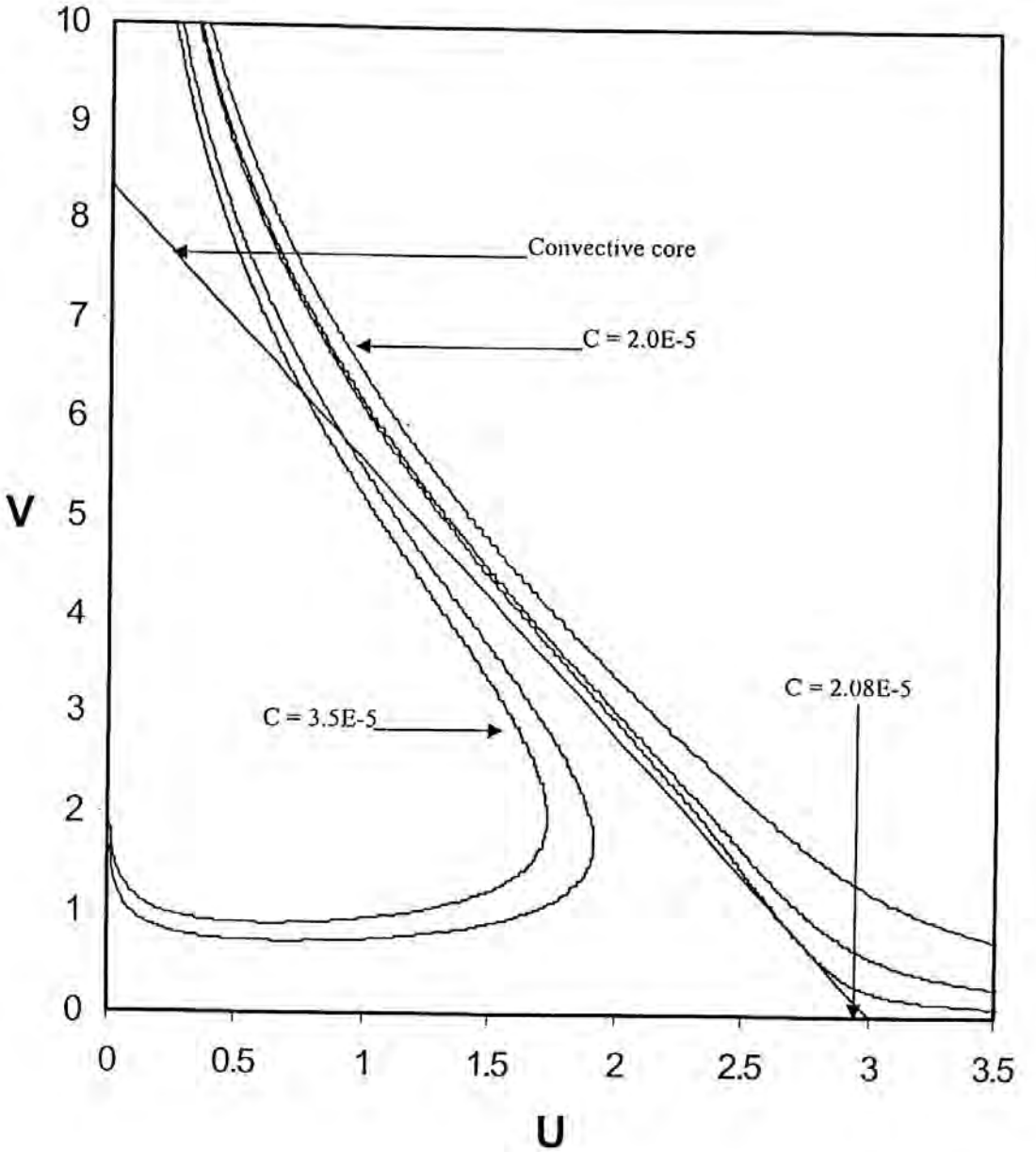

Figure 1: The core solution and the envelope solutions with different values of C in the U-V plane.

The complete solution:

From the table 1 we find that

$$p_f = 37.8 \qquad t_f = 0.638 \qquad q_f = 0.201 \qquad U_f = 2.47 \qquad V_f = 1.55$$

Also $l_f = 1$, at $x = x_f$, since all the energy is produced in the core.

With these values as our boundary conditions we have to solve the core equations, namely equations (75), (76), (78), and (79) inwards numerically. In order to do this we need the correct value of D. This can be done by integrating the energy equation.

Total luminosity, $L = \int_0^{r_1} 4\pi r^2 \rho(r) \varepsilon \, dr$

$$= \frac{\varepsilon_0 X X_{CN}}{4\pi} \left(\frac{\mu G}{\Re}\right)^{16} \frac{M^{18}}{R^{19}} \int_0^{x_1} p^2 t^{14} x^2 \, dx,$$

$$= L \, D \int_0^{x_f} p^2 t^{14} x^2 \, dx, \qquad \text{from(81)}$$

or, $$D \int_0^{x_f} p^2 x^2 t^{14} dx = 1 \qquad (104)$$

Introducing polytropic variables we can write

$$\frac{1}{D} = \int_0^{x_f} p^2 x^2 t^{14} dx = \left(\frac{5}{2}\right)^{1.5} p_c^{0.5} t_c^{17} \int_0^{\eta_f} \eta^2 \theta^{19} \, d\eta \qquad (105)$$

Substituting $\theta(\eta)$ from equation (85) we have

$$\frac{1}{D} = \left(\frac{5}{2}\right)^{1.5} p_c^{0.5} t_c^{17} \int_0^{\eta_f} \eta^2 \left(1 - \frac{\eta^2}{6} + \frac{\eta^4}{80}\right)^{19} d\eta. \qquad (106)$$

Since p and t are continuous at x_f we have

$$p_f = p_c \theta_f^{5/2} \qquad \text{and} \qquad t_f = t_c \theta_f$$

Now substituting the value of U_f in equation (89) and V_f in equation (90) we have

$$\eta_f = 1.343775$$

and hence using this η_f in equation (85) we get

$$\theta_f = 0.739812$$

Therefore, $p_c = \left(p_f / \theta_f^{5/2}\right) = 80.295$ and $t_c = \left(t_f / \theta_f\right) = 0.8624$

Now substituting the values of p_c, t_c, and η_f equation (106) and evaluating the integration we have

$$D = 4.51$$

Using this D in equation (79) we have integrated the core equation again by the fourth order Runge-Kutta method from the interface downward up to $x = 0.001$. The envelope solution and the core solution together give the complete internal

structure of the star. We are however yet to find the luminosity and the radius of the star.

From equations (80) and (81) we have

$$L R^{0.25} = \frac{128 C M^{4.25} \pi^{2.5} ac}{3\kappa_0 \left(\frac{\Re}{\mu G} \right)^{5.75}} \tag{107}$$

and

$$L R^{19} = \frac{\varepsilon_0 X X_{CN} \left(\frac{\mu G}{\Re} \right)^{16} M^{18}}{4\pi D} \tag{108}$$

Eliminating L from equation (107) and (108) we have

$$R^{18.75} = \frac{\varepsilon_0 X X_{CN} (3\kappa_0) \left(\frac{\mu G}{\Re} \right)^{10.25} M^{13.75}}{512 x C D a c \pi^{3.5}} \tag{109}$$

Substituting all the values of the constants and parameters in equation (109), we have

$$R = 1.39 R_{\odot}$$

And using this value of R in equation (108) we have the value of L, that is,

$$L = 38.9 L_{\odot}$$

The complete structure of model star is given in table 2.

Table 2 : Complete structure of the model star M=2.5, X=0.90, Y=0.09, Z=0.01 (Solar Unit)

x=r/R	p	t	q=Mr/M	logρ	Lr/L
1.000	0.00E+00	0.00E+00	1.00E+00		1.000
0.990	5.44E-09	2.40E-03	1.00E+00	-6.001	1.000
0.900	9.42E-05	2.44E-02	1.00E+00	-2.770	1.000
0.800	3.20E-03	5.66E-02	9.98E-01	-1.604	1.000
0.700	3.20E-02	9.84E-02	9.90E-01	-0.844	1.000
0.600	2.03E-01	1.54E-01	9.61E-01	-0.236	1.000
0.500	1.02E+00	2.28E-01	8.85E-01	0.294	1.000
0.400	4.33E+00	3.30E-01	7.28E-01	0.761	1.000
0.300	1.51E+01	4.67E-01	4.73E-01	1.153	1.000
0.203	3.78E+01	6.38E-01	2.01E-01	1.416	1.000
0.200	3.87E+01	6.43E-01	1.94E-01	1.423	0.998
0.100	6.73E+01	8.04E-01	2.89E-02	1.566	0.573
0.000	8.03E+01	8.62E-01	0.00E+00	1.612	0.000

iii. Effect of variation of Mass and Chemical Composition

If the chemical compositions remain same then there is a effect of varying mass on the other physical quantities, namely, luminosity L, effective temperature T_{eff}, and radius R.

We have $$C = \frac{3\kappa_0}{128\pi^{2.5} ac}\left(\frac{\Re}{\mu G}\right)^{5.75} LR^{0.25} M^{-4.25}, \qquad (80)$$

$$D = \frac{\varepsilon_0 XX_{CN}}{4\pi}\left(\frac{\mu G}{\Re}\right)^{16} \frac{M^{18}}{LR^{19}}, \qquad (81)$$

From equations (80) and (81) we thus have logarithmic measures

$$\log L + 0.25 \log R - 4.25 \log M + \log(constant) = 0 \qquad (110)$$

and

$$\log L + 19 \log R - 18 \log M + \log(constant) = 0 \qquad (111)$$

Differentiating equations (110) and (111) gives

$$\frac{\delta L}{L} + 0.25 \frac{\delta R}{R} - 4.25 \frac{\delta M}{M} = 0 \qquad (112)$$

and

$$\frac{\delta L}{L} + 19 \frac{\delta R}{R} - 18 \frac{\delta M}{M} = 0 \qquad (113)$$

Eliminating $\frac{\delta L}{L}$ from equations (112) and (113) we get

$$\frac{\delta R}{R} = 0.73 \frac{\delta M}{M} \qquad (114)$$

Again eliminating $\frac{\delta R}{R}$ from equations (112) and (113) we get

$$\frac{\delta L}{L} = 4.07 \frac{\delta M}{M} \qquad (115)$$

From black body relationship we

$$L = 4 \pi \sigma R^2 T_{eff}^4 \qquad (116)$$

where σ is Stefan-Boltzmann's constant

Logarithmic differentiation of equation (116) gives

$$\frac{\delta L}{L} - 2\frac{\delta R}{R} - 4\frac{\delta T_{eff}}{T_{eff}} = 0 \qquad (117)$$

Substituting the values of $\frac{\delta R}{R}$ and $\frac{\delta L}{L}$ from equations (114) and (115) into equation (117) gives

$$\frac{\delta T_{eff}}{T_{eff}} = 0.65\frac{\delta M}{M} \qquad (118)$$

From equations (114), (115), and (118) it is evident that as M increases R and T_{eff} increase slightly, but the increase in L is quite sharp.

If mass is kept constant then there are some effect on the physical quantities, L, R, and T_{eff} for the variation of κ_0, X, and Z.

From the logarithmic differentiation of equations (80) and (81) we get

$$\frac{\delta L}{L} + 0.25\frac{\delta R}{R} + \frac{\delta \kappa_0}{\kappa_0} = 0 \qquad (119)$$

and

$$\frac{\delta L}{L} + 19\frac{\delta R}{R} - \frac{\delta X}{X} - \frac{\delta Z}{Z} = 0 \qquad (120)$$

Eliminating $\frac{\delta L}{L}$ from equations (119) and (120) we get

$$\frac{\delta R}{R} = 0.53\left(\frac{\delta \kappa_0}{\kappa_0} + \frac{\delta X}{X} + \frac{\delta Z}{Z}\right) \qquad (121)$$

Again eliminating $\frac{\delta R}{R}$ from equations (119) and (120) we get

$$\frac{\delta L}{L} = -1.013\frac{\delta\kappa_0}{\kappa_0} - 0.013\left(\frac{\delta X}{X} + \frac{\delta Z}{Z}\right) \qquad (122)$$

Substituting the values of $\frac{\delta R}{R}$ and $\frac{\delta L}{L}$ from equations (121) and (122) into equation (117) gives

$$\frac{\delta T_{eff}}{T_{eff}} = -0.28\frac{\delta\kappa_0}{\kappa_0} - 0.023\left(\frac{\delta X}{X} + \frac{\delta Z}{Z}\right) \qquad (123)$$

But κ_0 depends on X. Therefore the change in κ_0 is in effect due to the change in X. Equations (121) - (123) indicate that any increase in X and Z slightly increases R but decreases L and T_{eff}. This is expected because R and T_{eff} vary inversely, the mass being constant.

iv. Summary and Discussion

We have determined the structure of a 2.5 solar mass in which the abundance of elements has taken as X = 0.90, Y = 0.09, Z = 0.01. We have also assumed that the opacity is mixed i.e. due to both electron scattering and free-free transition. We have solved the equations of structure numerically by the forth order Runge-Kutta method in which the step length has been taken as h = 0.001. To determine the structure we have followed a simple fitting method devised by Cowling (1936). It is found that if the mass and chemical compositions are prescribed then the distribution of the thermodynamic variables inside the star as well as its total luminosity, radius and effective temperature can be uniquely

determined. It is interesting to see that our results obtained by simple fitting method do not vary significantly from the recent calculation of W. Brunish (e.g., Bohm-Vitense) by regorous treatment of the problem. If the mass varies keeping the composition fixed, then all variables L, T_{eff} and R are found to vary. For an increase in M the position of the star in the HR diagram is slightly shifted toward the upper end of the MS. If the mass is constant then a decrease in the hydrogen content of the star increases luminosity and effective temperature. But as time goes on in the MS lifetime of a star its hydrogen content gradually diminishes giving rise to the helium content. That means, as an MS star ages its position in the HR diagram slowly moves along the MS toward the hot end. The position of an MS star in the HR diagram is thus determined mainly by its mass and chemical composition.

V. References

Bohm-Vitense E., Introduction to Stellar Astrophysics, Volume 3: Stellar Structure and Evolution, Cambridge University Press, 1992

Cowling T.G., 1936, MNRAS, 96, 42

Harm R. and Schwarzschild, M., 1955, ApJ. Suppl. Series, 1, 319

Henyey L.G., Wilets L., Bohm K.H., LeLevier R. Levee, R.D., 1959, ApJ, 129, 628

Huang S.S., 1960, ApJ, 131, 452

Kushwaha R.S., 1957, ApJ, 125, 242

Morton D.C., 1959, ApJ, 129, 20

Rajput B.S., and Yog Prakash, 1977, Mathematical Physics, Pragati Prakashan, India.

Reiz A., 1954, ApJ., 120, 342

SECTION 2

YOUNG STELLAR CLUSTERS

A. Studies of Three young Stellar Clusters With Constant Mass Evolution

Chapter 1. Star Formation

i. Current view of star formation

In recent years there have been some advancements in understanding the physical conditions of star formation (SF). It is now generally understood that SF occurs in dense molecular clouds. Evidence in its support comes from observation of dark molecular clouds in which young stellar like objects, called T Tauri stars, are seen embedded in the densest parts of the clouds. The ages of these objects are of the order of million years (e.g. Herbig 1962). Since this age is much less than the age of the galaxy they must have formed very recently. The most favourable star forming region to observe is perhaps the Orion complex. The region has been extensively studied for the last few decades. Recent summary of the region is available in Genzel and Stutzki (1989), and Hillenbrand (1997). Sites of active SF are located in the southern A and northern B clouds, the largest concentration of young stars being centred on the Trapezium cluster in the Orion A cloud. That SF is presently occurring in the region is also substantiated by the youth of the complex (e.g. Brown et al 1995; O'Dell & Wong 1996; and Hillenbrand 1997). Similar phenomena are observed in other regions such as the Ophiums-Scorpus-Centaurus region. Most stars in the Taurus cloud are believed to have formed in the past few million years (e.g. Hartmann 2003). SF is thus an ongoing process, and dense clouds are identified as sites of SF.

The classical view of SF was based on fragmentation of a molecular cloud due to gravitational instability, fragmentation process stopping at the minimum 'Jeans mass' scale (Jeans 1929). Jeans' calculation was of course very simple and mathematically not very consistent because of the so called "Jeans swindle' (e.g. Binney and Tremaine 1987). Further analysis of various equilibrium configurations (see Larson 2003) indicates that if gravity is strong, the minimum scale on which collapse can occur is always approximately the Jeans scale. However recent investigations have shown that SF is a very complicated problem involving many phenomena other than simply gravity and thermal energy. In recent times many theories have been advanced for SF. Some reviews are found in Adams (1998); Sigalotti & Klapp (2001); MacLow & Klessen (2004): and Larson (2003). Stars are found to form on different scales. On the largest scale stars form in giant molecular cloud (GMC) complexes, each complex containing several GMCs. Each GMC again contains small scale filamentary or clumpy structures (e.g. Blitz & William 1999). Molecular clouds are also found to have internal turbulent motion and magnetic field. Role of turbulence and magnetic field in cloud evolution and SF has been under extensive study for the last few decades (e.g. Larson 1979, Nakano 1984, McKee et al 1993, Basu & Mouschovias 1994, MacLow & Klessen 2004). It is found that although turbulence and magnetic field have important effect on cloud evolution they cannot hold a cloud against gravity for long . Molecular clouds are in fact transient objects. They form, evolve, give birth to stars and disperse. The general outline is that, interstellar turbulence compresses diffuse interstellar matter to high density where atomic gas is converted to molecular gas (Hollenbach et al 1971). Large scale shock generated by turbulence produces large density fluctuations leading to SF. The feed back effects of newly formed stars then quickly destroy the star forming cloud and recycle their matter back into diffuse state (see Larson 2003).

Small scale SF occurs in cloud cores or clumps either in singles or in groups (e.g. Lada & Lada 2003). Cluster formation is also found in simulation of

Klessen & Burkert 2001, Bonnell & Bate 2002, Bonnell et al 2003 and others. SF is a twin problem: (i) formation of protostars in collapsing cloud cores, and (ii) the distribution of stellar masses in clusters. To develop a complete theory of SF accounts must be taken of all the phenomena that may be involved in the formation process, namely, turbulence, magnetic field, gravity, protostellar interaction, rotation, feed back energy etc. Such a theory is yet to exist. Shu et al (1987) developed a model for formation of isolated single stars in which stars are formed by the inside-out collapse of a singular isothermal sphere which is initially in quasistatic equilibrium, supported against gravity by magnetic and thermal pressure, and evolves due to slow ambipolar diffusions process. Although some objections are there against some aspects of the process (e.g. Basu & Mouschovious 1994, Whitworth et al 1996, Larson 2001), the simplicity and elegance of the model have led to its wide use as a 'standard model' of SF.

As reviewed by Larson (2003), some progress in understanding the process of SF has recently come from collapse calculation of prestellar cores (e.g. Basu & Mouschovious 1994; Matsumoto et al 1997; Bate 1998; Lai 2000). All calculation indicates that when a core undergoes collapse, a small pressure supported object (i.e. an embryonic star) with mass of the order of 10^{-2} $M_{\odot}$ or less forms at the centre with an accompanying circumstellar disk. The embryo grows accreting more matter from the disk, the accretion being high initially but declining with time due to depletion of the envelope. Mass distribution of stars, the so-called mass function, is determined by competitive accretion. Protostellar accretion rate based on gravo-turbulent fragmentation has been discussed by Schmeja & Klessen (2004).

ii. Stellar Clusters

In the vast stellar system most of the stars are moving at random in space either alone, or with one or at most a couple of companions, as binary or multiple

systems. But a small number of stars of the entire population is observed to be associated with groups of different sizes and shapes. These groups have been called star clusters. On the basis of their size, shape, galactic distribution and the number as well as the physical characteristics of stellar content, two distinct types of clusters have been recognized, namely, the globular clusters, and the galactic or open clusters.

(a) Globular Clusters

Globular clusters are gravitationally bound concentrations of approximately ten thousand to one million stars, spread over a volume of several tens to about 200 light years in diameter. Globular clusters were always *thought* or suspected to be physical objects, agglomerations or swarms of stars held together by their mutual gravity, all close together and at about the same distance. Radial velocity measurements have revealed that most globular clusters are moving in highly eccentric elliptical orbits that take them far outside the Milky Way; they form a halo of roughly spherical shape which is highly concentrated to the Galactic Center, but reaches out to a distance of several 100,000 light years, much more than the dimension of the Galaxy's disk. They populate the halo or bulge of the Milky way and other galaxies with a significant concentration toward the Galactic Center. Spectroscopic study of globular clusters shows that they are much lower in heavy element abundance than stars such as the Sun that form in the disks of galaxies. Thus, globular clusters are believed to be very old and formed from an earlier generation of stars (*Population II*), which have formed from the more primordial matter present in the young galaxy just after (or even before) its formation. The Hertzprung-Russel diagrams (HRD) for globular clusters typically have short main sequences and prominent horizontal branches, this represents very old stars that have evolved past giant or super-giant phases. Comparison of the measured HRD of each globular cluster with theoretical model

HRDs derived from the theory of stellar evolution provides the possibility to derive, or estimate, the age of that particular cluster. It is perhaps a bit surprising that almost all globular clusters seem to be of about the same age; there seems to be a physical reason that they all formed in a short period of time in the history of the universe, and this period was apparently long ago when the galaxies were young. Semi-recent estimates yield an age of 12 to 20 billion years; the best value for observation is perhaps 14 to 16 billion The disk stars, by contrast, have evolved through many cycles of starbirth and supernovae, which enrich the heavy element concentration in star-forming clouds and may also trigger their collapse. Globular clusters typically contain a number of variable stars, they also contain a large number of white dwarfs and, at least in some cases, many neutron stars, some of which show up as pulsars. Our galaxy has about 200 globular clusters, most in highly eccentric orbits that take them far outside the Milky Way. Most other galaxies have globular cluster systems as well, in some cases containing several thousands of globulars. Some of the globular clusters are M2 to M5, M9, M10, M12 to M15, M19, M22, M28, M30, M53 to M56, M62, M68 to M72, M75, M79, M80, M92, etc including some early known NGC 104, NGC 4833, NGC 5139, and NGC 6397.

(b) Open Clusters

The open (or galactic) clusters are small in size, flattened in shape and are mostly distributed close to the galactic plane. The number of stars contained in the galactic cluster, usually lies between 10^2 to 10^3 and these stars have normal metal abundance like the sun. Galactic clusters are strongly concentrated near the galactic plane. Open clusters are physically related groups of stars held together by mutual gravitational attraction. Therefore, they populate a limited region of space, typically much smaller than their distance from us, so that they are all roughly at the same distance. They are believed to originate from large cosmic gas

and dust clouds (diffuse nebula) in the Milky Way, and to continue to orbit the galaxy through the disk. In many clouds visible as bright diffuse nebulae, star formation still takes place at this moment, so that we can observe the formation of new young star clusters. The process of formation takes only a considerably short time compared to the lifetime of the cluster, so that all member stars are of similar age. Also, as all the stars in a cluster formed from the same diffuse nebula, they are all of similar initial chemical composition. So open clusters are of great interest for astrophysicists because of the said properties of the stars in a cluster. They represent samples of stars of constant age and/or constant chemical composition, suited for study with respect to stellar structure and evolution, and to fix lines or loci in many state diagrams such as the color-magnitude diagram (CMD), or Hertzsprung-Russell diagram (HRD). Comparing the "standard" HRD, derived from nearby stars with sufficiently well-known distances, or the theory of stellar evolution, with the measured CMD of star clusters, provides a considerably good method to determine the distance of star clusters. Comparing their HRD with stellar theory provides a reasonable way to estimate the age of star clusters. The result that all the cluster HRDs can be explained by the theory of stellar evolution gives convincing evidence for this theory, and moreover for the underlying physics including nuclear and atomic physics, quantum physics and thermodynamics. Over 1100 open clusters are known in our milky way galaxy, and this is probably only a small percentage of the total population which is probably some factor higher; estimates of as many as about 100,000 Milky Way open clusters have been given. Most open clusters have only a short life as stellar swarms. As they drift along their orbits, some of their members escape the cluster, due to velocity changes in mutual closer encounters, tidal forces in the galactic gravitational field, and encounters with field stars and interstellar clouds crossing their way. An average open cluster has spread most of its member stars along its path after several 100 million years; only few of them have an age counted by billions of years. The escaped individual stars continue to orbit the Galaxy on their own as field stars. All field stars in our galaxy and the external galaxies are

thought to have their origin in clusters quite probably. Some of the open clusters are extreme young clusters which are observed to be embedded in nebulosities. Stars of these clusters have been born recently out of nebulous matter associated with them, as only the more massive members have had enough time to settle on to the main sequence, but the fainter, less massive ones are still in the process of gravitational contraction and are yet to settle on the main sequence. Some of the extreme young clusters are NGC 2264, NGC 6383, NGC 1976, NGC 6611, IC 5146 and the Orion Nebula cluster.

iii. Pre Main Sequence Evolution of Stars

The evolution of a protostar toward the main sequence can be divided into two distinct phases - the hydrodynamic phase and the quasihydrostatic phase. Both these phase together is called the pre-main-sequence phase of star's evolution. The study of pre-main-sequence stellar evolution has developed in such a way that it is the early phase, that is, the hydrodynamic phase which is still less well understood while the evolutionary behavior of a star in the quasihydrostatic phase is well established.

The first numerical calculations on the evolution of a contracting star was made by Henyey, LeLevier and Levee (1955) under the assumption of radiative energy transport. They also assume that loss of gravitational potential energy is the only source of radiating energy in the system, until the star reaches the main-sequence when it derives the energy from nuclear source. Their calculation predicts that contracting stars evolve with a gradually increasing surface temperature and luminosity. Brownlee and cox (1961) carried out similar work with improved energy generation laws and obtained results in general agreement with Henyey et al.

Su-Shu-Huang (1961) attempts to evaluate the plausibility of the theory of Henyey et al. for the pre-main-sequence evolution of stars. By comparing the observed distribution of pre-main-sequence stars on the HR diagram of NGC 2264 with a theoretically constructed HR diagram for contracting stars based on the theory of Henyey et al. He found the discrepancy between the theory and observation. However, due to some uncertainties in both the theoretical and observational work Huang was not prepared to reach a firm confirmation.

Soon it was realised by various authors (e.g. McCrea and Williams, 1962) that a greater understanding of the initial conditions of the problem was necessary. But it was Hayashi (1961) who investigated the problem in great details and concluded that the evolution of a protostar to a self luminous star occurred on a short time scale by the dynamical collapse of the protostar. At the end of dynamical collapse the protostar enters its quasistatic phase with a completely convective structure and then slowly evolves almost vertically downward on the HR diagram along a track known as " Hayashi track'. When the luminosity decreases sufficiently the star develops a radiative core and turns left to follow the 'Henyey track'. Subsequent calculations carried out by a number of authors (e.g. Hayashi and Hoshi, 1961; Hayashi and Nakano, 1963; Iben, 1965; Bodenheimer, 1965 and Ezer and cameron, 1967) are in general agreement with the results obtained by Hayashi. Calculations of evolution during the quasistatic contraction as outlined above are also found to be generally consistent with the observation. It is now generally accepted that a pre-main-sequence star, in its quasistatic equilibrium, has two distinct phases - a convective phase and a radiative phase. Following the work of Henyey, LeLevier and Levee (1955), and Hayashi (1961), the basic structure of the pre-main-sequence star is thus well understood. At low temperatures, below about 3500 K, the dominant contribution to the opacity of the stellar atmosphere comes from negligible hydrogen ions. This leads to the existence of a deep convective zone and the star behaves very similar to a polytrope of index 3/2. As the density increases a Kramers type opacity becomes

operative and the star then evolves similar to a polytrope with index 3. Detailed calculations by Faulkner, Griffiths and Hoyle (1963) and Ezer and Cameron (1963) obtained very good agreement with the simpler homogeneous polytropic models. In recent years some significant works have been done on PMS evolution. In modern theory the evolution of a star from its early proto-stellar phase to the zero age main sequence is predominantly governed by accretion and deuterium burning together with gravitational contraction. There is also the concept of a so called 'birthline' (Stahler 1983) where the subsolar mass stars first appear as visible objects. Although the theories differ in details the over all shape of the standard evolutionary tracks constructed by the modern theory (e.g. D'Antona & Mazzitelli 1994, Swenson et al 1994, Palla & Stahler 1993) do not look significantly different from Hayashi - Henyey tracks. In our calculation we follow the Hayashi - Henyey method. For simplicity, instead of interpolating mass by using standard tracks we use the approximate polytropic method based on Hayashi - Henyey picture.

Hayashi track:

Consider a star of low effective temperature and low density. For cool stars of large radii the opacity will be generated by negligible hydrogen ions. A convenient power law fit for the opacity is given by

$$\kappa = \kappa_0 P^{\frac{1}{2}} T^4 \tag{124}$$

where κ_0 is a constant whose value is about $10^{-16.72}$.

Now $$ds = -\kappa \rho \, dr \tag{125}$$

$$T^4 = \frac{3}{4} T_{eff}^4 \left(s + \frac{2}{3} \right) \tag{126}$$

where s is the optical depth, κ is the opacity, and T is the temperature at any point in the stellar atmosphere.

For the atmosphere we have

$$\frac{1}{\rho} \frac{dP}{dr} = -\frac{GM}{R^2} \tag{127}$$

From equations (125) and (127) we get

$$\frac{dP}{ds} = \frac{GM}{\kappa R^2} \tag{128}$$

Then by equation (126) we have

$$P^{\frac{1}{2}} \frac{dP}{ds} = \frac{4GM}{3R^2 \kappa_0 T_{eff}^4 \left(s + \frac{2}{3} \right)} \tag{129}$$

Integrating this with the boundary condition that $P = 0$ at $s = 0$ we have

$$P^{\frac{3}{2}} = \frac{2GM}{\kappa_0 R^2 T_{eff}^4} \ln\left(\frac{3}{2} s + 1 \right) \tag{130}$$

The Schwarzschild (1958) condition for convection is

$$\frac{T}{P} \frac{dP}{dT} < \frac{\gamma}{\gamma - 1},$$

which for $\gamma = \frac{5}{3}$ gives, $\frac{T}{P}\frac{dP}{dT} < \frac{5}{2}$

Substituting (126), (128), and (130) we find that convection occurs if

$$\ln\left(\frac{3}{2}s+1\right) \geq \frac{16}{15}$$

i.e., for $s \geq 1.267$.

This is a reasonable for s to define the stellar surface. So we conclude that the star is fully convective.

For a convective star

$$P \sim T^{5/2}$$

$$\frac{P}{P_c} = \left(\frac{T}{T_c}\right)^{5/2} \tag{131}$$

where P_c and T_c are central pressure and temperature. Substituting for P_c and T_c from equations (62) and (64) we have throughout the convective layer

$$P = \frac{b_n}{(c_n)^{5/2}} \frac{T^{5/2}}{M^{1/2} R^{3/2}}$$

But at the boundary $s = 1.267$ between the star and the atmosphere P is continuous, hence

$$\frac{b_n}{(c_n)^{\frac{5}{2}}}\left(\frac{T^{\frac{5}{2}}}{M^{\frac{1}{2}}R^{\frac{3}{2}}}\right)_{s=1.267} = \left[\frac{2GM}{\kappa_0 R^2 T_{eff}^4}\ln\left(\frac{3}{2}s+1\right)\right]^{\frac{2}{3}}_{s=1.267}$$

This gives $$T_{eff} = \frac{c_n^{\frac{15}{16}}}{b_n^{\frac{6}{31}}}\left(\frac{2.13G}{\kappa_0}\right)^{\frac{4}{31}} M^{\frac{7}{31}} R^{\frac{1}{31}}$$

Using the black body relationship we finally have

$$L = 4\pi R^2 \sigma T_{eff}^4 = cM^{\frac{28}{31}} R^{\frac{66}{31}} = cM^{0.9} R^{2.19} \qquad (132)$$

where $$c = 4\pi\sigma\left[\frac{c_n^{1.94}}{b_n^{0.77}}\left(\frac{2.13G}{\kappa_0}\right)^{0.52}\right]$$

Therefore $$T_{eff} \propto M^{\frac{7}{31}} R^{\frac{1}{31}}$$

and

$$L \propto M^{\frac{28}{31}} R^{\frac{66}{31}}$$

Eliminating R we have

$$L \propto M^{-\frac{434}{31}} T_{eff}^{66}$$

Therefore, for constant mass,

$$\log L = 66 \log T_{eff} + constant \qquad (133)$$

Henyey track:

If a polytropic model of star is assumed, then from equations (62) and (64) we have, on dimensional grounds

$$P \sim \frac{GM^2}{R^4}, \qquad \rho \sim \frac{M}{R^3}, \quad \text{and} \quad T \sim \frac{GM}{R} \tag{134}$$

From $L_r = -4\pi r^2 \frac{4ac}{3} \frac{T^3}{\kappa \rho} \frac{dT}{dr}$ we have

$$L \sim \frac{16\pi ac}{3\kappa} R^2 \left(\frac{GM}{R}\right)^4 \frac{R^3}{M} \frac{1}{R}$$

$$= \frac{16\pi ac}{3\kappa} M^3$$

i.e., $$L \propto \frac{M^3}{\kappa} \tag{135}$$

If we use the numerical calculation of Henyey et al. with detailed opacity table, we have (Huang 1961) .

$$L \propto M^{5.4} R^{-0.79} \tag{136}$$

Now from black body relationship we have

$$R^2 = \frac{L}{4\pi\sigma T_{eff}^4} \tag{137}$$

Hence eliminating R from (136) and (137) we get

$$L \propto M^{5.4} \left(\frac{T_{eff}^2}{L^{0.5}} \right)^{0.79}$$

or, $$L \propto M^{3.87} T_{eff}^{1.133}$$

Therefore, for constant M,

$$\log L = 1.133 \log T_{eff} + constant \tag{138}$$

This relation gives the path in the ($logL$, $logT_{eff}$) diagram along which a radiative star moves as it decreases its radius. Equation (133) and (138) together give the constant mass lines for contracting stars. Schematic representation of the evolutionary track for a given mass, following the Hayashi and Henyey is shown in figure 2. Similarly, for a group of contracting stars the constant time lines, the isochrones, can easily be found to be given by

$$\log L = 1.44 \log T_{eff} - 1.02 \log t + constant \tag{139}$$

Now that we have L-M-R relationships for both convective and radiative contracting stars we can summarise to see that the evolution of a PMS star, assuming that the only source of energy is gravitational, is governed by the following equations:

$$£ = 4\pi\sigma\Re^2 T_{eff}^4 \tag{140}$$

$$£ = c m^{0.9} \Re^{2.13} \quad \text{(convective)} \tag{141}$$

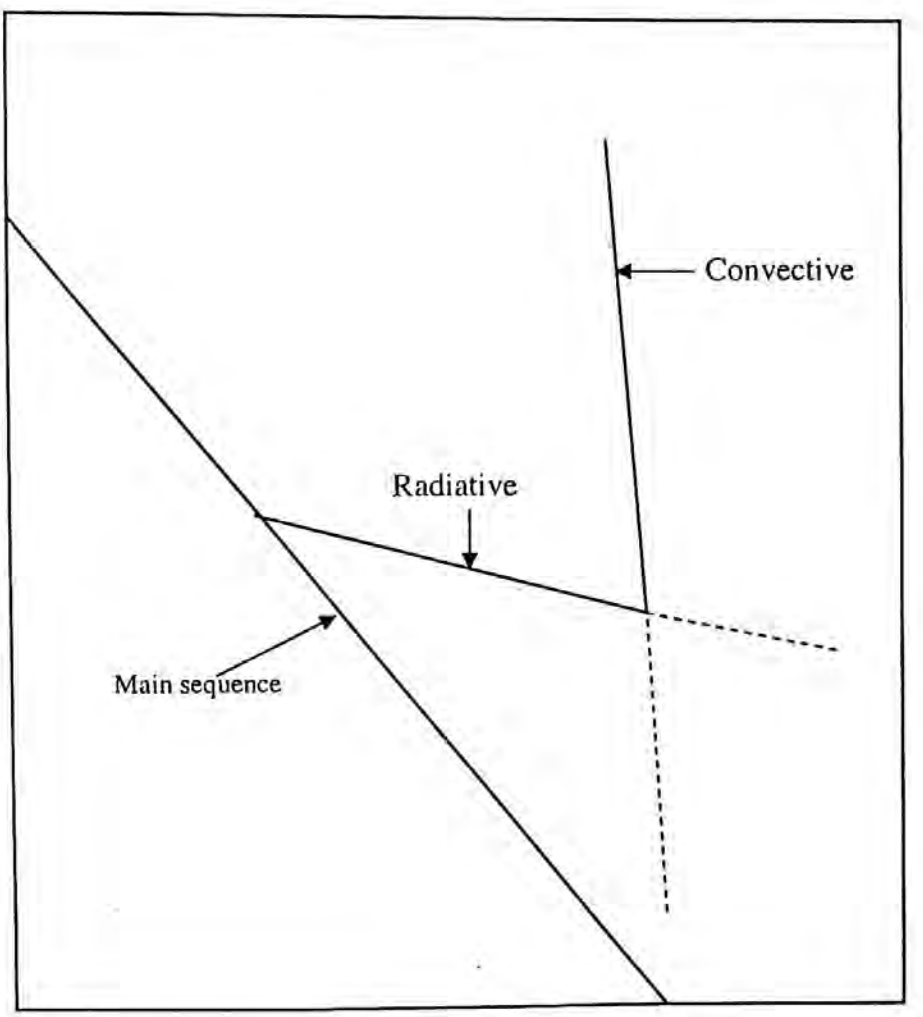

Figure 2: A Schematic representation of the evolutionary track in the HR diagram.

$$£ \propto m^{5.4}\Re^{-0.79} \qquad \text{(radiative)} \qquad (142)$$

$$£\,dt = -dE = \frac{2}{7}\left(\frac{3\gamma-4}{\gamma-1}\right)d\left(\frac{Gm^2}{\Re}\right) \qquad \text{(convective)} \qquad (143)$$

$$£\,dt = -dE = \frac{1}{2}\left(\frac{3\gamma-4}{\gamma-1}\right)d\left(\frac{Gm^2}{\Re}\right) \qquad \text{(radiative)} \qquad (144)$$

where the variables have now been expressed in italics.

iv. References

Adams F. C., 1998, ASP Conference series, Vol. 148

Basu S. and Mouschovias T. Ch., 1994, ApJ, 432, 720

Bate M. R., 1998, ApJ., 508 L95

Binney J. and Tremaine S., 1987, Galactic Dynamics (Princeton: Princeton Univ. Press)

Blitz L. and Williams J. P., 1999, The Origin of Stars and Planetary Systems ed C J Lada and N D Kylafis (Dordrecht: Kluwer) pp 3 28

Bodenheimer P., 1965, ApJ, 142, 451

Bonnell I. A., Bate M. R. and Vine S. G., 2003, MNRAS, 343, 413-418

Brown A.G.A., de Geus E.J., and de Zeeuw P.T., 1995, AA 289, 101

Brownlee R. R. and Cox A. N., 1961, Sky and Telescope, 32, 252

D'Antona F. and Mazzitelli I., 1994, ApJS, 90, 467

Ezer D. and Cameron A. G. W., 1963, Icarus, 1, 422

Ezer D. and Cameron A. G. W., 1967, Can.J.Phys., 45, 3429

Faulkner J. Griffiths K. and Hoyle F., 1963, MNRAS, 126, 1

Genzel R., and Stutzki J., 1989, ARAA, 27, 41

Hartmann L., 2003, ApJ. 585 398-405

Hayashi C., 1961, PASJ, 13, 450

Hayashi C., and Hoshi R., 1961, PASJ, 13, 442

Hayashi C., and Nakano T., 1963, Prog.Theo.Phys.Japan, 30, 470

Henyey L. G., Lelevier R and Levee R. D., 1955, PASP, 67,154

Herbig G. H., 1962, Advances in Astronomy and Astrophysics 1 47-103

Hillenbrand L. A., 1997, AJ, 113, 1733

Hollenbach D. J., Werner M. W., and Salpeter E. E., 1971, ApJ, 163, 165

Huang S. S., 1961, ApJ, 134, 12

Iben I. Jr., 1965, Ap.J, 142,1447

Jeans J. H., 1929, Astronomy and Cosmogony (Cambridge: Cambridge Univ. Press; reprinted by Dover, New York, 1961)

Lada C. J. and Lada E. A., 2003, ARA&A, 41, 57

Lai D., 2000, ApJ. 540 946-961

Larson R. B., 1979, MNRAS, 186 479-490

Larson R. B., 2001, The Formation of Binary Stars (IAU Symp. 200) ed H Zinnecker and R D Mathieu(San Francisco: Astron. Soc. Pacific) pp 93-106

Larson R. B., 2003, Rep. Prog. Phys., 66, 1651-1697

Mac Low M-M and Klessen R S 2004 Rev. Mod. Phys. 76 125-194

Matsumoto T., Hanawa T., and Nakamura F., 1997, ApJ. 478 569-584

McCrea W. H. and Williams I. P., 1962, Observatory, 82, 247

McKee C. F., Zweibel E. G., Goodman A. A. and Heiles C., 1993, Protostars and Planets III ed E H Levy and J I Lunine (Tucson: Univ. of Arizona Press) pp 327-366

Nakano T., 1984, Fundam. Cosmic Phys., 9 139-231

O'Dell C. R., and Wong S. K., 1996, AJ, 111, 846

Palla F. and Stahler S. W., 1993, ApJ, 418, 414

Schmeja S. and Klessen R. S., 2004, A&A, 419, 405

Schwarzschild, M., 1958, Structure and Evolution of Stars, Chicago Univ. Press, Dover.

Shu F. H., Adams F. C., and Lizano S., 1987, Ann. Rev. Astron. Astrophys. 25 23-81

Sigalotti L. Di G and Klapp J, 2001, Intl. J. Mod. Phys. D 10 115-211

Stahler S. W., 1983, ApJ., 274, 822-829

Swenson F. J., Faulkner J., Rogers F. J., and Iglesias C. A., 1994, ApJ, 425, 286

Whitworth A. P., Bhattal A. S., Francis N. and Watkins S. J., 1996, MNRAS, 283, 1061-1070

Chapter 2. The Young Clusters NGC 2264, NGC 1976, and the Orion Nebula Cluster

i. Introduction of the Clusters

Young open clusters provide information relating to star formation process and stellar evolution history (Herbst and Miller 1982; Adams et al. 1993; Sung et al. 1997). In this section we investigate three young clusters, NGC 2264, NGC 1976, and the Orion Nebula cluster. By analysing the observational data we intend to gather some information about cluster properties.

NGC 2264 is a well known young open cluster situated in the Orion arm. The location of the cluster is at α (right ascension) = $06^h\ 40^m\ 58^s$, δ (declination) = $+09^o\ 53'\ 42''$(2000). This cluster has been continually studied by various authors over a long period of time. Walker (1956) studied three colour photoelectric and photographic observations to investigate the colour-magnitude diagram of an extremely young cluster of stars. Relative proper motions of 245 stars in the cluster region were determined by Vasilevskis et al. (1965) with a probable error of ± 0.001 arcsec yr^{-1} and the probability of cluster membership for individual stars has also been derived. Out of these 245 stars, only 140 stars have p$\geq$ 50 per cent. According to Sanders (1976) most of the field stars would have been separated if one assumes p $\geq$ 50 per cent as a selection criterion. Mendoza and Gomez (1980) have carried out UBVRI photometry for 70 stars in the cluster field. Adams et al. (1983) performed UBVRI H_α photographic photometry and video camera observations for NGC 2264 using the criteria for PMS member selection could not separate H_α emission/non emission stars clearly. Kwon and Lee (1983), Sagar and Joshi (1983), Shulov et al. (1983), Perez et al. (1987) also

vastly studied the cluster NGC 2264. Sung et al. (1997) has been obtained UBVRI H_α CCD photometry for the young cluster NGC 2264. By constructing the HR diagram they determined the typical age and age spread of NGC 2264 and discussed the age discrepancy between turn-off age and turn-on age of the cluster. Park et al. (2000) has been obtained the UBVRI and H_α CCD photometry of NGC 2264 in the southern region around the Cone Nebula. UBV data for the cluster are available in obswww.unige.ch/webda. The parameters of the cluster are reddening (mag) = 0.051, distance modulus (mag) = $9^m.28$, age ~ 5 Myr.

NGC 1976 is located at a distance of about 1500 light-years towards the Northwestern and of the Orion A cloud. It is the main part of a large cloud of gas and dust which extends over 10 degrees well over half the constellation Orion. The parameters of NGC 1976 as found in obswww.unige.ch/webda are α (right ascension) = 5 32.9, δ (declination) = -5 25 (1950), distance (pc) = 399, reddening (mag) = 0.05, distance modulus (mag) = 8.16, log age = 7.11. UBV photometry of many authors (e.g., Johnson (1957), Walker (1969), Penston et al. (1975), McNamara (1976), Warren et al. (1977), Bastian et al. (1979), Shulov et al. (1983), Menzies et al. (1990), Penprase (1992), Frasca et al. (2003) etc.) are available in "all available UBV data" in the database of the said website. In our study we are concerned with only V and B-V data with uniform reddening of amount $E_{B-V} = 0.05$ and the estimated distance modulus of $8^m.16$.

The Orion Nebula cluster is extremely young and nearest, the distance being ~ 500 pc. It is projected against a dark cloud extending roughly from $\alpha = 5^h 28^m$ to $\alpha = 5^h 33^m$ and $\delta = -4^\circ 25'$ to $\delta = -6^\circ 30'$. Optical photometry for the cluster is available among others from (1) the CCD surveys of Prosser et al. (1994), Herbig and Terndrup (1986), (2) the photoelectric surveys of Duncan (1993), Van Altena et al. (1988), Rydgren and Vrba (1984), Cohen and Kuhi (1979), Walker (1969), and (3) the photographic surveys of Jones and Walker (1988), Andrews (1981), Parenago (1954). This cluster has been investigate in detail by Hillenbrand

(1997) using *VRI* data and D'Antona and Mazzitelli (1994) tracks. In our calculation we have taken (*V,B-V*) data from Walker (1969) and used polytropic method. The parameters of the cluster as in Walker (1969) are reddening (E_{B-V}) = 0.06 and distance modulus (*D.M.*) = $8^m.37$.

ii. Conversion of observational data to theoretical quantities

We have not carried out any observation of our own. We have used published data from recent observation of three young clusters, namely, NGC 2264, NGC 1976 and the Orion Nebula cluster. All these clusters are very young and nearest and hence suited for observational studies. We have taken data for all clusters in three colour photometry units *U*, *B*, and *V*. For NGC 2264 and NGC 1976 data have been taken from obswww.unige.ch/webda, and for the Orion Nebula cluster we have taken UBV data from Walker (1969). In the web we have found that some of the star have multiple measures. In that case we have used the average measure of the data. Uniform reddening of amounts E_{B-V} =0.051, E_{B-V}=0.05, and E_{B-V} =0.06 have been estimated for the clusters NGC 2264, NGC 1976, and the Orion Nebula cluster respectively, while the respective distance modulii have been given by $9^M.28$, $8^M.16$, and $9^M.37$.

In the study of clusters, we mainly measure photometry of the stars. In our calculations we have use three colour photometry units *U*, *B* and *V*. In the *UBV* system of photometry an object is observed through filters that allow light of only certain wave length to be transmitted. The wavelengths of light transmitted by *U*-filters are short and in the ultraviolet while the *B* and *V* filters admit the transmission of light at the blue and visual wavelength respectively. As all our calculations are in terms of $logL$ and $logT_{eff}$, it is necessary to convert the practical measurements *V* and *B-V* into theoretical quantities $log£$ and $logT_{eff}$. This can easily be done following standard method.

From apparent visual magnitude of stars, bolometric magnitude M_{bol}, are obtained by applying bolometric correction *B.C.*

$$M_{bol} = V + B.C. - D.M. \qquad (145)$$

where *D.M.* is the distance modulus for the clusters, *B.C.* is the bolometric correction.

The *B.C.* depends on the surface temperature of the star. It is not obtained by direct observation. At very low and high temperatures the *B.C.* is quite large and to some extent uncertain. However for intermediate temperature T_{eff} : *B.C.* scale is fairly accurately known.

Transformation of M_{bol} to bolometric luminosity can conveniently be done by referring to solar data to give

$$\log\left(\frac{£}{L_\Theta}\right) = \frac{1}{2.5}\left(4.75 - M_{bol}\right) \qquad (146)$$

where 4.75 is the bolometric magnitude of the sun. Combining equations (145) and (147) gives

$$\log\left(\frac{£}{L_\Theta}\right) = 1.9 - 0.4\left(V + B.C. - D.M.\right) \qquad (148)$$

It is of primary importance, therefore, to use accurate empirical scales of bolometric corrections, colours, and effective temperatures to convert the theoretically derived parameters from observational parameters. The conversion of *B-V* into $logT_{eff}$ is one full of appreciable uncertainties as there exists, no complete $logT_{eff}$: *B-V: B.C.* scale which is universally accepted. Most of the improvements and additions in the last decade to Flower's (1977) scales rely on new temperature measurements of early-type stars (e.g., Humphreys & McElroy

1984; Malagnini et al. 1986; Massey, Parker, & Garmany 1989; Fitzpatrick & Garmany 1990; Chlebowski & Garmany 1991; Napiwotzki, Schonberner, & Wenske 1993); some additions have been made to the cool end as well (Habets & Heintze 1981; Humphreys & McElroy 1984). However, we adopt $logT_{eff}$: *B-V* : *B.C.* scale of Flower (1996), as in table 3. Because it is most recent and it covers a wide range of temperature.

Table 3 : B-V:logTeff:BC scale, Flowers (1996)

B-V	logTeff	B.C.		B-V	logTeff	B.C.		B-V	logTeff	B.C.
-0.35	4.7538	-4.720		0.37	3.8368	0.026		1.09	3.6699	-0.482
-0.34	4.7031	-4.506		0.38	3.8338	0.025		1.10	3.6682	-0.494
-0.33	4.6551	-4.197		0.39	3.8307	0.022		1.11	3.6666	-0.505
-0.32	4.6098	-3.861		0.40	3.8277	0.020		1.12	3.6649	-0.517
-0.31	4.5670	-3.534		0.41	3.8247	0.018		1.13	3.6633	-0.528
-0.30	4.5266	-3.234		0.42	3.8217	0.015		1.14	3.6616	-0.540
-0.29	4.4884	-2.966		0.43	3.8187	0.012		1.15	3.6599	-0.552
-0.28	4.4523	-2.73		0.44	3.8157	0.009		1.16	3.6583	-0.564
-0.27	4.4183	-2.523		0.45	3.8127	0.006		1.17	3.6566	-0.576
-0.26	4.3863	-2.341		0.46	3.8098	0.003		1.18	3.6550	-0.588
-0.25	4.3561	-2.177		0.47	3.8068	-0.001		1.19	3.6533	-0.601
-0.24	4.3276	-2.028		0.48	3.8039	-0.004		1.20	3.6516	-0.614
-0.23	4.3008	-1.891		0.49	3.8010	-0.008		1.21	3.6500	-0.626
-0.22	4.2755	-1.762		0.50	3.7981	-0.012		1.22	3.6483	-0.640
-0.21	4.2517	-1.641		0.51	3.7952	-0.016		1.23	3.6467	-0.652
-0.20	4.2294	-1.525		0.52	3.7923	-0.021		1.24	3.6450	-0.666
-0.19	4.2083	-1.414		0.53	3.7895	-0.025		1.25	3.6434	-0.679
-0.18	4.1885	-1.307		0.54	3.7866	-0.030		1.26	3.6417	-0.694
-0.17	4.1699	-1.205		0.55	3.7838	-0.035		1.27	3.6401	-0.707
-0.16	4.1524	-1.107		0.56	3.7811	-0.039		1.28	3.6384	-0.722
-0.15	4.1360	-1.013		0.57	3.7783	-0.045		1.29	3.6368	-0.736
-0.14	4.1205	-0.923		0.58	3.7756	-0.050		1.30	3.6351	-0.752
-0.13	4.1060	-0.839		0.59	3.7729	-0.055		1.31	3.6335	-0.766
-0.12	4.0923	-0.759		0.60	3.7702	-0.061		1.32	3.6318	-0.782
-0.11	4.0795	-0.684		0.61	3.7676	-0.067		1.33	3.6301	-0.798
-0.10	4.0674	-0.614		0.62	3.7649	-0.073		1.34	3.6285	-0.814
-0.09	4.0560	-0.549		0.63	3.7623	-0.079		1.35	3.6268	-0.831
-0.08	4.0453	-0.488		0.64	3.7598	-0.085		1.36	3.6251	-0.848
-0.07	4.0353	-0.432		0.65	3.7572	-0.091		1.37	3.6235	-0.865
-0.06	4.0258	-0.381		0.66	3.7547	-0.098		1.38	3.6218	-0.883
-0.05	4.0169	-0.334		0.67	3.7523	-0.104		1.39	3.6201	-0.901

B-V	logTeff	B.C.	B-V	logTeff	B.C.	B-V	logTeff	B.C.
-0.04	4.0084	-0.290	0.68	3.7498	-0.111	1.40	3.6184	-0.920
-0.03	4.0005	-0.252	0.69	3.7474	-0.117	1.41	3.6167	-0.939
-0.02	3.9930	-0.216	0.70	3.7450	-0.124	1.42	3.6149	-0.960
-0.01	3.9859	-0.184	0.71	3.7426	-0.132	1.43	3.6132	-0.980
0.00	3.9791	-0.155	0.72	3.7403	-0.139	1.44	3.6114	-1.002
0.01	3.9728	-0.129	0.73	3.7380	-0.146	1.45	3.6096	-1.024
0.02	3.9667	-0.106	0.74	3.7358	-0.153	1.46	3.6078	-1.047
0.03	3.9609	-0.085	0.75	3.7335	-0.161	1.47	3.6060	-1.071
0.04	3.9555	-0.067	0.76	3.7313	-0.168	1.48	3.6041	-1.096
0.05	3.9502	-0.050	0.77	3.7291	-0.176	1.49	3.6022	-1.122
0.06	3.9452	-0.036	0.78	3.7270	-0.184	1.50	3.6002	-1.150
0.07	3.9404	-0.024	0.79	3.7249	-0.192	1.51	3.5982	-1.178
0.08	3.9358	-0.013	0.80	3.7228	-0.200	1.52	3.5961	-1.209
0.09	3.9314	-0.004	0.81	3.7207	-0.208	1.53	3.5940	-1.241
0.10	3.9271	0.004	0.82	3.7186	-0.216	1.54	3.5918	-1.276
0.11	3.9229	0.010	0.83	3.7166	-0.225	1.55	3.5895	-1.312
0.12	3.9189	0.015	0.84	3.7146	-0.233	1.56	3.5872	-1.350
0.13	3.915	0.019	0.85	3.7126	-0.242	1.57	3.5847	-1.393
0.14	3.9113	0.022	0.86	3.7107	-0.250	1.58	3.5822	-1.437
0.15	3.9076	0.024	0.87	3.7088	-0.259	1.59	3.5795	-1.486
0.16	3.9040	0.026	0.88	3.7068	-0.268	1.60	3.5767	-1.539
0.17	3.9004	0.028	0.89	3.7049	-0.277	1.61	3.5738	-1.595
0.18	3.8969	0.029	0.90	3.7031	-0.285	1.62	3.5707	-1.658
0.19	3.8935	0.031	0.91	3.7012	-0.295	1.63	3.5674	-1.728
0.20	3.8902	0.032	0.92	3.6994	-0.304	1.64	3.5640	-1.802
0.21	3.8869	0.033	0.93	3.6976	-0.313	1.65	3.5604	-1.885
0.22	3.8836	0.033	0.94	3.6958	-0.322	1.66	3.5565	-1.978
0.23	3.8804	0.034	0.95	3.6940	-0.332	1.67	3.5525	-2.078
0.24	3.8771	0.034	0.96	3.6922	-0.342	1.68	3.5482	-2.191
0.25	3.8740	0.035	0.97	3.6904	-0.352	1.69	3.5436	-2.318
0.26	3.8708	0.035	0.98	3.6887	-0.361	1.70	3.5387	-2.460
0.27	3.8676	0.035	0.99	3.6869	-0.372	1.71	3.5335	-2.620
0.28	3.8645	0.035	1.00	3.6852	-0.382	1.72	3.5279	-2.803
0.29	3.8614	0.035	1.01	3.6835	-0.392	1.73	3.5220	-3.007
0.30	3.8583	0.034	1.02	3.6818	-0.403	1.74	3.5157	-3.239
0.31	3.8552	0.034	1.03	3.6800	-0.414	1.75	3.5090	-3.502
0.32	3.8521	0.033	1.04	3.6783	-0.426	1.76	3.5018	-3.805
0.33	3.8490	0.032	1.05	3.6766	-0.437	1.77	3.4941	-4.152
0.34	3.8460	0.031	1.06	3.6750	-0.448	1.78	3.4860	-4.544
0.35	3.8429	0.030	1.07	3.6733	-0.459	1.79	3.4772	-5.004
0.36	3.8399	0.028	1.08	3.6716	-0.471	1.80	3.4678	-5.535

iii. Masses and ages of stars in the cluster

Masses and ages of stars in a cluster are usually determined by interpolating from the standard mass lines and time lines. This is a tedious job. We attempt to determine the values of the parameters algebraically by solving two sets of simultaneous equations satisfied by PMS stars.

It is found convenient to express £, m, $\Re$, and T_{eff} in solar units such that £ = $LL_{\odot}$, m= $MM_{\odot}$, $\Re = RR_{\odot}$. $T_{eff} = TT_{\odot}$ and t in units of t_s such that $t = \tau t_s$

where

$$t_s = \frac{2}{7}\left(\frac{3\gamma-4}{\gamma-1}\right)\frac{GM_{sun}^2}{L_{sun}R_{sun}}$$

Doing this equations (140)- (144) reduces to the following nondimensioal forms

$$L = R^2 T^4 \tag{149}$$

$$L = 0.134 M^{0.9} R^{2.13} \quad \text{(convective)} \tag{150}$$

$$L = M^{5.4} R^{-0.79} \quad \text{(radiative)} \tag{151}$$

$$L\,d\tau = -\frac{M^2}{R^2}\,dR \quad \text{(convective)} \tag{152}$$

$$L\,d\tau = -1.75\frac{M^2}{R^2}\,dR \quad \text{(radiative)} \tag{153}$$

From equation (150) we have

$$R = 2.57\left(\frac{L^{0.47}}{M^{0.42}}\right) \tag{154}$$

and hence $$\frac{dR}{d\tau} = 1.2\left(\frac{L^{-0.53}}{M^{0.42}}\right)\frac{dL}{d\tau} \tag{155}$$

Substituting from equations (154) and (155) into equation (152) and simplifying we obtain

$$L^{-2.47}\, dL = -5.5\, M^{-2.42}\, d\tau$$

which integrates to

$$L = \left(8.08\, M^{-2.42}\, \tau + L_0^{-1.47}\right)^{-0.67} \tag{156}$$

where L_0 refers to the initial value of L.

Again from equations (149) and (154) we have

$$T^4 = 0.16\, M^{0.84}\, L^{0.06}$$

Hence $$T_{eff} = 0.63\, M^{0.21}\, L^{0.01}\, T_{esun} \tag{157}$$

From equations (156) and (157) we thus have logarithmic measures of the luminosity and effective temperature of a convective star of mass M as

$$\log L = -0.68 \log\left(8.08\, M^{-2.42}\, \tau + L_0^{-1.47}\right) \tag{158}$$

$$\log T_{eff} = 0.21 \log M + 0.015 \log L + 3.56 \quad (159)$$

where we have used $T_{esun} = 5780K$.

Again from equation (151) we have

$$R = \left(\frac{M^{6.84}}{L^{1.265}} \right) \quad (160)$$

hence $$\frac{dR}{d\tau} = -1.265 L^{-2.265} M^{6.84} \frac{dL}{d\tau} \quad (161)$$

Substituting R and $\frac{dR}{d\tau}$ in equation (153) we have

$$L^{0.735} dL = \frac{1}{2.2155} M^{4.83} d\tau \quad (162)$$

Which integrates to

$$L = \left(0.12 M^{4.84} \tau + L_0^{0.265}\right)^{3.76} \quad (163)$$

Again from equations (149) and (160) we have

$$L = M^{3.86} T_{eff}^{1.13} T_{esun}^{-1.13} \quad (164)$$

From equations (163) and (164) we thus have logarithmic measures of the luminosity and effective temperature of a radiative star of mass M as

$$\log L = 3.76 \log\left(0.12 M^{4.84} \tau + L_0^{0.265}\right) \quad (165)$$

$$\log T_{eff} = 0.885(\log L - 3.86 \log M + 4.25) \qquad (166)$$

Between the convective and radiative phase there is an intermediate regime. If we assume instantaneous change from one phase to the other, then at the transition point we must have

$$L_{convective} = L_{radiative}$$

Eliminating R from equation (150) and (151) we have, at the transition point,

$$L = 0.54M^{4.18} \qquad (167)$$

This gives the initial radius for the radiative stars. Eliminating M in terms of $logT_{eff}$ and using appropriate boundary condition we find from equation (167),

$$\log L = 15.21 \log T_{eff} - 54.29 \qquad (168)$$

This is a line in the HR diagram which separates the convective and radiative stars. Now, if $logL$ and $logT_{eff}$ are known for the stars, then the masses and ages can easily be determined by solving the two sets of equation, namely (158)-(159) and (165)-(166), depending on whether the stars are convective and radiative.

Following Flower (1996) we have converted the (V, B-V) data for the three clusters into theoretical quantities of $logL$ and $logT_{eff}$ and then drawing the line (168) on the theoretical HR diagram we have separated the convective and radiative stars. The resulting HR diagram with the line for NGC 2264 is shown in figure 3. Since the other diagrams look similar they have not been included. It is found that for NGC 2264 stars numbered 13, 37, 69, 146, 229, 237, 238, 239, 332, 528, 536 are convective while for the other two clusters the convective stars are

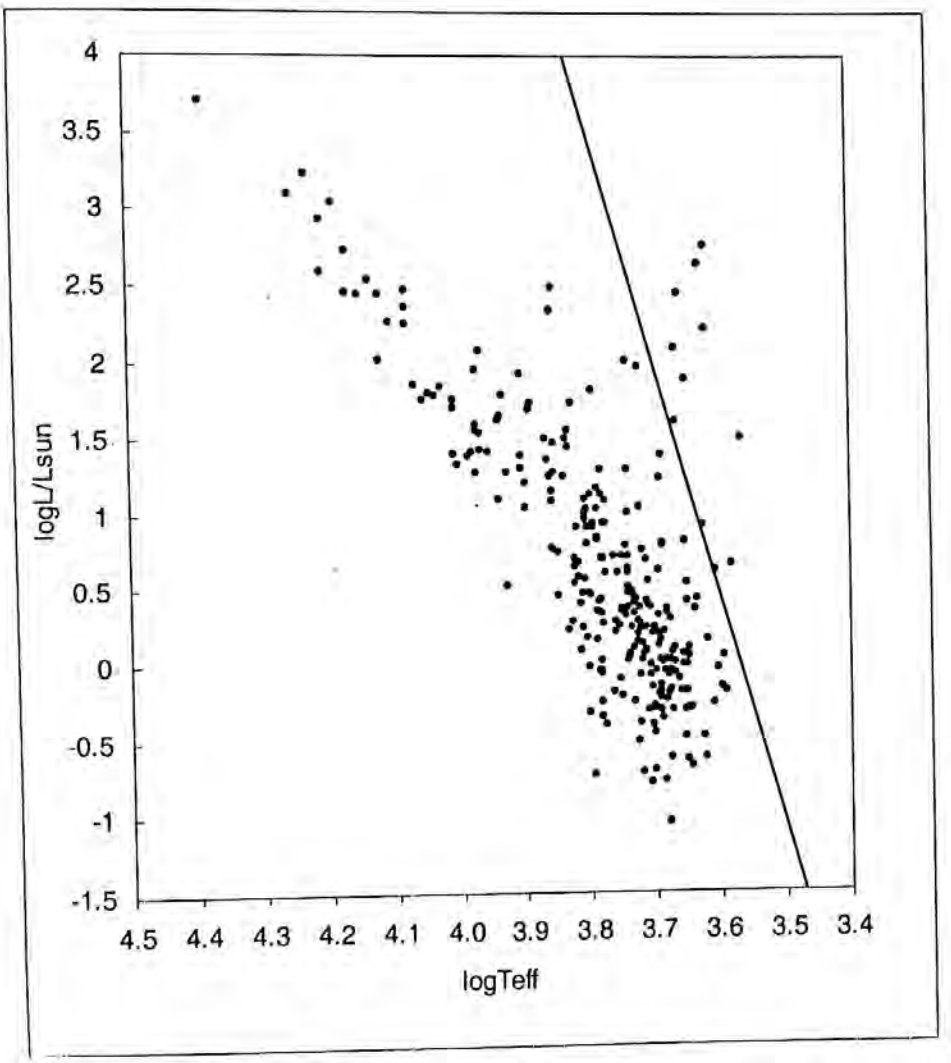

Figure 3: HR diagram of NGC 2264 with a line of separation of convective and radiative star

identified as stars numbered 748, 857, 866, 895, 1049, 1072, 1267, 1315, 1326, 1328, 1421, 1472, 1519, 1563, 1658, 1724, 2029, 2448, 2455, 2479, 2670, 2773 for NGC 1976, and 1036, 1049, 1267, 1315, 1328, 1342, 1472, 1724, 2160, 2478 for the Orion Nebula cluster. The others are radiative stars. Stars falling on the line of separation can be treated as falling on either side. Once the convective or radiative natures of the stars known it become easy to determine the masses and

ages of the stars from equations (158)-(159) and (165)-(166). With values of $logL$ and $logT_{eff}$ as obtained by the conversion of observational data for all three clusters we have solved the equations to find $logM$ and $log\tau$. The results of all our calculation, for all the three clusters, are given in table 4, table 5, and table 6.

Stars in

Table 4 : Masses and ages of the cluster NGC 2264 (Solar Unit)

Star No.	$\log L/L_\odot$	LogTeff	Mass $M/M_\odot$	Age	Star No.	$\log L/L_\odot$	LogTeff	Mass $M/M_\odot$	Age
1	-0.009	3.707	1.032	0.704	175	-0.497	3.625	0.815	1.068
2	1.715	3.890	2.550	0.037	176	-0.194	3.592	0.999	0.200
3	0.148	3.618	1.203	0.112	177	1.988	3.740	3.319	0.003
4	0.218	3.834	1.085	1.102	178	3.696	4.386	5.952	0.005
5	-0.029	3.801	0.957	1.630	179	1.748	4.008	2.402	0.076
6	2.318	3.858	3.734	0.006	180	0.463	3.810	1.276	0.499
7	3.027	4.189	4.561	0.009	181	1.787	4.045	2.398	0.085
8	0.414	3.650	1.380	0.091	182	1.544	3.973	2.178	0.101
10	1.121	3.798	1.904	0.081	184	0.018	3.719	1.041	0.734
11	-0.718	3.719	0.671	5.079	186	-0.165	3.598	1.012	0.215
12	-0.304	3.643	0.903	0.778	187	2.252	4.106	3.037	0.039
13	1.487	3.567	0.849	0.001	189	1.088	3.807	1.856	0.096
14	-0.252	3.734	0.877	1.713	190	0.698	3.778	1.499	0.209
15	-0.014	3.657	1.064	0.395	192	0.090	3.813	1.019	1.314
16	-0.710	3.701	0.682	4.316	193	1.680	3.894	2.491	0.042
17	0.451	3.849	1.234	0.681	194	0.416	3.787	1.260	0.469
18	-0.388	3.723	0.814	2.235	195	0.556	3.807	1.351	0.383
19	-0.518	3.727	0.751	3.247	196	1.030	3.804	1.796	0.109
20	1.490	3.837	2.311	0.043	197	-0.793	3.707	0.646	5.609
21	0.046	3.738	1.044	0.815	199	-0.235	3.692	0.911	1.124
22	-1.046	3.680	0.566	8.685	202	2.062	3.967	2.980	0.027
23	0.198	3.727	1.151	0.492	203	0.505	3.743	1.368	0.250
24	2.462	4.080	3.504	0.020	204	-0.193	3.655	0.958	0.655
25	2.470	3.855	4.097	0.004	205	1.350	3.865	2.087	0.078
26	0.895	3.819	1.641	0.176	206	2.529	4.136	3.512	0.023
27	0.798	3.804	1.564	0.201	208	0.629	3.743	1.474	0.179
28	0.694	3.822	1.452	0.302	209	1.074	3.858	1.778	0.151
29	1.538	3.834	2.383	0.037	210	0.332	3.734	1.242	0.364
30	1.382	3.986	1.960	0.163	212	3.222	4.229	4.985	0.007
31	1.494	3.868	2.269	0.055	213	0.193	3.694	1.174	0.351
32	0.472	3.740	1.344	0.267	214	0.431	3.731	1.320	0.273
34	1.237	3.840	1.983	0.086	215	1.944	3.973	2.764	0.038
35	1.526	3.967	2.164	0.101	216	0.992	3.740	1.832	0.063
36	1.325	4.001	1.876	0.204	217	0.216	3.723	1.167	0.449
37	2.740	3.620	1.232	0.000	220	1.725	3.825	2.681	0.021
38	1.381	3.687	2.396	0.006	221	0.743	3.849	1.468	0.327
39	1.090	3.940	1.698	0.253	222	1.641	3.936	2.366	0.062
42	0.368	3.740	1.263	0.354	223	1.238	3.861	1.956	0.102
43	1.386	3.904	2.076	0.095	224	1.018	3.790	1.801	0.099
46	1.918	3.904	2.851	0.025	225	0.346	3.790	1.206	0.575
50	2.918	4.208	4.217	0.013	226	1.770	3.931	2.562	0.044
54	0.097	3.670	1.127	0.342	227	0.906	3.804	1.668	0.151
58	-0.466	3.699	0.789	2.238	228	1.154	3.858	1.865	0.123

Star No.	$\log L/L_\odot$	LogTeff	Mass $M/M_\odot$	Age	Star No.	$\log L/L_\odot$	LogTeff	Mass $M/M_\odot$	Age
59	-0.191	3.660	0.955	0.693	229	2.428	3.662	2.044	0.000
60	0.772	3.689	1.665	0.058	230	0.788	3.689	1.681	0.055
62	0.664	3.816	1.433	0.311	231	2.586	4.208	3.459	0.030
64	-0.413	3.705	0.812	2.043	232	1.828	4.026	2.490	0.069
65	0.934	3.795	1.707	0.130	233	1.798	3.795	2.857	0.012
66	0.716	3.750	1.545	0.151	234	0.642	3.822	1.408	0.345
67	1.280	3.781	2.117	0.045	235	0.227	3.810	1.108	0.909
68	0.936	3.776	1.731	0.108	236	1.084	3.776	1.891	0.072
69	2.626	3.629	1.376	0.000	237	2.196	3.620	1.347	0.000
70	1.166	3.790	1.967	0.067	238	1.874	3.652	2.006	0.001
73	1.956	3.723	3.296	0.002	239	2.082	3.667	2.285	0.001
74	2.714	4.170	3.833	0.018	301	0.604	3.776	1.420	0.261
76	0.021	3.743	1.025	0.908	302	0.358	3.752	1.245	0.407
77	0.006	3.668	1.068	0.437	305	0.137	3.725	1.112	0.568
78	-0.313	3.655	0.891	0.925	306	0.254	3.778	1.150	0.666
79	-0.730	3.795	0.632	9.072	307	0.096	3.734	1.079	0.686
80	-0.039	3.602	1.087	0.147	311	-0.056	3.787	0.951	1.573
81	-0.646	3.650	0.733	2.225	312	0.146	3.790	1.070	0.960
83	3.088	4.257	4.518	0.011	318	0.402	3.813	1.227	0.596
84	0.834	3.790	1.614	0.161	320	1.114	3.784	1.914	0.072
85	-0.210	3.678	0.933	0.905	321	0.162	3.804	1.070	1.028
87	1.294	3.904	1.965	0.120	322	0.418	3.729	1.312	0.276
88	2.431	4.152	3.275	0.032	325	0.544	3.711	1.431	0.158
89	-0.771	3.685	0.664	4.412	326	0.273	3.825	1.127	0.901
90	0.514	3.927	1.215	0.959	332	0.655	3.582	1.145	0.019
91	0.713	3.765	1.527	0.177	335	0.237	3.715	1.189	0.390
92	1.044	3.723	1.913	0.043	336	0.274	3.760	1.179	0.542
93	0.388	3.711	1.304	0.246	355	0.229	3.736	1.166	0.492
94	1.434	3.834	2.240	0.049	364	-0.196	3.762	0.889	1.873
95	-0.629	3.675	0.728	2.748	365	0.058	3.658	1.109	0.327
96	0.149	3.692	1.145	0.389	366	-0.003	3.687	1.049	0.561
98	0.930	3.778	1.722	0.113	370	0.786	3.745	1.615	0.119
99	1.266	3.855	1.998	0.090	389	0.238	3.701	1.200	0.336
100	1.614	3.940	2.321	0.069	390	1.411	3.956	2.035	0.126
103	1.696	4.008	2.328	0.086	395	0.361	3.684	1.307	0.189
104	1.044	3.897	1.702	0.214	396	-0.086	3.678	1.005	0.641
105	-0.367	3.687	0.845	1.524	404	0.473	3.736	1.349	0.255
106	0.342	3.752	1.233	0.425	411	0.681	3.713	1.551	0.109
107	2.354	4.080	3.285	0.026	412	-0.105	3.663	1.004	0.564
108	0.814	3.790	1.594	0.170	413	-0.177	3.675	0.954	0.797
109	2.450	4.170	3.274	0.034	416	-0.109	3.755	0.941	1.408
110	0.101	3.647	1.147	0.239	424	0.609	3.694	1.505	0.105
112	1.400	4.008	1.951	0.178	428	0.428	3.781	1.273	0.435
114	0.996	3.807	1.757	0.122	439	0.269	3.725	1.203	0.397
115	-0.055	3.698	1.010	0.726	443	0.050	3.717	1.062	0.662

Star No.	$\log L/L_{\odot}$	LogTeff	Mass $M/M_{\odot}$	Age	Star No.	$\log L/L_{\odot}$	LogTeff	Mass $M/M_{\odot}$	Age
116	0.952	3.807	1.712	0.137	447	0.426	3.634	1.406	0.058
117	0.251	3.755	1.167	0.551	451	-0.316	3.711	0.857	1.666
118	0.906	3.795	1.678	0.140	454	0.118	3.719	1.104	0.561
121	0.604	3.757	1.438	0.221	455	0.013	3.684	1.062	0.516
125	0.704	3.781	1.501	0.211	457	-0.251	3.684	0.907	1.074
126	-0.312	3.672	0.882	1.116	466	0.324	3.781	1.197	0.569
127	-0.278	3.610	0.938	0.418	469	0.534	3.822	1.320	0.455
128	1.200	3.897	1.868	0.145	480	-0.080	3.723	0.978	0.993
131	5.046	4.527	12.109	0.000	481	0.040	3.648	1.105	0.297
132	1.744	4.056	2.320	0.101	483	-0.356	3.781	0.798	3.235
133	0.283	3.675	1.255	0.212	490	-0.058	3.784	0.951	1.548
134	0.750	3.719	1.610	0.097	491	0.209	3.685	1.192	0.301
136	0.044	3.594	1.149	0.075	493	0.463	3.801	1.283	0.465
137	2.009	4.121	2.602	0.075	497	-0.191	3.692	0.935	0.997
138	1.584	3.973	2.230	0.092	498	-0.218	3.752	0.883	1.833
139	0.530	3.652	1.477	0.063	500	0.113	3.694	1.119	0.439
141	-0.070	3.668	1.021	0.544	502	-0.064	3.781	0.950	1.542
142	2.433	4.121	3.351	0.027	503	0.367	3.707	1.291	0.249
143	1.418	3.967	2.029	0.132	504	-0.157	3.705	0.946	1.032
144	0.361	3.638	1.347	0.085	505	0.400	3.734	1.294	0.303
145	1.410	3.979	2.002	0.146	507	0.199	3.705	1.169	0.390
146	1.594	3.667	2.476	0.005	509	-0.053	3.677	1.026	0.573
147	1.284	3.740	2.181	0.027	511	-0.047	3.685	1.023	0.622
148	0.206	3.760	1.132	0.648	514	0.333	3.682	1.287	0.201
149	0.009	3.692	1.053	0.575	516	-0.290	3.699	0.877	1.400
150	-0.303	3.647	0.902	0.810	517	0.054	3.738	1.049	0.798
151	0.580	3.816	1.363	0.386	519	0.762	3.858	1.476	0.332
152	2.238	4.080	3.066	0.035	520	0.453	3.798	1.278	0.467
153	-0.496	3.653	0.800	1.520	521	0.012	3.781	0.994	1.270
154	0.600	3.740	1.450	0.189	526	-0.329	3.801	0.800	3.467
155	-0.627	3.622	0.756	1.499	527	-0.408	3.776	0.776	3.543
156	-0.006	3.652	1.073	0.360	528	0.616	3.606	1.496	0.041
157	1.769	4.035	2.388	0.084	530	0.717	3.743	1.553	0.140
158	1.462	3.855	2.246	0.054	532	-0.199	3.694	0.929	1.038
159	1.276	3.973	1.856	0.195	535	0.417	3.713	1.325	0.232
161	-0.081	3.707	0.989	0.855	536	0.911	3.625	1.758	0.022
163	0.085	3.715	1.086	0.590	538	1.233	3.692	2.186	0.013
164	0.364	3.723	1.275	0.300	542	-0.256	3.781	0.847	2.512
165	1.270	3.927	1.908	0.149	603	-0.151	3.692	0.957	0.894
167	0.069	3.715	1.075	0.616	652	0.808	3.653	1.742	0.023
168	-0.190	3.650	0.963	0.607	672	0.064	3.672	1.104	0.385
169	0.310	3.745	1.216	0.432	673	0.015	3.677	1.068	0.472
172	1.842	4.067	2.440	0.085	675	0.321	3.696	1.266	0.249
173	-0.686	3.645	0.718	2.353	684	0.260	3.723	1.198	0.398
174	-0.315	3.690	0.869	1.371	1145	-0.298	3.699	0.873	1.430

Stars in

Table 5 : Masses and ages of the cluster NGC 1976 (Solar Unit)

Star No.	$\log L/L_\odot$	LogTeff	Mass $M/M_\odot$	Age	Star No.	$\log L/L_\odot$	LogTeff	Mass $M/M_\odot$	Age
748	2.291	3.522	0.452	0.000	1943	0.111	3.625	1.171	0.152
767	0.096	3.792	1.037	1.112	1952	-0.218	3.645	0.950	0.615
775	1.066	3.908	1.712	0.217	1953	1.246	3.752	2.115	0.035
784	0.856	3.807	1.616	0.176	1955	0.966	3.678	1.882	0.025
793	0.088	3.762	1.053	0.900	1956	1.298	3.874	2.010	0.096
804	0.404	3.770	1.265	0.421	1967	0.060	3.672	1.101	0.389
819	0.467	3.731	1.348	0.247	1970	4.199	4.356	8.197	0.001
824	0.830	3.760	1.642	0.123	1971	-0.034	3.657	1.052	0.419
832	-0.128	3.673	0.983	0.681	1988	-0.059	3.585	1.088	0.081
837	0.894	3.865	1.590	0.249	1993	3.575	4.152	6.481	0.002
841	-0.400	3.750	0.794	2.861	1996	0.784	3.762	1.595	0.143
846	0.466	3.778	1.305	0.384	2001	0.285	3.713	1.225	0.334
857	3.083	3.522	0.397	0.000	2003	-0.223	3.743	0.886	1.715
866	1.886	3.657	2.115	0.001	2006	0.145	3.694	1.141	0.401
867	1.985	4.001	2.781	0.040	2007	-0.119	3.660	0.997	0.563
872	0.050	3.919	0.926	2.843	2013	0.008	3.770	0.999	1.176
878	1.132	3.792	1.924	0.075	2016	-0.010	3.801	0.968	1.552
895	0.825	3.622	1.719	0.028	2017	0.385	3.713	1.300	0.253
908	1.700	3.973	2.390	0.069	2020	0.456	3.709	1.360	0.199
917	0.692	3.750	1.523	0.161	2021	0.557	3.725	1.429	0.180
924	-0.358	3.727	0.826	2.142	2029	1.782	3.502	0.394	0.000
930	0.603	3.677	1.517	0.081	2030	0.459	3.768	1.309	0.357
936	-0.507	3.685	0.778	2.184	2031	2.977	4.121	4.636	0.007
952	0.311	3.707	1.249	0.291	2032	0.329	3.696	1.272	0.243
967	0.573	3.765	1.404	0.257	2033	0.574	3.717	1.451	0.156
972	0.188	3.787	1.100	0.843	2035	1.240	3.923	1.879	0.156
979	-0.530	3.729	0.745	3.397	2036	1.272	3.828	2.042	0.071
980	-0.672	3.734	0.683	5.067	2037	5.140	4.452	13.468	0.000
1001	1.654	3.919	2.412	0.054	2043	0.193	3.725	1.150	0.488
1005	-0.118	3.703	0.969	0.911	2050	0.361	3.725	1.271	0.309
1007	0.053	3.746	1.043	0.858	2054	3.163	4.189	4.947	0.007
1010	0.026	3.729	1.038	0.793	2057	-0.361	3.705	0.837	1.778
1022	0.908	3.816	1.657	0.166	2058	1.366	3.961	1.974	0.145
1023	-0.259	3.692	0.898	1.198	2060	-0.572	3.776	0.704	5.355
1026	0.312	3.757	1.208	0.479	2065	1.684	4.026	2.285	0.098
1034	1.138	3.880	1.820	0.151	2068	-0.225	3.663	0.934	0.795
1036	0.997	3.635	1.973	0.001	2069	0.482	3.668	1.419	0.103
1037	1.078	3.752	1.913	0.057	2074	2.420	3.894	3.874	0.006
1042	0.252	3.620	1.279	0.078	2078	-0.089	3.655	1.019	0.482
1044	2.216	4.008	3.175	0.024	2080	1.412	4.026	1.943	0.190
1045	-0.304	3.711	0.863	1.611	2083	2.734	4.170	3.879	0.017
1048	0.206	3.642	1.225	0.156	2084	0.476	3.627	1.455	0.037
1049	0.912	3.596	1.279	0.010	2085	1.946	3.993	2.732	0.042

Star No.	$\log L/L_\odot$	LogTeff	Mass $M/M_\odot$	Age	Star No.	$\log L/L_\odot$	LogTeff	Mass $M/M_\odot$	Age
1050	-0.339	3.694	0.855	1.514	2086	1.194	3.822	1.957	0.083
1051	0.439	3.768	1.294	0.376	2089	-0.425	3.721	0.798	2.415
1054	-0.311	3.746	0.839	2.210	2100	0.700	3.653	1.633	0.035
1058	0.391	3.608	1.400	0.022	2102	1.556	4.026	2.117	0.134
1064	-0.370	3.667	0.855	1.241	2104	0.900	3.736	1.740	0.078
1072	0.556	3.587	1.230	0.031	2111	-0.378	3.717	0.823	2.063
1073	-0.646	3.855	0.639	10.709	2115	0.009	3.665	1.073	0.414
1075	0.249	3.682	1.224	0.256	2118	1.250	3.967	1.836	0.200
1076	0.371	3.707	1.295	0.246	2120	-0.049	3.747	0.980	1.135
1077	-0.119	3.685	0.980	0.759	2124	1.422	3.961	2.042	0.127
1084	-0.222	3.678	0.927	0.935	2125	0.957	3.798	1.726	0.126
1089	0.905	3.825	1.644	0.180	2128	0.169	3.698	1.155	0.390
1090	-0.071	3.635	1.043	0.338	2131	3.051	3.887	5.670	0.001
1092	-0.311	3.692	0.870	1.379	2133	0.034	3.629	1.116	0.213
1097	1.940	4.056	2.607	0.063	2143	-0.084	3.653	1.023	0.464
1102	-0.362	3.680	0.851	1.402	2145	0.122	3.719	1.107	0.554
1111	-0.174	3.752	0.907	1.635	2151	0.590	3.837	1.351	0.441
1117	1.670	3.865	2.526	0.034	2152	-0.234	3.658	0.932	0.768
1122	-0.006	3.752	1.002	1.058	2153	0.465	3.765	1.317	0.343
1125	0.229	3.684	1.208	0.278	2160	0.222	3.639	1.240	0.139
1126	1.700	4.008	2.334	0.085	2164	0.767	3.707	1.639	0.078
1139	1.072	3.828	1.812	0.120	2167	0.777	3.690	1.667	0.059
1144	0.234	3.624	1.262	0.092	2168	-0.147	3.632	0.999	0.407
1154	-0.320	3.673	0.876	1.164	2172	-0.088	3.653	1.021	0.469
1158	0.798	3.784	1.585	0.168	2173	-0.064	3.618	1.060	0.241
1159	0.612	3.620	1.585	0.012	2174	0.550	3.804	1.349	0.381
1170	-0.032	3.740	0.995	1.023	2181	0.254	3.667	1.240	0.204
1175	0.646	3.790	1.442	0.264	2186	-0.445	3.655	0.824	1.342
1179	0.572	3.807	1.364	0.368	2187	0.002	3.680	1.057	0.510
1180	0.376	3.770	1.244	0.453	2188	0.152	3.723	1.124	0.533
1185	-0.347	3.692	0.852	1.520	2189	1.266	3.945	1.880	0.168
1188	0.161	3.670	1.171	0.283	2194	0.167	3.705	1.147	0.426
1189	0.226	3.795	1.119	0.816	2200	1.092	3.828	1.834	0.114
1195	0.216	3.757	1.141	0.616	2211	-0.567	3.647	0.770	1.720
1196	1.246	3.927	1.881	0.158	2216	0.481	3.687	1.401	0.139
1197	0.630	3.668	1.550	0.064	2217	0.275	3.707	1.222	0.322
1199	0.923	3.768	1.727	0.103	2219	1.562	3.834	2.418	0.035
1211	-0.402	3.745	0.795	2.776	2222	0.776	3.770	1.580	0.157
1212	0.646	3.760	1.472	0.202	2233	-0.056	3.689	1.016	0.661
1216	-0.178	3.699	0.937	1.034	2236	-1.138	3.657	0.544	8.988
1218	-0.312	3.736	0.845	2.042	2237	0.174	3.703	1.154	0.410
1229	0.610	3.729	1.471	0.162	2238	1.271	3.768	2.125	0.040
1241	1.016	3.792	1.796	0.102	2240	0.146	3.668	1.161	0.289
1251	0.048	3.787	1.012	1.206	2243	-0.049	3.567	1.107	0.009
1255	-0.175	3.682	0.951	0.853	2244	0.332	3.662	1.304	0.148

Star No.	logL/$L_\odot$	LogTeff	Mass M/$M_\odot$	Age	Star No.	logL/$L_\odot$	LogTeff	Mass M/$M_\odot$	Age
1259	1.257	3.840	2.007	0.082	2247	1.116	3.843	1.842	0.121
1260	-0.133	3.625	1.013	0.346	2248	0.687	3.768	1.500	0.195
1267	1.457	3.509	0.450	0.000	2249	-0.167	3.690	0.949	0.916
1270	0.416	3.711	1.326	0.227	2252	0.671	3.721	1.534	0.124
1281	0.862	3.834	1.592	0.216	2254	-0.173	3.640	0.979	0.502
1284	0.997	3.694	1.896	0.031	2257	0.370	3.719	1.284	0.281
1287	0.395	3.755	1.271	0.376	2261	0.376	3.711	1.295	0.254
1293	0.433	3.694	1.355	0.176	2263	-0.182	3.667	0.956	0.732
1301	-0.956	3.792	0.554	15.596	2264	-0.758	3.652	0.685	3.085
1304	0.214	3.719	1.170	0.432	2267	0.624	3.787	1.426	0.273
1306	1.635	3.819	2.552	0.025	2268	-0.260	3.653	0.921	0.776
1307	1.098	3.837	1.829	0.120	2271	2.709	4.121	3.951	0.014
1315	1.319	3.567	0.873	0.001	2276	0.170	3.652	1.191	0.209
1319	0.322	3.678	1.282	0.197	2281	-0.077	3.768	0.951	1.436
1322	0.564	3.723	1.437	0.172	2284	1.757	4.035	2.371	0.087
1326	1.008	3.617	1.578	0.012	2290	0.971	3.831	1.703	0.159
1328	0.381	3.590	1.298	0.064	2292	0.749	3.682	1.649	0.056
1346	-0.039	3.665	1.042	0.476	2294	0.125	3.696	1.126	0.433
1347	0.008	3.736	1.022	0.884	2297	-0.088	3.653	1.021	0.469
1350	-0.031	3.743	0.994	1.040	2298	-0.288	3.643	0.912	0.741
1352	-0.443	3.660	0.822	1.412	2299	-0.226	3.639	0.949	0.576
1353	-0.375	3.660	0.856	1.168	2300	-0.011	3.696	1.038	0.632
1356	0.013	3.698	1.052	0.602	2302	1.174	3.919	1.811	0.179
1357	0.506	3.778	1.337	0.346	2303	-0.256	3.723	0.881	1.580
1360	-0.249	3.705	0.895	1.319	2305	0.031	3.640	1.105	0.267
1361	0.496	3.792	1.317	0.398	2307	-0.394	3.727	0.809	2.352
1364	0.496	3.781	1.326	0.364	2308	2.102	4.080	2.827	0.048
1365	0.582	3.678	1.497	0.089	2310	0.269	3.698	1.226	0.295
1366	0.209	3.647	1.224	0.169	2312	-0.246	3.667	0.920	0.877
1372	0.369	3.765	1.243	0.441	2314	2.964	4.252	4.211	0.015
1374	1.046	3.795	1.825	0.097	2316	-0.132	3.723	0.949	1.139
1377	-0.403	3.725	0.806	2.365	2317	0.194	3.745	1.135	0.588
1378	0.100	3.734	1.082	0.678	2320	-0.651	3.665	0.724	2.640
1381	0.286	3.668	1.262	0.190	2324	1.020	3.828	1.757	0.137
1391	0.892	3.816	1.642	0.173	2328	0.524	3.762	1.366	0.287
1393	0.377	3.725	1.283	0.296	2329	0.970	3.865	1.664	0.206
1394	1.110	3.784	1.910	0.073	2334	-0.765	3.663	0.677	3.534
1395	0.324	3.673	1.287	0.183	2335	-0.295	3.635	0.913	0.673
1402	-0.216	3.689	0.923	1.027	2338	-0.652	3.711	0.701	4.015
1403	-0.394	3.629	0.864	0.824	2339	1.182	3.804	1.966	0.073
1404	0.641	3.725	1.502	0.142	2340	0.812	3.828	1.552	0.234
1409	0.600	3.723	1.468	0.156	2342	1.404	3.816	2.228	0.045
1410	-0.468	3.643	0.819	1.249	2345	0.656	3.757	1.483	0.192
1414	0.604	3.776	1.420	0.261	2346	0.792	3.807	1.556	0.208
1415	0.475	3.755	1.334	0.304	2347	-0.267	3.684	0.899	1.121

Star No.	$\log L/L_\odot$	LogTeff	Mass $M/M_\odot$	Age	Star No.	$\log L/L_\odot$	LogTeff	Mass $M/M_\odot$	Age
1420	-0.048	3.740	0.985	1.066	2349	-0.511	3.670	0.784	1.897
1421	0.305	3.585	1.247	0.075	2353	0.169	3.665	1.180	0.258
1422	0.659	3.747	1.495	0.173	2354	-0.302	3.680	0.882	1.190
1423	0.602	3.760	1.433	0.227	2357	-0.135	3.687	0.970	0.808
1425	0.460	3.709	1.363	0.196	2358	0.798	3.784	1.585	0.168
1426	0.160	3.757	1.103	0.713	2364	0.510	3.778	1.340	0.342
1427	0.038	3.699	1.066	0.574	2366	3.300	4.301	4.978	0.009
1429	0.869	3.687	1.765	0.041	2367	-0.058	3.727	0.988	0.974
1430	0.081	3.685	1.105	0.434	2368	0.189	3.602	1.246	0.052
1439	0.038	3.727	1.047	0.754	2369	-0.236	3.662	0.929	0.804
1440	0.173	3.713	1.146	0.455	2370	0.966	3.784	1.752	0.108
1441	2.430	3.908	3.862	0.007	2373	-0.269	3.677	0.902	1.047
1445	2.285	4.121	3.068	0.039	2374	0.806	3.790	1.587	0.173
1455	0.843	3.755	1.661	0.112	2375	-0.274	3.645	0.919	0.725
1457	1.324	3.792	2.158	0.045	2376	0.010	3.701	1.048	0.631
1467	0.958	3.784	1.744	0.110	2381	0.229	3.660	1.227	0.199
1469	0.562	3.658	1.498	0.065	2382	-0.220	3.653	0.943	0.691
1470	0.485	3.660	1.430	0.088	2385	0.846	3.650	1.786	0.017
1472	0.333	3.585	1.241	0.068	2387	1.712	4.056	2.276	0.109
1474	0.796	3.776	1.592	0.157	2388	0.725	3.682	1.626	0.060
1477	-0.219	3.696	0.917	1.114	2391	0.242	3.790	1.134	0.750
1478	-0.160	3.653	0.978	0.580	2393	0.934	3.795	1.707	0.130
1484	0.407	3.707	1.323	0.222	2396	1.686	3.877	2.529	0.036
1485	-0.585	3.655	0.758	1.983	2397	0.391	3.731	1.289	0.304
1487	-0.107	3.660	1.004	0.543	2402	-0.484	3.709	0.776	2.549
1491	2.470	4.080	3.521	0.020	2404	0.704	3.762	1.520	0.177
1492	0.798	3.813	1.554	0.215	2405	0.314	3.729	1.233	0.366
1505	0.181	3.713	1.151	0.445	2408	0.055	3.731	1.055	0.749
1507	1.047	3.884	1.719	0.194	2409	-0.470	3.668	0.804	1.667
1509	0.076	3.689	1.099	0.457	2410	2.256	4.106	3.044	0.038
1510	0.362	3.699	1.294	0.232	2412	0.089	3.685	1.110	0.424
1511	1.450	3.931	2.117	0.098	2413	0.060	3.757	1.040	0.926
1513	0.936	3.894	1.598	0.274	2418	1.759	4.045	2.358	0.091
1518	0.031	3.663	1.088	0.379	2419	-0.368	3.709	0.832	1.878
1519	1.688	3.673	2.624	0.004	2420	1.483	3.884	2.230	0.064
1523	0.130	3.738	1.098	0.652	2422	3.873	4.418	6.473	0.004
1526	0.244	3.770	1.150	0.639	2423	0.766	3.778	1.561	0.174
1530	-0.774	3.701	0.656	5.096	2424	0.855	3.887	1.530	0.321
1538	0.733	3.825	1.483	0.280	2425	0.935	3.755	1.755	0.087
1539	0.904	3.757	1.720	0.098	2427	0.199	3.675	1.194	0.271
1540	0.834	3.650	1.773	0.018	2428	1.030	3.868	1.721	0.181
1541	0.261	3.696	1.221	0.295	2432	-0.024	3.596	1.102	0.112
1544	-0.322	3.642	0.894	0.801	2433	0.634	3.784	1.438	0.259
1546	2.604	4.106	3.746	0.017	2434	-0.223	3.713	0.905	1.322
1552	0.222	3.667	1.217	0.225	2436	0.317	3.660	1.293	0.151

Star No.	$\log L/L_{\odot}$	LogTeff	Mass $M/M_{\odot}$	Age	Star No.	$\log L/L_{\odot}$	LogTeff	Mass $M/M_{\odot}$	Age
1554	0.334	3.717	1.258	0.305	2438	-0.167	3.647	0.978	0.542
1555	-0.162	3.650	0.979	0.558	2441	0.896	3.757	1.712	0.100
1561	0.608	3.734	1.465	0.171	2442	0.806	3.727	1.655	0.091
1562	1.394	3.986	1.974	0.158	2444	0.176	3.627	1.216	0.125
1563	0.596	3.548	0.797	0.009	2445	0.730	3.778	1.528	0.192
1567	-0.105	3.677	0.994	0.663	2446	0.156	3.600	1.223	0.056
1572	-0.616	3.627	0.758	1.548	2447	0.598	3.773	1.417	0.259
1574	0.077	3.743	1.060	0.783	2448	1.846	3.502	0.390	0.000
1575	0.699	3.819	1.460	0.291	2452	0.485	3.690	1.401	0.144
1581	0.256	3.734	1.187	0.447	2454	-0.353	3.705	0.841	1.741
1582	-0.028	3.689	1.033	0.612	2455	0.089	3.564	1.030	0.098
1585	-0.430	3.604	0.860	0.618	2466	1.318	3.813	2.120	0.055
1587	0.212	3.662	1.214	0.215	2467	-0.062	3.738	0.979	1.082
1589	-0.480	3.672	0.798	1.771	2471	0.186	3.752	1.124	0.640
1590	1.062	3.801	1.835	0.098	2473	1.326	3.931	1.966	0.133
1605	1.974	3.940	2.876	0.028	2474	0.640	3.792	1.435	0.274
1608	0.136	3.672	1.152	0.311	2475	0.010	3.668	1.071	0.431
1615	0.117	3.685	1.129	0.392	2476	0.396	3.618	1.394	0.039
1617	-0.193	3.755	0.895	1.747	2478	0.772	3.736	1.612	0.111
1620	0.063	3.625	1.138	0.179	2479	0.455	3.522	0.612	0.008
1621	-0.012	3.648	1.071	0.348	2482	-0.052	3.673	1.028	0.549
1623	1.084	3.787	1.877	0.081	2486	0.606	3.784	1.414	0.279
1626	0.670	3.790	1.463	0.248	2491	-0.218	3.680	0.927	0.944
1627	1.544	4.008	2.126	0.125	2494	0.942	3.719	1.806	0.055
1634	2.229	4.136	2.936	0.048	2495	-0.024	3.672	1.047	0.495
1643	0.142	3.703	1.132	0.448	2498	-0.403	3.694	0.823	1.797
1646	1.238	3.822	2.009	0.074	2500	0.642	3.834	1.397	0.378
1647	0.214	3.760	1.137	0.634	2501	-0.602	3.667	0.744	2.349
1648	-0.532	3.750	0.734	4.010	2502	-0.137	3.625	1.010	0.350
1649	1.213	3.685	2.170	0.012	2507	0.682	3.810	1.453	0.284
1653	-0.031	3.725	1.006	0.889	2509	-0.001	3.655	1.074	0.371
1654	1.658	3.967	2.342	0.073	2510	1.110	3.868	1.805	0.148
1657	0.558	3.813	1.347	0.400	2512	-0.263	3.690	0.897	1.190
1658	0.530	3.604	1.486	0.054	2519	0.686	3.760	1.507	0.181
1659	0.733	3.647	1.673	0.025	2521	-0.030	3.642	1.064	0.332
1660	1.737	4.035	2.343	0.091	2524	0.170	3.738	1.124	0.586
1662	0.899	3.768	1.702	0.110	2526	0.584	3.673	1.503	0.081
1664	2.622	4.170	3.628	0.022	2534	0.704	3.711	1.575	0.100
1667	0.264	3.620	1.288	0.074	2536	0.842	3.855	1.551	0.266
1671	1.291	3.884	1.989	0.105	2537	0.890	3.822	1.633	0.182
1683	0.790	3.837	1.522	0.265	2538	-0.634	3.678	0.725	2.870
1684	0.212	3.662	1.214	0.215	2542	-0.138	3.668	0.980	0.659
1685	1.086	3.927	1.710	0.234	2545	3.761	4.418	6.054	0.005
1689	-0.435	3.684	0.813	1.770	2547	0.045	3.687	1.080	0.490
1690	-0.036	3.606	1.087	0.161	2548	-0.115	3.665	0.996	0.593

Star No.	$\log L/L_\odot$	LogTeff	Mass $M/M_\odot$	Age	Star No.	$\log L/L_\odot$	LogTeff	Mass $M/M_\odot$	Age
1691	0.698	3.760	1.518	0.176	2552	0.492	3.787	1.318	0.385
1698	1.690	3.979	2.366	0.073	2554	-0.349	3.663	0.868	1.127
1699	0.007	3.731	1.025	0.851	2564	2.944	4.252	4.161	0.016
1705	0.062	3.701	1.081	0.547	2565	0.016	3.606	1.121	0.131
1708	2.597	4.121	3.696	0.018	2566	0.760	3.807	1.526	0.226
1709	0.129	3.694	1.130	0.420	2569	0.092	3.770	1.050	0.947
1712	0.989	3.798	1.759	0.116	2570	0.698	3.804	1.473	0.260
1716	3.905	4.418	6.597	0.004	2571	0.636	3.807	1.418	0.312
1717	0.609	3.685	1.514	0.092	2574	0.192	3.770	1.115	0.731
1719	0.769	3.765	1.578	0.152	2575	1.216	3.776	2.046	0.050
1724	1.201	3.647	2.124	0.013	2576	0.380	3.740	1.272	0.343
1728	4.546	4.527	8.986	0.001	2579	0.498	3.629	1.472	0.036
1729	-0.113	3.663	0.999	0.577	2583	0.023	3.768	1.009	1.110
1731	0.128	3.770	1.073	0.863	2587	0.128	3.750	1.088	0.728
1732	0.196	3.776	1.113	0.757	2588	-0.158	3.668	0.969	0.698
1736	0.987	3.655	1.936	0.011	2591	0.171	3.598	1.236	0.047
1739	-0.398	3.645	0.853	1.040	2592	0.958	3.861	1.655	0.207
1740	1.918	4.080	2.533	0.075	2593	-0.131	3.684	0.974	0.770
1743	0.360	3.723	1.272	0.303	2597	0.354	3.657	1.326	0.126
1744	2.510	4.170	3.393	0.029	2598	0.252	3.781	1.146	0.685
1746	0.636	3.689	1.535	0.089	2599	1.651	3.956	2.349	0.069
1750	1.240	3.792	2.052	0.056	2600	0.153	3.602	1.219	0.063
1752	0.037	3.698	1.067	0.563	2603	0.794	3.868	1.495	0.327
1760	-0.144	3.757	0.920	1.570	2604	1.254	3.877	1.955	0.110
1764	-0.214	3.610	0.975	0.335	2605	0.476	3.816	1.281	0.503
1768	1.667	4.045	2.232	0.114	2606	0.619	3.747	1.460	0.192
1772	1.786	3.945	2.564	0.046	2608	2.326	4.170	3.041	0.046
1773	0.099	3.677	1.123	0.371	2609	0.939	3.887	1.609	0.260
1774	0.102	3.738	1.080	0.702	2610	0.788	3.781	1.578	0.169
1775	-0.228	3.734	0.890	1.608	2612	-0.023	3.685	1.038	0.581
1785	0.364	3.672	1.320	0.157	2618	0.141	3.660	1.165	0.260
1786	0.214	3.667	1.211	0.230	2619	0.380	3.750	1.264	0.374
1787	0.376	3.627	1.370	0.058	2626	1.398	3.919	2.070	0.102
1789	0.962	3.804	1.724	0.131	2627	1.807	3.831	2.805	0.018
1790	-0.276	3.672	0.901	1.009	2628	0.564	3.736	1.424	0.198
1791	0.852	3.781	1.640	0.142	2630	-0.004	3.723	1.024	0.811
1792	1.850	4.067	2.452	0.083	2633	-0.058	3.717	0.996	0.883
1795	1.737	4.035	2.343	0.091	2642	-0.062	3.639	1.047	0.349
1798	1.346	3.861	2.086	0.077	2646	1.292	3.950	1.903	0.163
1799	0.365	3.635	1.353	0.077	2649	-0.015	3.622	1.089	0.219
1803	0.262	3.717	1.205	0.371	2651	0.241	3.692	1.209	0.299
1811	-0.251	3.660	0.922	0.822	2654	-0.018	3.727	1.012	0.876
1813	2.746	4.208	3.806	0.020	2660	0.658	3.804	1.438	0.288
1817	0.834	3.699	1.714	0.057	2668	0.766	3.919	1.420	0.491
1827	0.144	3.672	1.158	0.304	2669	1.654	3.945	2.370	0.064

Star No.	$\log L/L_{\odot}$	LogTeff	Mass $M/M_{\odot}$	Age		Star No.	$\log L/L_{\odot}$	LogTeff	Mass $M/M_{\odot}$	Age
1828	0.462	3.668	1.402	0.110		2670	0.928	3.613	1.538	0.015
1830	0.588	3.816	1.369	0.378		2675	0.519	3.707	1.414	0.162
1848	-0.086	3.668	1.011	0.568		2682	-0.204	3.672	0.941	0.825
1849	2.173	4.136	2.840	0.055		2686	0.934	3.801	1.700	0.137
1854	1.110	3.865	1.809	0.144		2687	1.046	3.868	1.737	0.173
1863	2.064	3.897	3.127	0.016		2695	0.588	3.781	1.401	0.286
1865	2.562	3.993	3.945	0.009		2699	1.946	3.986	2.743	0.041
1876	0.090	3.634	1.150	0.195		2700	0.938	3.837	1.663	0.182
1877	0.346	3.703	1.278	0.253		2703	0.199	3.768	1.121	0.704
1878	-0.171	3.713	0.933	1.151		2707	0.598	3.810	1.382	0.353
1879	-0.203	3.746	0.895	1.672		2711	3.452	4.252	5.634	0.005
1880	-0.161	3.755	0.913	1.609		2714	-0.213	3.707	0.914	1.219
1881	1.230	3.904	1.891	0.141		2721	0.990	3.865	1.684	0.195
1885	0.930	3.861	1.628	0.222		2728	-0.366	3.680	0.849	1.417
1889	2.718	3.961	4.423	0.005		2733	-0.232	3.709	0.902	1.308
1891	3.209	4.001	5.771	0.002		2752	0.841	3.765	1.648	0.125
1898	0.698	3.717	1.563	0.109		2753	0.606	3.784	1.414	0.279
1901	2.778	4.170	3.982	0.015		2762	1.612	4.026	2.189	0.117
1902	0.558	3.795	1.364	0.347		2770	0.513	3.743	1.375	0.245
1904	-0.361	3.705	0.837	1.778		2773	0.815	3.598	1.329	0.016
1905	1.506	3.993	2.101	0.125		2780	1.482	3.773	2.402	0.023
1906	0.051	3.707	1.070	0.597		2787	0.494	3.727	1.374	0.219
1919	0.401	3.713	1.312	0.242		4101	-0.145	3.663	0.980	0.632
1931	-0.126	3.667	0.989	0.624		4110	-2.008	3.750	0.304	160.475
1933	3.110	4.208	4.729	0.008		4146	-0.421	3.544	0.901	0.022
1935	0.444	3.723	1.337	0.240		4147	-0.680	3.613	0.737	1.556
1937	0.009	3.694	1.052	0.586		4148	-1.050	3.629	0.584	5.393

Stars in

Table 6 : Masses and ages of the Orion Nebula cluster

Star No.	$\log L/L_\odot$	LogTeff	Mass $M/M_\odot$	Age	Star No.	$\log L/L_\odot$	LogTeff	Mass $M/M_\odot$	Age
867	2.084	4.008	2.935	0.035	1798	1.45	3.858	2.220	0.065
908	1.872	4.026	2.556	0.064	1803	0.33	3.721	1.249	0.395
1001	1.732	3.923	2.520	0.049	1813	2.81	4.208	3.963	0.017
1010	0.107	3.731	1.088	0.758	1817	0.86	3.961	1.458	0.522
1026	0.412	3.750	1.289	0.400	1849	2.06	4.056	2.794	0.049
1037	1.172	3.750	2.028	0.055	1865	2.64	3.993	4.137	0.008
1036	1.054	3.637	1.952	0.018	1891	3.34	4.026	6.122	0.002
1042	0.329	3.622	1.337	0.142	1881	1.32	3.908	1.994	0.122
1044	2.296	4.008	3.330	0.021	1904	-0.25	3.699	0.898	1.480
1049	1.010	3.592	1.200	0.006	1905	1.58	3.993	2.198	0.108
1052	0.284	3.643	1.282	0.211	1889	2.65	3.979	4.195	0.007
1058	0.466	3.610	1.462	0.079	1902	0.64	3.801	1.425	0.329
1073	-0.562	3.858	0.670	9.198	1901	2.93	4.208	4.257	0.013
1077	-0.039	3.687	1.027	0.771	1919	0.50	3.715	1.392	0.238
1089	0.986	3.837	1.711	0.177	1932	3.35	4.229	5.368	0.005
1092	-0.231	3.694	0.912	1.348	1933	3.23	4.229	4.997	0.007
1090	-0.042	3.652	1.050	0.562	1931	0.00	3.667	1.067	0.576
1097	2.012	4.056	2.722	0.054	1955	1.05	3.680	1.976	0.037
1102	-0.012	3.662	1.062	0.570	1970	4.01	4.208	8.070	0.001
1111	-0.093	3.755	0.950	1.501	1993	3.62	4.136	6.736	0.002
1117	1.746	3.871	2.632	0.033	1996	0.89	3.770	1.689	0.138
1122	0.075	3.755	1.051	0.981	2031	3.17	4.170	5.031	0.006
1125	0.309	3.685	1.266	0.303	2036	1.33	3.846	2.090	0.079
1126	1.790	4.017	2.448	0.075	2043	0.27	3.727	1.202	0.482
b67	-0.065	3.665	1.026	0.678	2035	1.32	3.915	1.982	0.128
1139	1.156	3.828	1.906	0.108	2037	5.69	4.610	16.799	0.000
1144	0.311	3.625	1.320	0.156	2054	3.32	4.229	5.279	0.006
1154	-0.241	3.675	0.918	1.180	2054a	2.15	4.067	2.926	0.042
1158	0.894	3.784	1.679	0.152	2057	-0.28	3.707	0.877	1.696
1159	0.689	3.622	1.657	0.048	2058	1.51	3.986	2.110	0.125
1179	0.640	3.807	1.421	0.342	2065	1.78	4.026	2.420	0.080
1185	-0.267	3.694	0.892	1.480	2068	0.14	3.692	1.139	0.503
1189	0.291	3.801	1.158	0.789	2102	1.58	3.986	2.203	0.105
1195	0.298	3.760	1.196	0.579	2104	0.44	3.734	1.328	0.324
1196	1.334	3.931	1.976	0.138	2124	1.49	3.956	2.140	0.107
1197	0.709	3.670	1.623	0.087	2134	3.15	3.871	6.096	0.001
1199	1.004	3.770	1.810	0.102	2143	-0.15	3.675	0.968	0.936
1211	-0.321	3.747	0.833	2.534	2153	0.54	3.770	1.375	0.334
1241	1.097	3.798	1.877	0.101	2160	1.25	3.516	0.501	0.000
1251	0.128	3.787	1.061	1.076	2164	0.85	3.701	1.733	0.081
1267	1.436	3.516	0.486	0.000	2222	0.85	3.768	1.654	0.149
1259	1.320	3.846	2.075	0.081	2219	1.63	3.831	2.525	0.033
1270	0.504	3.711	1.398	0.228	2233	0.04	3.692	1.073	0.654

Star No.	$\log L/L_\odot$	LogTeff	Mass $M/M_\odot$	Age	Star No.	$\log L/L_\odot$	LogTeff	Mass $M/M_\odot$	Age
1281	0.950	3.837	1.675	0.194	2248	0.74	3.770	1.550	0.200
1284	1.073	3.696	1.982	0.042	2244	0.55	3.653	1.492	0.112
1306	1.713	3.825	2.662	0.025	2252	0.72	3.719	1.584	0.137
1307	1.184	3.846	1.913	0.115	2257	0.46	3.721	1.348	0.283
1315	1.371	3.571	0.897	0.001	2261	0.50	3.701	1.402	0.212
1319	0.395	3.677	1.340	0.221	2267	0.71	3.784	1.508	0.240
1322	0.662	3.719	1.528	0.161	2271	2.71	4.092	4.023	0.012
1328	0.450	3.592	1.316	0.052	2268	-0.18	3.655	0.964	0.841
1347	-0.462	3.738	0.771	3.377	2276	0.27	3.652	1.262	0.243
1342	2.366	3.468	0.247	0.000	2284	1.79	4.026	2.431	0.079
1346	0.042	3.667	1.093	0.518	2290	1.06	3.837	1.790	0.146
1360	-0.254	3.719	0.885	1.732	2294	0.21	3.698	1.180	0.446
1350	0.038	3.745	1.034	1.005	2292	0.83	3.682	1.734	0.070
1357	0.582	3.790	1.388	0.350	2302	1.26	3.915	1.917	0.148
1361	0.593	3.798	1.389	0.362	2303	-0.13	3.719	0.953	1.261
1372	0.414	3.778	1.266	0.494	2310	0.29	3.699	1.242	0.359
1378	0.133	3.736	1.101	0.735	2314	2.99	4.229	4.330	0.013
1381	0.315	3.665	1.288	0.244	2317	0.27	3.738	1.191	0.531
1391	0.995	3.819	1.742	0.152	2316	0.24	3.725	1.183	0.512
1394	1.208	3.787	2.021	0.069	2342	1.48	3.816	2.337	0.043
1404	0.716	3.723	1.573	0.145	2346	0.86	3.810	1.619	0.199
1414	0.682	3.778	1.485	0.250	2345	0.72	3.760	1.540	0.195
1425	0.545	3.713	1.430	0.208	2353	0.25	3.665	1.239	0.290
1426	0.286	3.752	1.193	0.564	2358	0.86	3.784	1.647	0.165
1429	0.940	3.689	1.840	0.056	2366	3.48	4.356	5.347	0.007
1430	0.161	3.687	1.157	0.455	2375	-0.20	3.647	0.962	0.808
1441	2.502	3.880	4.106	0.005	2387	1.73	4.035	2.332	0.096
1440	0.209	3.715	1.169	0.510	2391	0.40	3.765	1.264	0.467
1445	2.431	4.152	3.275	0.033	2397	0.46	3.747	1.327	0.349
1457	1.408	3.792	2.269	0.043	2396	1.77	3.884	2.642	0.034
1467	1.038	3.784	1.829	0.105	2405	0.40	3.731	1.292	0.361
1474	0.884	3.776	1.678	0.146	2404	0.76	3.760	1.577	0.176
1472	0.400	3.587	1.262	0.056	2418	4.13	4.488	7.198	0.003
b276	-1.926	3.752	0.319	138.800	2422	4.06	4.452	7.072	0.003
1491	2.576	4.092	3.718	0.017	2418a	1.96	4.080	2.600	0.069
b284	-0.746	3.837	0.609	12.751	2423	0.84	3.778	1.634	0.166
1487	-0.028	3.662	1.052	0.595	2420	1.55	3.877	2.327	0.057
1505	0.219	3.721	1.171	0.522	2422	4.01	4.452	6.856	0.003
1507	1.115	3.887	1.787	0.179	2425	1.02	3.757	1.843	0.088
1513	1.013	3.900	1.666	0.251	2424	0.94	3.894	1.602	0.287
1511	1.534	3.945	2.206	0.091	2433	0.70	3.792	1.491	0.262
1526	0.323	3.768	1.207	0.576	2434	-0.14	3.715	0.948	1.265
1539	0.978	3.760	1.794	0.101	2436	0.33	3.673	1.290	0.256
1538	0.814	3.834	1.548	0.266	2441	0.98	3.760	1.794	0.101
1546	2.652	4.092	3.891	0.014	2444	0.25	3.629	1.272	0.192

Star No.	$\log L/L_{\odot}$	LogTeff	Mass $M/M_{\odot}$	Age	Star No.	$\log L/L_{\odot}$	LogTeff	Mass $M/M_{\odot}$	Age
1541	0.361	3.696	1.296	0.291	2442	0.86	3.734	1.702	0.109
1544	-0.244	3.643	0.936	0.893	2445	0.82	3.776	1.611	0.174
1555	-0.082	3.652	1.025	0.626	2454	-0.27	3.707	0.882	1.661
1562	1.562	3.967	2.211	0.097	2467	0.02	3.740	1.026	1.016
1561	0.692	3.734	1.540	0.170	2466	1.40	3.807	2.241	0.049
1567	-0.038	3.678	1.034	0.712	2474	0.70	3.807	1.476	0.291
1572	-0.538	3.629	0.793	1.703	2475	0.05	3.668	1.094	0.521
1581	0.274	3.760	1.179	0.615	2478	0.63	3.592	1.278	0.027
1589	-0.400	3.673	0.836	1.764	2482	0.03	3.675	1.077	0.582
1590	1.139	3.801	1.921	0.092	2486	0.71	3.784	1.508	0.240
1608	0.236	3.672	1.223	0.322	2491	-0.14	3.682	0.971	0.958
1626	0.760	3.762	1.572	0.181	2494	1.00	3.717	1.869	0.064
1627	1.664	4.026	2.258	0.106	2500	0.70	3.855	1.424	0.410
1634	2.331	4.152	3.086	0.042	2507	0.75	3.831	1.494	0.305
1647	0.243	3.768	1.151	0.705	2509	0.14	3.680	1.147	0.455
1646	1.323	3.819	2.118	0.066	2512	-0.18	3.692	0.939	1.173
1649	1.281	3.690	2.252	0.022	2519	0.77	3.762	1.583	0.175
1654	1.738	3.967	2.456	0.063	2526	0.64	3.678	1.551	0.114
1657	0.644	3.816	1.416	0.360	2524	0.25	3.740	1.178	0.562
1664	2.739	4.189	3.841	0.019	2536	0.92	3.846	1.635	0.222
1660	1.868	4.056	2.498	0.077	2534	0.80	3.707	1.671	0.100
1662	0.948	3.781	1.737	0.129	2545	3.83	4.418	6.290	0.004
1671	1.375	3.884	2.091	0.092	2547	0.12	3.689	1.131	0.509
1683	0.877	3.825	1.617	0.214	2548	-0.03	3.667	1.044	0.634
1698	1.774	3.986	2.476	0.065	2552	0.58	3.798	1.379	0.373
1699	0.096	3.734	1.079	0.793	2565	0.09	3.608	1.171	0.236
1712	1.072	3.787	1.863	0.098	2564	3.13	4.301	4.493	0.013
1709	0.681	3.687	1.578	0.113	2566	0.84	3.813	1.596	0.215
1716	3.969	4.418	6.854	0.003	2574	0.27	3.773	1.168	0.677
1731	0.186	3.784	1.100	0.913	2575	1.29	3.773	2.142	0.050
1724	1.260	3.643	2.028	0.010	2576	0.49	3.755	1.343	0.343
1732	0.284	3.787	1.165	0.727	2579	0.63	3.611	1.610	0.049
1728	4.614	4.527	9.358	0.001	2569	0.19	3.778	1.110	0.861
1736	1.054	3.650	2.022	0.025	2587	0.21	3.752	1.140	0.685
1744	2.493	4.121	3.473	0.024	2591	0.24	3.600	1.289	0.135
1743	0.423	3.731	1.313	0.336	2597	0.46	3.653	1.415	0.144
1740	2.002	4.080	2.663	0.063	2605	0.59	3.810	1.373	0.399
1768	1.751	4.045	2.347	0.096	b1201	-0.39	3.548	0.916	0.412
1795	1.821	4.035	2.463	0.077	b1202	-0.60	3.615	0.770	1.780
1774	0.229	3.736	1.166	0.574	b1203	-0.97	3.630	0.611	5.448
1789	1.043	3.810	1.803	0.126					

iv. References

Adams F. C. and Lin D.N.C., 1993, Protostars and Planets III ed E. H. Levy and J. I. Lunine (Tucson: Univ. of Arizona Press) pp 721-748

Adams M. T., Strom K. M. and Strom S. E., 1983, ApJS, 53, 893

Andrews A.D., 1981, "Orion Nebula" (Armagh Observatory Press)

Bastian U., Mundt R., 1979, A&ASuppl, 36, 57

Chlebowski T. and Garmany C.D., 1991, ApJ, 368, 241

Cohen M., Kuhi L.V.: 1979, ApJS 41, 743

D'Antona F. and Mazzitelli I., 1994, ApJS, 90, 467

Duncan D. K., 1993, ApJ, 406, 172

Fitzpatrick E.L. and Garmany C.D., 1990, ApJ, 363, 119

Flower P. J., 1977, A&A, 54, 31

Flower P. J., 1996, ApJ, 469, 355-365

Frasca A., Alcala J.M., Covino E., Catalano S., Marilli E., Paladino R., 2003, A&A, 405, 149

Habets G.M.H.J. and Heintze J.R.W., 1981, A&AS, 46, 193

Herbig G. H. and Terndrup D. M., ApJ, 307, 609

Herbst W. and Miller D. P., 1982, AJ, 87, 1478

Hillenbrand L. A., 1997, AJ, 113, 1733

Humphreys R. M. and McElroy D. B., 1984, ApJ, 284, 565

Jones B.F. and Walker M.F., 1988, AJ, 95, 1755

Johnson H.L., 1957, ApJ, 126, 134

Kwon S. M. and Lee S. W., 1983, JKAS, 16, 7

Malagnini M.L., Morossi C., Rossi L. and Kurucz R.L., 1986, A&A, 162, 140

Massey P., Parker J.W. and Garmany C.D., 1984, AJ, 98, 1305

McNamara B.J., 1976, Astron. J., 81, 845

Mendoza E. E. and Teresa G., 1980, MNRAS, 190, 623-630

Menzies J.W., Marang F., Westerhuys J.E., 1990, South African Astron. Obs. Circ, 14, 33

Napiwotzki R., Schonberner D. and Wenske V., 1993, A&A, 268, 653

Parenago P.P., 1954, Trudy Sternberg Astron. Inst. 25

Park B. G., Sung H., Bessel M. S. and Kang Y. H., 2000, Astron. J., 120, 894-908

Penprase B.E., 1992, ApJS, 83, 273

Penston M.V., Hunter J.K., O'Neil A., 1975, MNRAS, 171, 219

Perez M. R., The P. S. and Westerlund B. E., 1987, PASP, 99, 1050

Prosser C.F.F., Stauffer J.R., Hartmann L.W., Soderblom D.R., Jones B.F., Werner M.W. and McCaughrean M.J., 1994, ApJ, 421, 517

Rydgren A.E., Vrba F.A., 1984, Astron. J., 89, 399

Sagar R. and Joshi U., 1983, MNRAS, 205, 747-758

Sanders W. L., 1976, Astr. Astrophys., 45, 131

Shulov O.S., Kopatskaya G.N., Khudyakova T.N. , 1983, Trudy Astron. Obs. Leningrad, 38, 76

Sung H. Bessel M. S. and Lee S. W., 1997, Astron. J., 114, 2644

Van Altena W. F., Lee J. F., Lu P. K., and Upgren A. R., 1988, AJ, 95, 1744

Vasilevskis S., Sanders W. L. and Balz A.G.A.Jr., 1965, AJ, 70, 797

Walker M. F., 1956, ApJS, 2, 365

Walker M. F., 1969, ApJ, 155, 447

Warren P.R., Hesser J.E.,1977, ApJS, 34, 115

Chapter 3. Some Properties of the Clusters

i. Mass function

One of the fundamental characteristics of stellar clusters is the existence of a mass function $\xi(M)$, being defined as the number of stars per unit mass range. Another way of defining it is the number of stars per unit logarithmic mass range, $\xi(logM)$ (Miller & Scalo 1979). The relation between two is

$$\xi(M) = \xi(\log M)\frac{d\log M}{dM} \tag{169}$$

Mass function at birth i.e. when stars formed are known as the initial mass function (IMF). IMF can be derived from present day mass function by correcting it for evolutionary effects. However, for very young clusters no such correction is necessary. IMF can be computed by direct count of the number of stars as function of mass. Because all the stars formed are present in young clusters. Salpeter (1955) first computed the mass function for stars in the solar neighbourhood. He considered all stars in the mass range $0.4M_{\odot}$ to $10M_{\odot}$ and obtained a MF slope of – 2.35. Since then lot of observational works have been done on IMF's for both field stars and cluster type stars. Kroupa (2001) investigated the variation of IMF in some great detail. According to him IMF inferred from galactic field stars can be described by a multiple part power law IMF

$$\xi(M) \propto M^{-\alpha} \tag{170}$$

where $\alpha_0 = +0.3 \pm 0.7$, $0.01 \le m \le 0.08$

$$\alpha_1 = +1.3\pm0.5\,, \qquad 0.08 \le m \le 0.5$$

$$\alpha_2 = +2.3\pm0.3\,, \qquad 0.5 \le m \le 1.0$$

$$\alpha_3 = +2.3\pm0.7\,, \qquad 1.00 \le m$$

Kroupa claims this form to be universally valid. He also concludes that the single star IMFs for young clusters between $0.1M_{\odot}$ to $1M_{\odot}$ are systematically steeper than the galactic field IMF. However the field stars IMF or the universality of IMF is not our concern. Our main interest is in cluster IMF. Advances in recent observational studies of cluster IMFs have come from Massey et al. (1995); Phelps et al. (1993); Lada & Lada (2003); Hillenbrand (1997); Sung & Lee (1995); Subramanium & Sagar (1995); and many others. Some reviews are also available in Scalo (1998) and Hunter et al (1997). It is generally observed that the IMF is not the same over all mass ranges. There is also variation in IMF between clusters. Perhaps the most reliable information about cluster IMF comes from the observational studies of the Orion complex by Hillenbrand 1997. After extensive study of the region he finds that over most of the mass range the IMF can be described as a power law form, the average slope being consistent with standard Miller-Scalo (1979) or Salpeter (1955) mass spectra. A turn over is also found at the low mass end, the peak being in the region $(0.2 - 0.4)M_{\odot}$. Similar turn over has also been observed by Lada & Lada (2003) at $(0.1 - 0.3)M_{\odot}$.

In the previous chapter we have determined masses and ages of individual stars in each of clusters NGC 2264, NGC 1976, and the Orion Nebula cluster following PMS evolution. With the masses from the tables (4, 5, 6) we have computed the number of star per unit mass, $\xi(M)$, for each cluster. Results are shown in diagram (figure 4, figure 5, figure 6) as plots of $log\xi(M)$ against $logM$. It is found that the mass distribution follows a power law form over most of the mass range in each cluster, the cluster, the slope being always close to Salpeter's

value $\Gamma = -2.35$. For NGC 2264 $\Gamma = -2.5$ for $1.2M_{\odot} \leq M \leq 10.23M_{\odot}$. There is a turn about at M = 0.89. For NGC 1976 the turn is at 0.89. For the range $1.34M_{\odot} \leq M \leq 16.2M_{\odot}$, $\Gamma = -2.6$. For the ONC we find $\Gamma = -2.55$ for $1.06M_{\odot} \leq M \leq 12.59M_{\odot}$, the turning point being at M = 1.06.

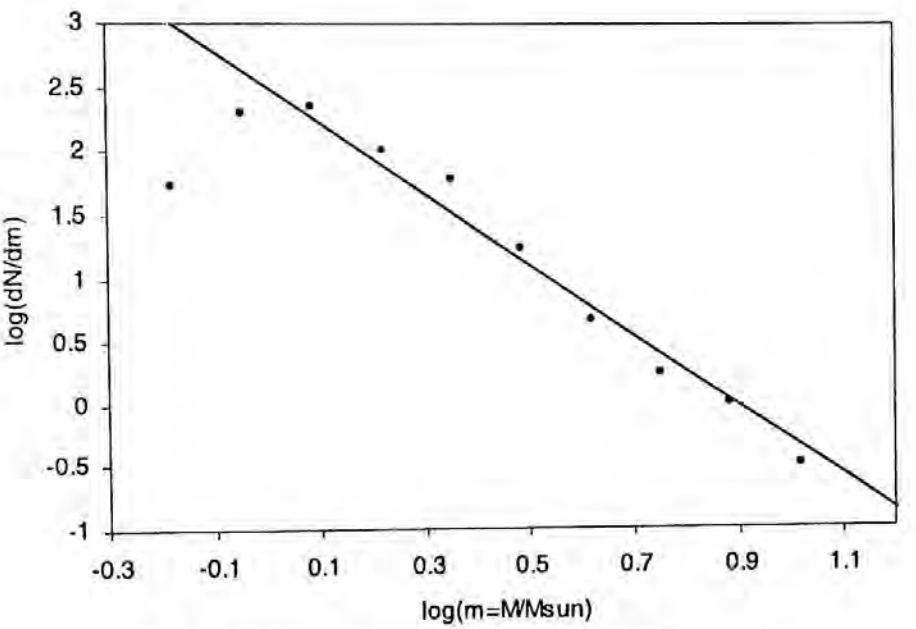

Figure 4: Mass function of the cluster NGC 2264.

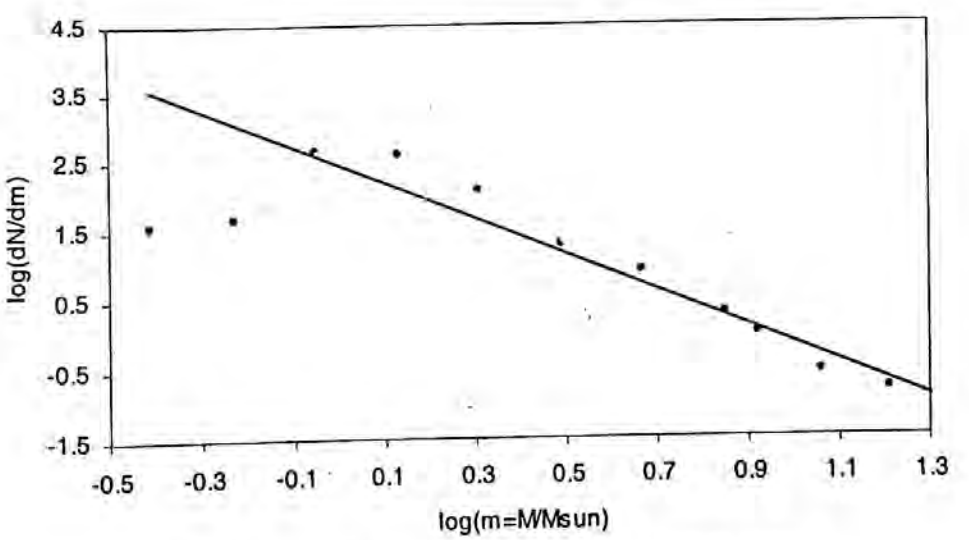

Figure 5: Mass function of the cluster NGC 1976.

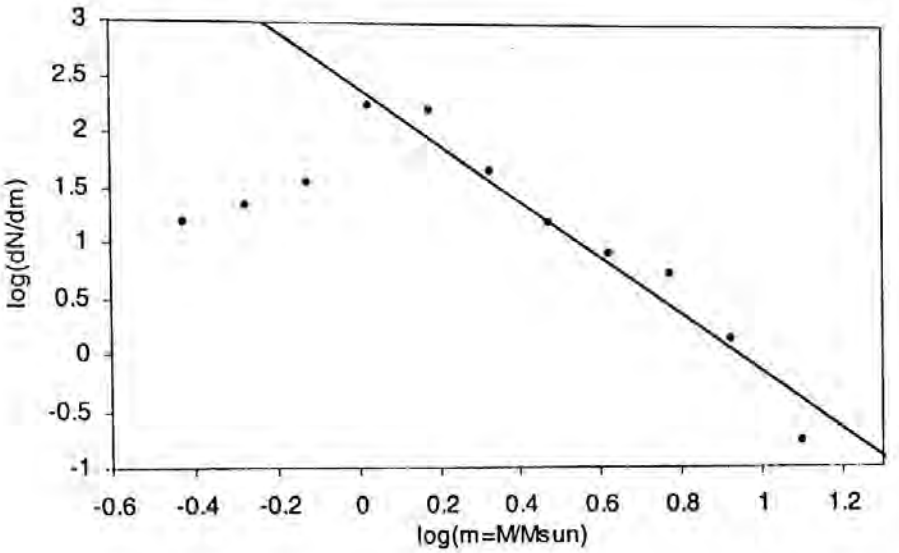

Figure 6: Mass function of the Orion Nebula cluster.

ii. The age distribution of stars

In observation of most young clusters and associations considerable spread in ages of stars is found (e.g. Williams and Cremin 1969, Brown et al 1995, Hillenbrand 1997) indicating the existence of a stellar formation rate. Observational evidences are also there for time varying formation rates (e.g. Iben & Talbot 1966, Hillenbrand 1997). In the previous chapter we have algebracally calculated the ages of the individual stars of the clusters. Hence the number of stars formed per unit time can also be calculated. With a suitable interval of age we count the number of stars in the interval and calculate the formation rate for the clusters. Formation rates are shown in figure 7 for cluster NGC 2264, figure 8 for NGC 1976, and figure 9 for Orion Nebula cluster. The diagrams clearly show that a definite age spread exists for the stars in each cluster. The spread being of the order of a few million years. The other outstanding feature of the distribution diagram is that the number of stars decreases with increasing age. That means the rate of star formation increases with the passage of time. It is interesting to see

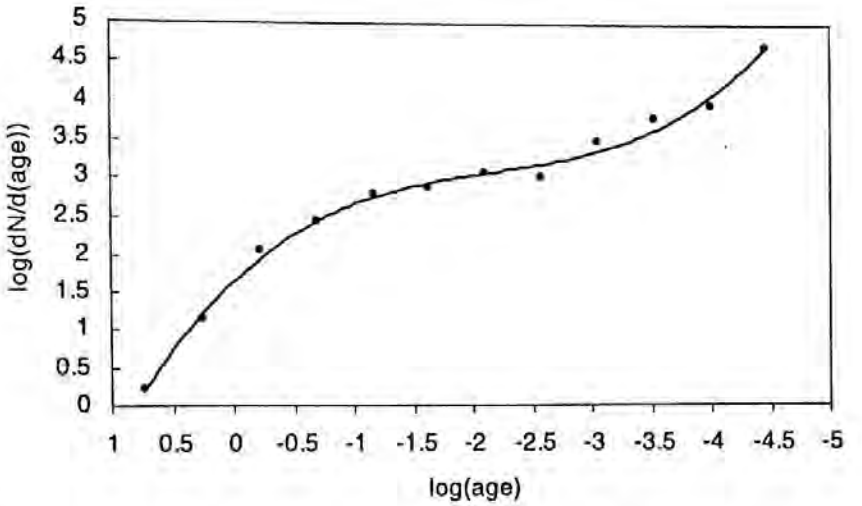

Figure 7: Age distribution of the cluster NGC 2264, solid line- the polynomial fit.

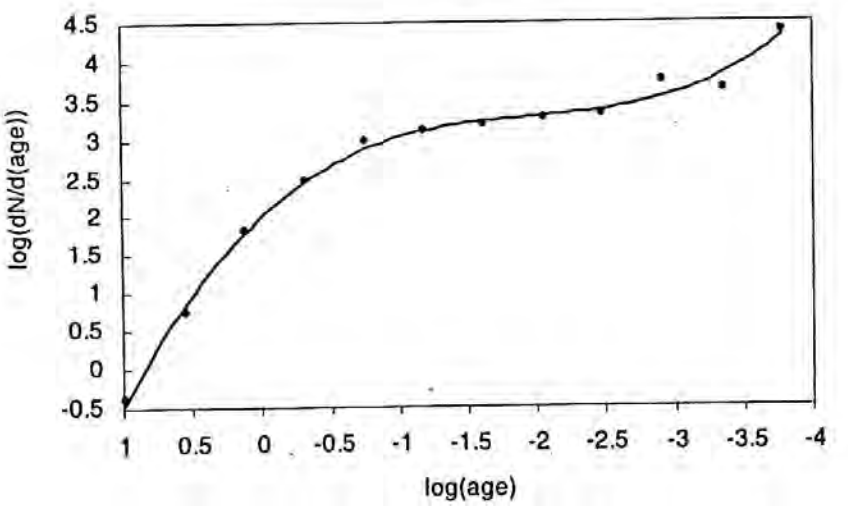

Figure 8: Age distribution of the cluster NGC 1976, solid line- the polynomial fit.

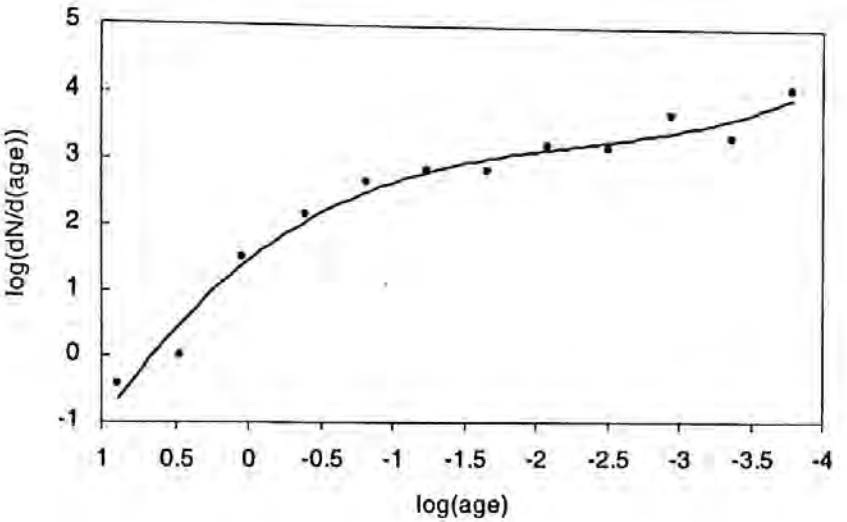

Figure 9: Age distribution of the Orion Nebula cluster, solid line- the polynomial fit.

that, in all cases, the distribution in the log–log plane looks very similar. The distribution is always found to follow a polynomial relationship of the form

$$\log\left(\frac{dN}{d\log t}\right) = -a(\log t)^{-3} - b(\log t)^{-2} - c(\log t)^{-1} + d \qquad (171)$$

where $a = 0.089,\ 0.128,\ 0.09$

$b = 0.58\ ,\ 0.758,\ 0.635$

$c = 1.5\ \ ,\ 1.64\ \ ,\ 1.75$

$d = 1.64\ ,\ 2.01\ \ ,\ 1.46$

respectively for NGC 2264, NGC 1976, and ONC. It is found that the coefficients do not vary much between the clusters.

iii. Mass-age correlation

By means of correlation diagram any relationship stellar mass and age can easily be determined. To establish such a relashion we plot our calulated stellar ages against their masses for the three clusters NGC 2264, NGC 1976, and the ONC in figure 10, figure 11, and figure 12 respectively. A corelation is found to exist all the three clusters.

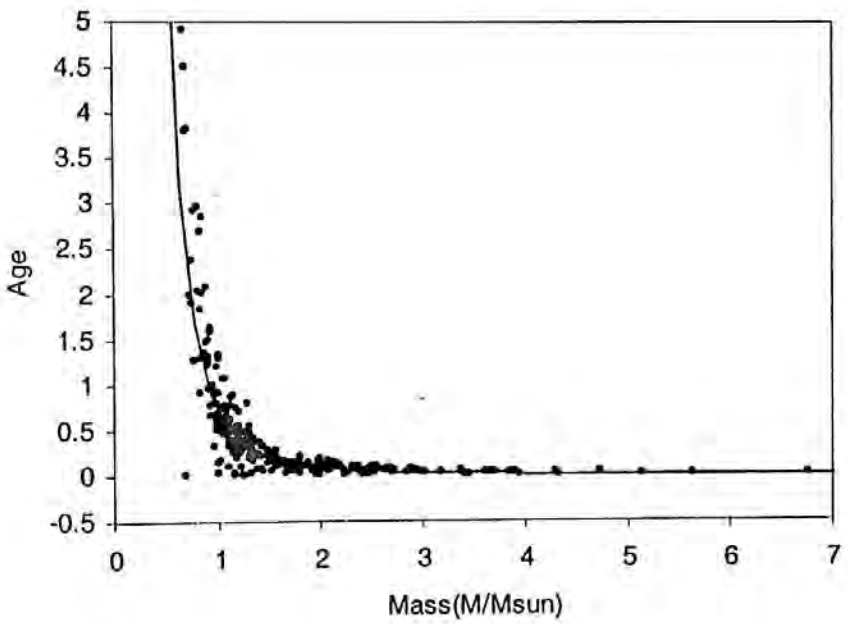

Figure 10: Mass age correlation of NGC 2264 cluster, solid line- the exponential fit.

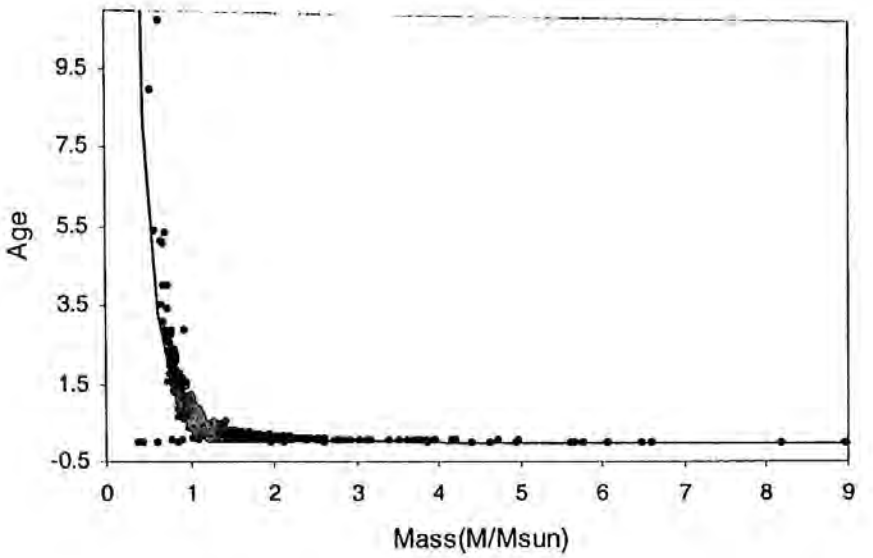

Figure 11: Mass age correlation of NGC 1976 cluster, solid line- the exponential fit.

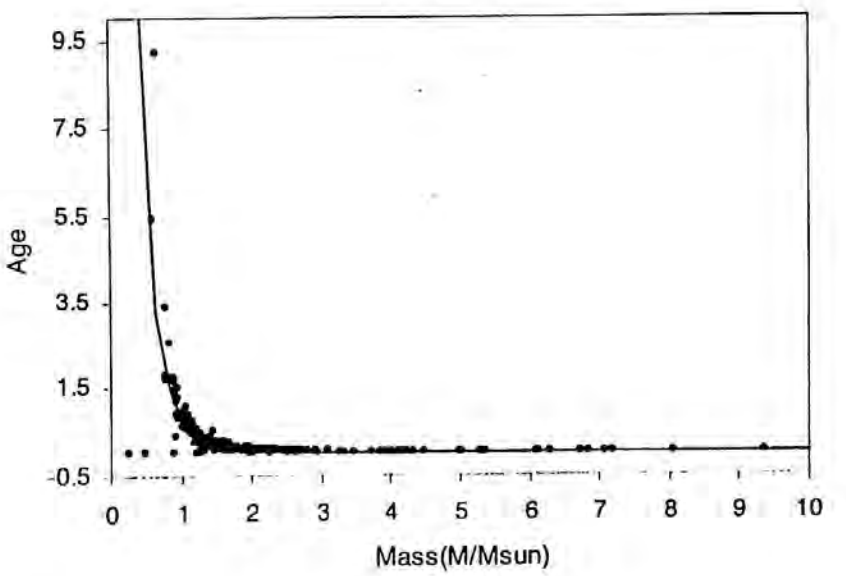

Figure 12: Mass age correlation of the Orion Nebula cluster, solid line- the exponential fit.

For NGC 2264 the relationship is given by

$$Age = 0.53\left(\frac{M}{M_{sun}}\right)^{-2.93}$$

For NGC 1976 that is

$$Age = 0.58\left(\frac{M}{M_{sun}}\right)^{-3.0}$$

while for the Orion Nebula cluster the relationship is obtained as

$$Age = 0.62\left(\frac{M}{M_{sun}}\right)^{-3.01}$$

For the clusters under discussion the relationship can be generalised to be given by a form

$$t = a\left(\frac{M}{M_{sun}}\right)^{-b} \tag{172}$$

where t is the age of a star of mass M, Msun is the usual solar mass, a and b are constants with values

$$a = 0.55 \pm 0.05$$
$$b = 2.95 \pm 0.05$$

iv. Summary and discussion

By analysing the obsevational data for the young clusters NGC 2264, NGC 1976, and the Orion Nebula cluster we have determined the masses and ages of the cluter stars by approximated polytropic method and investigated some cluster properties, namely, mass functions, formation rate, and mass-age correlation. From the mass frequency diagrams figure 4, figure 5, and figure 6 it is seen that

the clusters short of low mass stars. For the high mass stars the distribution is linear in the *log-log* plane having a slope close to Salpeter's value in each case. Regarding the formation rate and mass-age correlation we have obtained some interesting result. If the formation rate is plotted against age in the *log-log* plane then the distribution is found to obey a polynomial form of relationship equation (171) while for the mass-age correlation the distribution is given by a power law fit (equation 172). However not to much emphasis should be given to this result. Because our estimates are approximated and crude in many respects. In our calculation we have not considered any effect of rotation and magnetic field in PMS evolution. Rotation has significanct effect on PMS evolutionary tracks (e.g. Roxburgh 1966). Although the time lines may remains unaltered due to rotational effect the mass given to the stars clearly altered (Williams and Cremin 1969). Effects of magnetic field in the process of star formation have been extensively studied by many authors (e.g. Basu and Mouschovious 1994, MacLow and Klessen 2004). However its effect on PMS evolution is not very clearly understood. It is, of course, known that in the presence of a magnetic field, mass loss becomes a very effective machanism for retarding the rotation of a star. If an appreciable change in mass has occured during the phase of interest then the evolutionary tracks should be modified. There are two possible effects. Firstly, if considerable mass loss was occuring at the time of observation, the luminosity of the star may be modified as a result of some of the energy generated in the star being used up to eject material instead of being emitted as radiation. Secondly, if the stars have evolved for most of their lives as a larger mass star than their present mass, then the age we have given them will be too large. So of mass loss is there, then both the deduced mass and age nedd to be modified. Finally, we have calculated masses and ages of the stars by simple polytropic method whereas the proper way to do so is to use theoretical evolutionary tracks. It will be interesting to see how the empirical results that we have obtained by the simple method compare with results obtained by investigating young clusters by using theoretical mass lines and isochrones constructed properly.

V. References

Basu S. and Mouschovias T. Ch., 1994, ApJ, 432, 720

Brown A.G.A., de Geus E.J., and de Zeeuw P.T., 1995, AA 289, 101

Hillenbrand L. A., 1997, AJ, 113, 1733

Hunter D. A., Light R. M., Holtzman J. A., Lynds R., O' Neil E. J. Jr., and Grillmair C. J., 1997, ApJ, 478, 124

Iben I. Jr. and Talbot R. J., 1966, ApJ, 144, 968

Kroupa P., 2001, MNRAS, 322 231-246

Lada C. J. and Lada E. A., 2003, ARA&A, 41, 57

Mac Low M-M and Klessen R S 2004 Rev. Mod. Phys. 76 125-194

Massey P., Johnson K. E., and DeGioia-Estwood K, 1995, ApJ, 454, 151

Miller G. E., and Scalo J. M., 1979, ApJ. Suppl., 41 513-547

Phelps R. L., and Janes K. A., 1993, AJ, 106, 1870

Roxburgh, I. W., 1966, ApJ, 143, 111

Salpeter E. E., 1955, ApJ., 121, 161

Scalo J. M., 1998, ASP Conf. Serie, Vol. 142, ed G Gilmore and D Howell

Subramanium A. and Sagar R., 1995, A&A, 297, 695

Sung H. and Lee S-W., 1995, JKAS, 28, 119

Williams I. P. and Cremin A. W., 1969, MNRAS, 144, 359

B. Observational tests of an accretion model of star formation in galactic clusters

Chapter 1. An accretion model of star formation

i. The scenario of the model

Most theoretical models of star formation assume that protostars result from fragmentation of interstellar gas clouds into stellar size units. Subsequently each unit evolves onto the main-sequence by direct contraction with essentially no change in mass. Bhattacharjee and Williams (1980) hereafter BW proposed an alternative scenario for star formation whereby a gas cloud is initially fragmented into similar mass stellar nuclei due to the passage of a plane shock wave. The stellar nuclei thus form at different times, in a sequence, the maximum spread in the formation time being the shock crossing time. Subsequently these nuclei increase in mass by accreting matter from the ambient gas. Accretion in the cluster as a whole continues till the exhaustion of the cloud material. The final mass of a star is determined by the time for which accretion proceeds. In general, the stellar nuclei forming first grow to a larger final mass as they have more time available to accrete. At the termination of the accretion process the cluster thus finishes up with stars of widely different masses and ages.

ii. Predictions of the model

Formation Rate(FR):

In observation of most young clusters and associations, in constant mass model, considerable spread in ages of stars is found (e.g. Williams and Cremin

1969, Brown et al. 1995, Hillenbrand 1997) indicating the existences of a stellar formation rate. Observational evidences are also there for time varying formation (e.g. Iben and Talbot 1966, Hillenbrand 1997). BW(1980), in their proposed model, obtained a time varying formation rate. If, in the proposed scenario, the gas cloud is of uniform density then as the shock passes over the cloud the number of fragments formed in any time interval will be proportional to the volume swept out by the shock in that time. In that case the number of stars formed in unit time will depend on the geometry of the cloud. In reality, a gas cloud is likely to be flattened in shape due to rotational effects. For such a cylindrical cloud of height h and cross section radius R, with the shock progressing in the plane of symmetry, the volume of the cloud swept out by the shock front in the time interval (t, $t+dt$) is $2h(2R\ v\ t - v^2\ t^2)^{1/2}dt$ where t is the formation time of a star, measured from when the shock first encounters the cloud, and v is the shock speed. With $2R/v = t_0$, the shock crossing time, the number of stars formed in unit time is found to be given by

$$\frac{dN}{dt} \propto \left(\frac{t}{t_0} - \frac{t^2}{t_0^2} \right)^{\frac{1}{2}} \qquad (173)$$

For the shock progressing along the axis, dN/dt has the uninteresting constant value 2 (BW 1980). In reality the rate is likely to be bounded by these two extreme cases. In our calculation we consider the time varying formation rate (173).

Mass function(MF):

Mass functions have been defined in chapter 3, section A. Advancements in the observational studies of MF have also been briefly discussed. There have also been some theoretical progresses in cluster IMFs. Previous work on IMF was mostly based on fragmentation scheme (e.g. Larson 1973, Elmegreen & Mathieu

1983, Zinnecker 1990). Recently a new idea has developed whereby the stars help determine their own masses. Using these ideas several authors have produced IMF models (e.g. Silk 1995, Nakano et al 1995). In the current picture of star formation attempts are being made to construct theoretical models of IMF following accretion in clusters (e.g. Bate & Bonnell 1997, Basu & Jones 2004, Bonnell et al 2001, Bonnell et al 2004). Accretion in SF has also been reviewed by Hartmann (1998). A significant piece of work is that of Bonnell et al (2001) in which the authors investigating competitive accretion in clusters obtained a 'two power law' mass spectrum with a slope $\gamma = -3/2$ for low mass stars and a steeper slope of $-2 \geq \gamma \geq -2.5$ (Salpeter $\gamma = -2.35$) for high mass stars, the different slopes being due to whether the cluster potential during the formation process was gas dominated or star dominated. Simulation of the problem by the same authors also results in mass spectrum in general agreement with these theoretical results. The elegance of this work is that it provides a physical mechanism for the turn over observed in cluster IMFs. However, according to Scalo (1998), while it may be easier to obtain a power law IMF of any desired index based on a variety of physical and geometrical model, a theoretical IMF with variance as a function of mass is preferred.

BW(1990), in their model, assuming different accretion times and same initial mass for stars obtained an analytical form of IMF with variation as a function of mass. In the model, stars are assumed to accrete matter at a rate given by Bondi-Hoyle (1944), i.e.

$$\frac{dM}{dt} \sim M^2 \rho \ .$$

In reality the density ρ is likely to decrease as accretion proceeds. For the problem in hand ρ may be assumed to be constant over the time scale of interest, ignoring any short period of ineffective accretion. Then the accretion rate can be taken as

$$\frac{dM}{dt} \sim M^2 \tag{174}$$

In the model stellar formation proceeds for $0 \leq t \leq t_0$. If effective accretion terminates simultaneously for all stars then a typical star formed at some t will have a longer accretion time and hence a larger final mass than a star formed at some $t + dt$ later. If M and $M - dM$ be respective final masses then the number of stars formed during the interval $(t, t + dt)$ will have their masses in the range $(M - dM, M)$. If M_2 (formed at $t = 0$) $\geq M \geq M_1$ (formed at $t = t_0$) be the final mass range in the cluster then the formation time of a typical star of final mass M can easily be found to be given by

$$\frac{t}{t_0} = \frac{M_1 (M_2 - M)}{M (M_2 - M_1)} \tag{175}$$

Eliminating t for (169), (174), and (175) gives the mass function

$$\xi(M) = \frac{dN}{dt} \propto \left(\frac{1}{M}\right)^2 \left\{\left(\frac{M_1}{M}\right)\left(\frac{M_2}{M}\right)\left(\frac{M - M_1}{M_2 - M_1}\right)\left(\frac{M_2 - M}{M_2 - M_1}\right)\right\}^{\frac{1}{2}} \tag{176}$$

IIR diagram

One known feature of young galactic clusters is the scatter of stellar points in the HR diagram. It is believed that the scatter is due to evolutionary effects of young contracting stars of different masses and ages (e.g. Palla & Stahler 1993, Tout et al 1999). In an accretion model the spread is found to be due to differential accretion rates arising out of density variation in the gas cloud. For each star with a given final mass there exists a definite but large region in the HR diagram through which the star must pass to reach the main sequence with that mass. The prediction of the model, referred to, is that the pre-main sequence (PMS) stellar

points should appear in the HR diagram in a region bounded by the MS and two evolutionary tracks corresponding to the extreme values of density variation in star forming cloud. For small molecular clouds these tracks correspond to $n(H) \approx 10^4$ at the centre and $n(H) \approx 10^2$ at the surface (see Evans 1978).

iii. References

Basu S. and Jones C. E., 2004, MNRAS, 347, 47

Bate M. R. and Bonnell I. A., 1997, MNRAS, 285, 33-48

Bhattacharjee S. K. and Williams I. P., 1980, A&A, 91, 85

Bondi H. and Hoyle F., 1944, MNRAS, 104, 273

Bonnell I. A., Clarke C. J., Bate M. R., and Pringle J. E., 2001b, MNRAS, 324, 573.

Bonnell I. A., Vine S. G. and Bate M. R., 2004, MNRAS, 349, 735

Brown A.G.A., de Geus E.J., and de Zeeuw P.T., 1995, AA 289, 101

Elmegreen B. G. and Mathieu R. D., 1983, MNRAS, 203, 305

Evans II N. J., 1978, In Protostars and Planets P, 153, ed. Gehrels. T, Univ. Arizona Press

Hartmann L., 1998, Accretion Processes in Star Formation (Cambridge: Cambridge Univ. Press)

Hillenbrand L. A., 1997, AJ, 113, 1733

Iben I. Jr. and Talbot R. J., 1966, ApJ, 144, 968

Larson R. B., 1973, Fundam. Cosmic Phys. 1 1-70

Nakano T., Hasegawa T., and Norman C., 1995, ApJ. 450 183-195

Palla F. and Stahler S. W., 1993, ApJ, 418, 414

Scalo J. M., 1998, ASP Conf. Serie, Vol. 142, ed G Gilmore and D Howell

Silk J., 1995, ApJ, 438, L41

Tout C. A., Livio M. and Bonnell I. A., 1999, MNRAS, 319, 360-376

Williams I. P. and Cremin A. W., 1969, MNRAS, 144, 359

Zinnecker H., 1990, in Physical Processes in Fragmentation and Star Formation, eds, R. Capuzzo-Dolcetta, C. Chiosi, & A. Di Fazio (Dordrecht: Kluwer), 201

Chapter 2. Pre Main Sequence Evolution of Accreting Stars

i. Mass accretion and energy balance

There are now several models available for the rate of accretion of interstellar matter by a star. We are, however, interested in a process of continuous accretion by a star which is essentially embedded in a gas cloud and moves slowly relative to the gas. We consider a protostellar object, embedded in a quiescent gas cloud, which is accreting matter at a rate given by Bondi (1952). As no significant nuclear energy can be released at this early stage of evolution, we assume that the only source of radiating energy is the gravitational energy of the star plus any energy coming in with the accreting matter.

The energy carried in by an element of mass dm in time dt is

$$\frac{1}{2}W^2\,dm - \frac{G\,m\,dm}{R_\infty} - \varepsilon_l$$

where m is the mass of the star, W the mean thermal velocity of the gas molecules, R_∞ the initial distance of the mass element from the centre of the star and ε_l the loss of energy due to any effect during its journey to the star. If $E(m,R)$ represents the total energy of a star of mass m and radius R, then from conservation of energy we have

$$E(m,R) + \frac{1}{2}W^2\,dm - \frac{G\,m\,dm}{R_\infty} - \varepsilon_l = £\,dt + E(m+dm,R+dR) \qquad (177)$$

where $£dt$ is the loss of energy through radiation in time dt. Castellani and Panagia (1971) have shown that ε_l represents only a fraction of the order of 10^{-3} of total incoming energy. Hence ε_l can be neglected. Initial potential energy of the element of mass is also very small compared to its thermal energy. Hence the potential energy term can also be neglected.

Equation (177) thus approximate to

$$£\,dt = E(m,R) - E(m+dm,R+dR) - \frac{1}{2}W^2\,dm \tag{178}$$

Substituting for E from equation (71) into (178) gives

$$£\,dt = -\frac{(3\gamma-4)}{(5-n)(\gamma-1)}\left\{\frac{Gm^2}{R} - \frac{G(m+dm)^2}{(R+dR)}\right\} + \frac{1}{2}W^2\,dm$$

which simplifies to

$$£\,dt = \frac{(3\gamma-4)}{(5-n)(\gamma-1)}\,d\left(\frac{Gm^2}{R}\right) + \frac{1}{2}W^2\,dm$$

For the convective model $n = 3/2$, and hence

$$£\,dt = \frac{2}{7}\left(\frac{3\gamma-4}{\gamma-1}\right)d\left(\frac{Gm^2}{R}\right) + \frac{1}{2}W^2\,dm \tag{179}$$

Similarly for the radiative model with $n = 3$ we have

$$£\,dt = \frac{1}{2}\left(\frac{3\gamma-4}{\gamma-1}\right)d\left(\frac{Gm^2}{R}\right) + \frac{1}{2}W^2\,dm \tag{180}$$

ii. Evolution of young star with mass accretion

The physical processes and the accretion rate of Bondi (1952) pose the over all problem for the evolution of a pre-main-sequence star accreting mass. If we assume that the gravitational contraction is the only source of energy available in the PMS phase then the equations characterising the evolution are

$$\frac{dm}{dt} = 2\pi G^2 m^2 \left(W^2 + V^2\right)^{-\frac{3}{2}} \rho_\infty$$

$$£ = 4\pi\sigma \Re^2 T_{eff}^{\ 4}$$

$$£ = c m^{0.9} \Re^{2.13} \qquad \text{(convective)}$$

$$£ \propto m^{5.4} \Re^{-0.79} \qquad \text{(radiative)}$$

$$£\, dt = \frac{2}{7}\left(\frac{3\gamma - 4}{\gamma - 1}\right) d\left(\frac{Gm^2}{\Re}\right) + \frac{1}{2} W^2\, dm \qquad \text{(convective)}$$

$$£\, dt = \frac{1}{2}\left(\frac{3\gamma - 4}{\gamma - 1}\right) d\left(\frac{Gm^2}{\Re}\right) + \frac{1}{2} W^2\, dm \qquad \text{(radiative)}$$

where G is the gravitational constant, m is the mass of the protostar, £ is the luminosity of the protostar, $\Re$ is the radius of the protostar, T_{eff} is the effective temperature, and W and ρ_∞ are respectively the mean thermal velocity of the gas molecules and density of the gas cloud at a "great distance" from the protostar.

It is found convenient to express £, m, $\Re$, and T_{eff} in solar units such that $£ = LL_{\odot}$, $m = MM_{\odot}$, $\Re = RR_{\odot}$, $T_{eff} = T\,T_{\odot}$ and t in units of t_s such that $t = \tau\, t_s$ where

$$t_s = \frac{2}{7}\left(\frac{3\gamma - 4}{\gamma - 1}\right)\frac{GM_{sun}^2}{L_{sun}R_{sun}}$$

Doing this the above equations reduces to the following nondimensional forms

$$\frac{dM}{d\tau} = K M^2 \tag{181}$$

$$L = R^2 T^4 \tag{182}$$

$$L = c_1 M^{0.9} R^{2.13} \qquad \text{(convective)} \tag{183}$$

$$L = M^{5.4} R^{-0.79} \qquad \text{(radiative)} \tag{184}$$

$$L\,d\tau = d\left(\frac{M^2}{R}\right) + A\,dM \qquad \text{(convective)} \tag{185}$$

$$L\,d\tau = \frac{7}{4}d\left(\frac{M^2}{R}\right) + A\,dM \qquad \text{(radiative)} \tag{186}$$

where

$$K = \frac{2\pi G^2 M_{sun} t_s \rho_{\infty}}{\left(W^2 + V^2\right)^{\frac{3}{2}}} \tag{187}$$

$$A = \frac{1}{2}\frac{W^2 M_{sun}}{L_{sun} t_s}$$

and c_1 is a constant whose numerical value is about 0.134.

For convective model, using the above equations, Bhattacharjee (1980) obtained a differential equation, which is

$$\frac{dL}{dM} = 5.15\left(\frac{L}{M}\right) + 5.78A\left(\frac{L^{1.47}}{M^{2.42}}\right) - \frac{5.78}{K}\left(\frac{L^{2.47}}{M^{4.42}}\right) \tag{188}$$

Once L is determined for a star of given mass its temperature is given by the black body relationship (182) as

$$T = L^{0.25} R^{-0.5}$$

or, substituting for R from equation (183) and inserting the numerical value of c_1 we obtain

$$T = L^{0.015} M^{0.21} \tag{189}$$

We have similar differential equation for the radiative model, which is given by

$$\frac{dL}{dM} = 3.82\left(\frac{L}{M}\right) - 0.45A\left(\frac{L^{-0.27}}{M^{-4.84}}\right) + \frac{0.45}{K}\left(\frac{L^{0.73}}{M^{-2.83}}\right) \tag{190}$$

while the black body relationship gives

$$T = L^{1.83} M^{-3.42} \tag{191}$$

In reality, there exists an intermediate regime where the convective phase gives way to the radiative phase. We shall assume an instantaneous change from one regime to the other such that

$$(L,T)_{conv.} = (L,T)_{rad.}$$

Thus at the transition point we must have

$$R = 1.99\ M^{1.54} \tag{192}$$

But R and M are both time varying functions. The functional relationship between R and M can be expressed in the form of a differential equation. Differentiating equation (183) w. r. to τ and by eliminating τ, $\frac{dL}{dM}$, and L by equations (183), and (188) we have

$$\frac{dR}{dM} = 2\left(\frac{R}{M}\right) + A\left(\frac{R^2}{M^2}\right) - \frac{c_1}{K}\left(\frac{R^{2.13}}{M^{3.1}}\right) \tag{193}$$

The solution of equation (193) which satisfies the equality (192) determines the mass and radius, and hence the luminosity at which the star enters its radiative phase. Obviously, this is the initial boundary condition for the radiative track.

It is obvious that no analytical solution of either set of equations is possible. Resort has to be made to numerical technique for solving these equations. It is necessary to specify K before any solution of the equations can be obtained. Since we are interested only in the general effects of the gas accretion on the evolution of stars, K can be chosen as a free parameter. For given value of K, evolutionary tracks for accreting stars can now be constructed using equations 188 – 193. BW(1980a) constructed evolutionary tracks for some different values of K. A schematic representation of such tracks is shown in figure 13. By investigating different aspects of young accreting stars BW(1980a) reached the following conclusions:

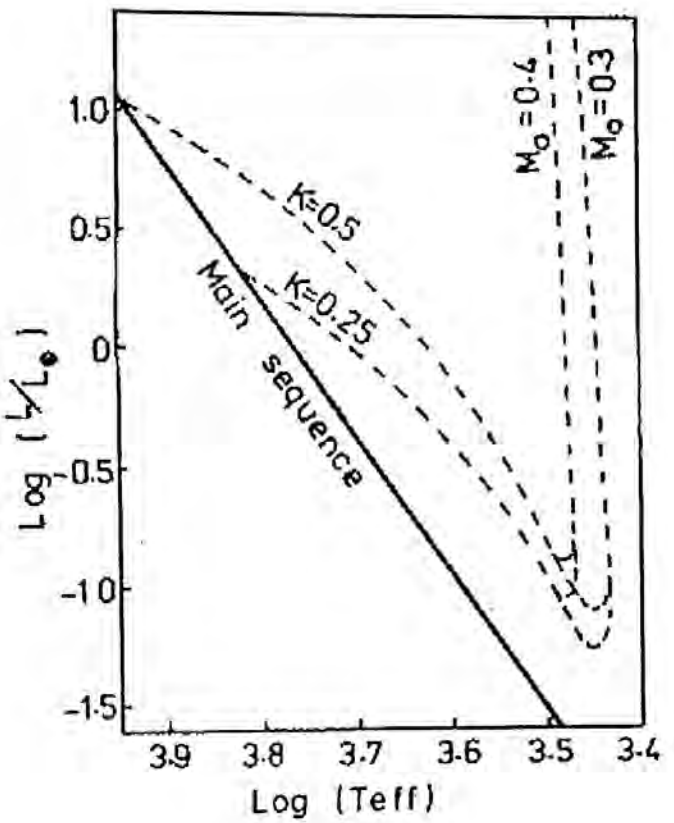

Figure 13: Evolutionary tracks in the HR diagram for contracting stars accreting matter. Tracks are shown for two different masses and two different accretion rates. (BW 1980a)

(a) The evolution of an accreting star is dominated by the accretion rate rather than the initial condition. Different accretion rates will cause a spread in the positions of the evolutionary tracks in the HR diagram. This spread is similar to the observed envelope of the pre-main-sequence stars in HR diagrams of young galactic clusters.

(b) From the observation of the present luminosity and temperature of a star there is no way of knowing about its past evolutionary behaviour.

(c) The masses of the pre-main-sequence stars can be determined uniquely, irrespective of mass accretion, from their observed positions in the HR diagram.

(d) The ages of the stars cannot be determined uniquely from their observed positions in an HR diagram, the ages being dependent on the past evolutionary behaviour of the stars.

iii. References

Bhattacharjee S. K. 1980, Ph.D. Thesis, University of London, UK.

Bhattacharjee S. K. and Williams I. P., 1980, A&A, 91, 85

Bhattacharjee S. K. and Williams I. P., 1980a, MNRAS, 192, 841

Bondi H., 1952, MNRAS, 112, 195

Castellani V. and Panagia N., 1971, Astrophys. Space Sci. 10, 122

Chapter 3. Observational Tests of the Theoretical Predictions

i. The observational data used

To test the theoretical predictions with observation we have considered seven clusters, namely, the ONC, NGC 1976, NGC 2264, NGC 6383, NGC 6716, NGC 6811, and NGC 1245 of these NGC 6716, NGC 6811, and NGC 1245 are of intermediate ages (~ 10^8 yrs) while the rest are very young (~ 10^6 yrs). The clusters have been considered in two groups depending on the nature of data used. In group 1 we have the clusters NGC 1976, NGC 2264, and NGC 6383. The remaining ones are in group 2. The well studied cluster NGC 2264 has been in both the groups. That NGC 1976, NGC 2264, the ONC have been recently investigated by many has been mentioned in the earlier chapter. The other clusters, namely, NGC 6383, NGC 6716, NGC 6811, and NGC 1245 have also been studied by numerous authors quite extensively in the last few decades (e.g. Shevchenko et al., (1992); Van Altena et al., (1988); Evans, T. L. (1978); Glushkova et al., (1999); Van de Ancker et al., (2000); Burke et al., (2004); Wee et al., (1996); Carraro et al., (1994); Qian et al., (1994); Flaccomio et al., (1999); etc). We have, however, taken data from sources easily accessible to us. The data source for NGC 1976 and NGC 2264 has been mentioned in chapter 2, section A. Although the web site has compiled data from many sources the majority of the data have come from Walker (1969), Warren et al. (1977), Van Altena et al. (1988), Shulov et al. (1983), and Shevchenko et al. (1992), for the NGC 1976 and Walker (1956), Medoza et al. (1980), and Sagar et al. (1983) for NGC 2264. For NGC 6383 the (V,B-V) data have been taken from Evans, T. L. (1978). Uniform reddening of amounts E_{B-V} = 0.35, has been estimated for the cluster while the

distance modulus has been given by $10^M.6$. As for the deduced mass functions we have taken data from Hillenbrand (1997) - ONC; Piskunov (1997) – NGC 6811; Piskunov (1997) – NGC 1245; Chun et al. (1996) - NGC 6716; and Sagar et al. (1983) - NGC 2264. It should be mentioned that these mass functions have been derived by using some trustworthy theoretical evolutionary tracks (e.g. D' Antona & Mazzitelli-1994, Swenson et al-1994, Iben-1967, Maeder-1980, Schaller et al-1992, etc) whereas we have determined mass functions of the clusters in group 1 by deriving stellar masses by the polytropic method.

ii. Comparison of the theoretical predictions with observation

Stellar ages and masses are usually determined from observational data by using theoretical evolutionary tracks. For accreting stars it is difficult to use PMS evolutionary tracks for determining masses and ages. However, Siess et al. (1997) has shown that the PMS evolutionary tracks for accreting stars converge to the standard tracks defined by their final masses. That means, the mass lines for accreting and non accreting star are identical. The same conclusion was also reached by BW(1980a) meaning that the masses of accreting star can be determined from their observed position in the HR diagram by using constant mass model. To estimate stellar masses in an accretion picture we can, therefore, use the same method as in chapter 2, section A. For NGC 1976 and NGC 2264 stellar masses have been given in table (4 and 5). For NGC 6383 we convert the data, corrected for both reddening and distance, to theoretical quantities of $logL$ and $logT_{eff}$ and determined masses by solving the two sets of equations (158-159) and (165-166) according as the stars are convective or radiative. The computed mass functions for the three clusters (group 1) are given in table 7.

Table 7 : Computed mass functions for three clusters

NGC 1976		NGC 2264		NGC 6383	
Δlogm	ΔN	Δlogm	ΔN	Δlogm	ΔN
-0.5-(-0.32)	6	-0.247-(-0.114)	11	-0.213-(0.082)	13
-0.32-(-0.14)	12	-0.114-(-0.019)	54	-0.082-0.051	21
-0.14-0.04	178	-0.019-0.152	84	-0.051-0.184	26
0.04-0.22	240	0.152-0.285	51	0.184-0.316	44
0.22-0.40	103	0.285-0.418	41	0.316-0.449	10
0.40-0.58	25	0.418-0.551	16	0.449-0.582	9
0.58-0.76	16	0.551-0.684	6	0.582-0.715	5
0.76-0.94	6	0.684-0.817	3		
0.94-1.12	3	0.817-0.950			
1.12-1.30	1	0.950-1.083	1		

In figure 14 we show the comparison of the predicted mass function with the observed mass function in a log-log plane. Clearly the agreement is found to be very good. It should be noted that the theoretical MF depend on the mass range (M_1, M_2). For the theoretical MF we have taken this mass range as (~0.1-50$M_\odot$) following Hillenbrand's (1997) extensive work on the ONC.

Polytropic mass estimates are not always reliable. That is why we have decided to compare the prediction with the deduced mass functions of the clusters in group 2. The deduced mass functions are of course in power law form and the ranges of stellar masses considered are selective. In our comparison we have obtained a *log-log* plot in figure 15 of the deduced mass functions of NGC 6811, NGC 2264, NGC 6716, NGC 1245, the ONC, and also of the theoretical mass function; the theoretical mass range being (0.1-50$M_\odot$). It is evident from the diagram that the theoretical MF agrees with observation in both cases. It should be noted that in the case of constant mass evolution the data for the ONC have been taken from Walker (1969) which in the present works we have taken Hillenbrand's (1997) mass function for comparison of the predicted mass

function. Because Hillenbrand's work is reliable. The agreement between the theory and Hillenbrand's (1997) work is quite remarkable.

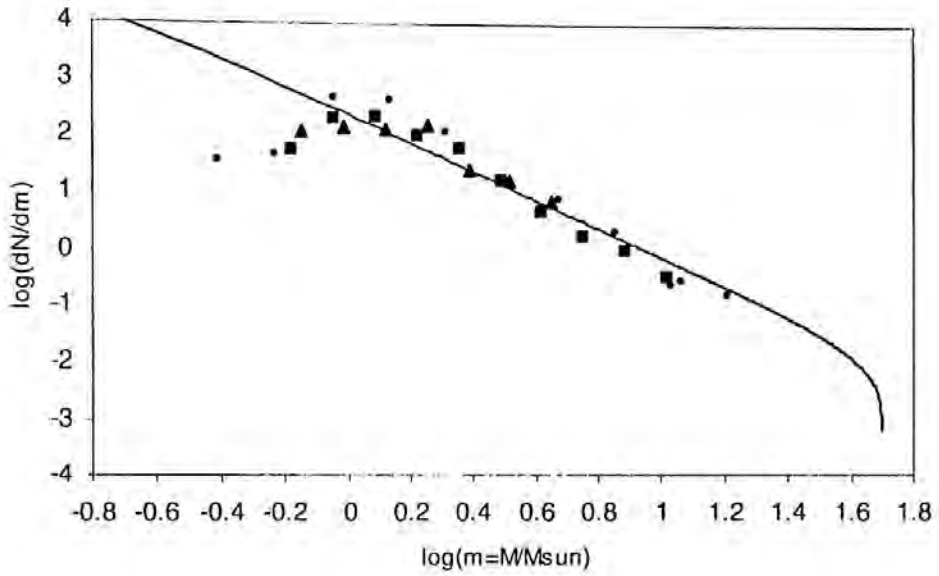

Figure 14: Comparison of the theoretical MF with observed MFs of some clusters deduced by polytropic method. Solid line - the theoretical MF, • - NGC 1976, ■ - NGC 2264, ▲ - NGC 6383.

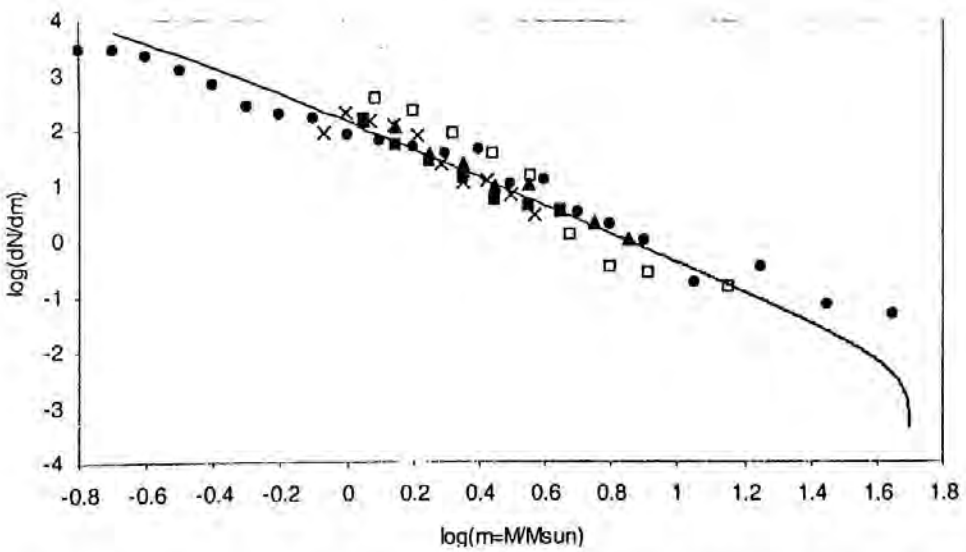

Figure 15: Comparison of the theoretical MF with deduced MFs of some clusters. Solid line - the theoretical MF, • - the ONC, ■ - NGC 6716, ▲ - NGC 2264, × - NGC 6811, □ - NGC 1245.

Although the masses of PMS accreting stars can be determined by constant mass evolutionary code their exact ages can not be determined because of uncertainties in their initial mass and the density of accreted material. Stellar age determination is, therefore outside the framework of this model. However, with masses estimated from the observational data, their relative formation times can be determined by using equation (4), and so the number of stars formed per unit time, i.e. the formation rate (FR) can also be calculated by star counts. We have calculated the formation rate for the clusters in group 1 with our polytropic mass estimates while for the clusters in group 2 we have considered two clusters, NGC 6811 and NGC 1245, for computing the FR with deduced masses. Due to non-availability of data on deduced masses of individual stars in other clusters it has not been possible to compare the FRs with deduced masses for these clusters. Our calculated data required to determine the FRs are shown in table 8.

Table 8 : Computed formation rate (FR) for three clusters

NGC 1976		NGC 2264		NGC 6383	
Δlog(FT)	ΔN	Δlog(FT)	ΔN	Δlog(FT)	ΔN
-2.0-(-1.8)	2	-1.4-(-1.2)	2	-1.6-(-1.4)	2
-1.8-(-1.6)	3	-1.2-(-1.0)	5	-1.4-(-1.2)	4
-1.6-(-1.4)	5	1.0-(-0.8)	14	-1.2-(-1.0)	9
-1.4-(-1.2)	16	-0.8-(-0.6)	40	1.0-(-0.8)	8
-1.2-(-1.0)	21	-0.6-(-0.4)	67	-0.8-(-0.6)	24
-1.0-(-0.8)	93	-0.4-(-0.2)	113	-0.6-(-0.4)	43
-0.8-(-0.6)	226	-0.2-0.0	25	-0.4-(-0.2)	20
-0.6-(-0.4)	202			-0.2-0.0	18
-0.4-(-0.2)	15				
-0.2-0.0	6				

where FT is the formation time and ΔN is the number of stars in the time interval Δlog(FT).

In figure 16 we compare the theoretical formation rate with the calculated formation rates for these clusters and the formation rate computed from the deduced masses for NGC 6811 and NGC 1245. The agreement between the theory and observation is again found to be very good.

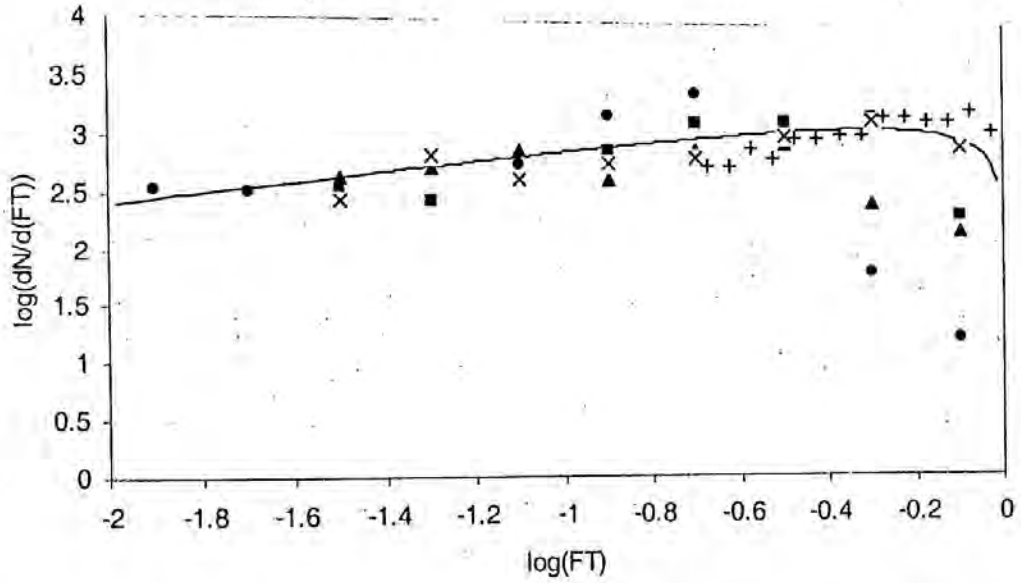

Figure 16: The theoretical FR as compared with observed FRs of some clusters. Solid line - the theoretical FRs, • - NGC 1976, ■ - NGC 2264, ▲ - NGC 6383, × - NGC 6811, + - NGC 1245.

For the comparison of the observed spread in the HR diagram, that is, the scatter of PMS stellar points we have drawn in figure 17 and figure 18 the limiting region bounded by the MS and the two evolutionary tracks corresponding to $n(H_2) = 10^4$ (curve 1) and $n(H_2) = 10^2$ (curve 2), as constructed by BW (1980a) with the simple polytropic method, superimposed on the HR diagram for the clusters NGC 1976 and NGC 2264. The main sequence has been taken to be given by a single straight line through the position of the Sun. Since the comparison with other clusters look alike they have not been included.

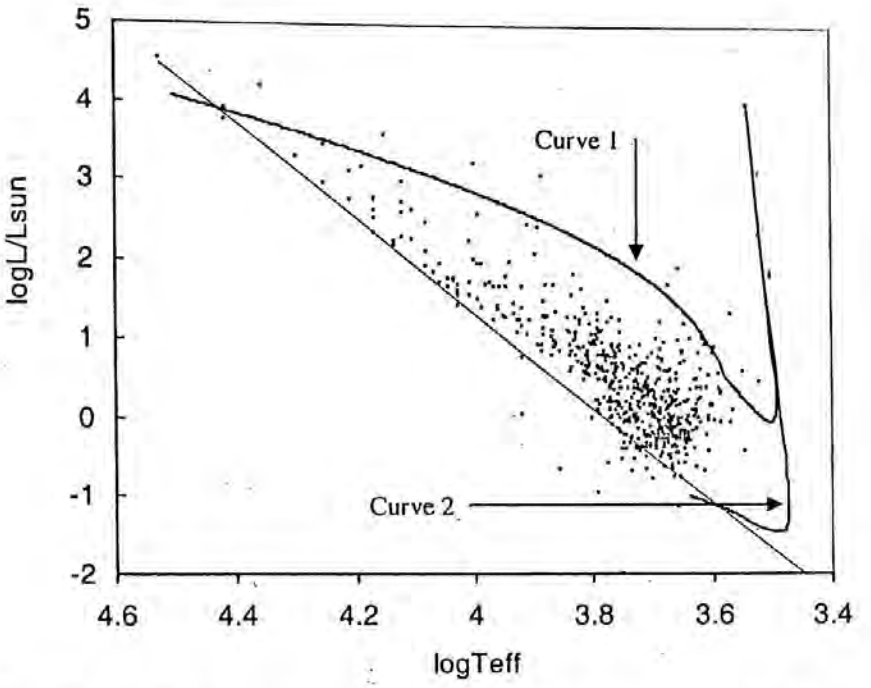

Figure 17: The predicted limiting region superimposed on the HR diagram of NGC 1976

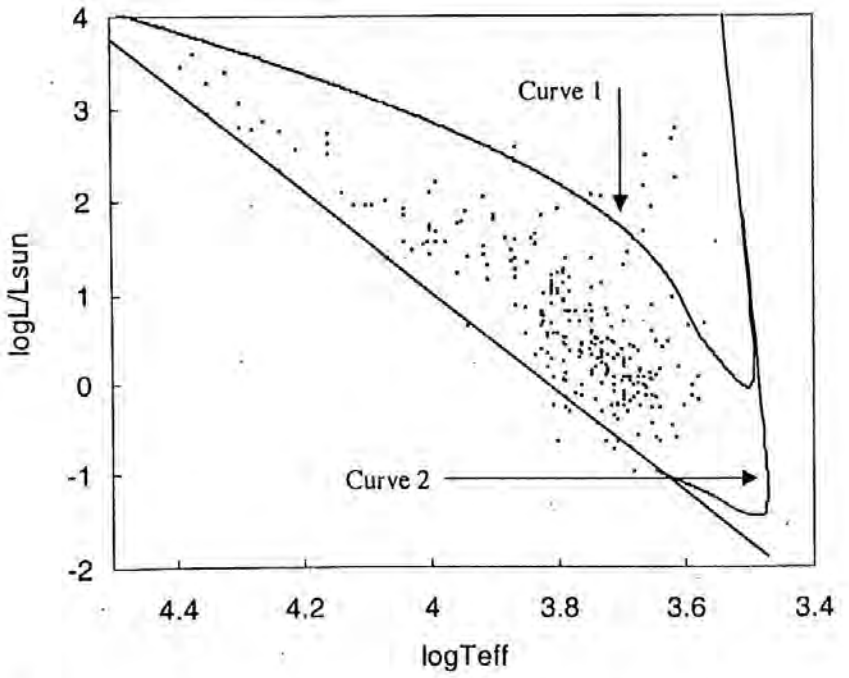

Figure 18: The predicted limiting region superimposed on the HR diagram of NGC 2264

iii. Discussion

We have tested the theoretical prediction of an accretion model of star formation about the existence of a mass function and a formation rate with observation of a number of galactic clusters. The mass function has been tested in figure 14 and figure 15. Figure 14 shows the comparison of the theoretical MF with the mass functions deduced by the simple polytropic method. Since the reliability of the mass estimates by simple polytropic method may sometimes be questioned, the theoretical prediction has also been tested with mass functions deduced by several authors by using trustworthy theoretical evolutionary tracks. Figure 15 shows such a comparison of the mass function. It is evident from the diagrams that the agreement between the theory and observation in both cases are very good. There is, however, some discrepancy in the low mass end. Some clusters are found short of low mass stars. It is satisfying to see that no such discrepancy occurs in the case of ONC. In fact, the theoretical MF agrees with the deduced mass function of the ONC over the whole range of stellar masses ($0.1 - 50M_{\odot}$), as estimated by Hillenbrand's (1997). This suggests that the apparent shortage of low mass stars in other clusters may probably due to observational effect.

In the conventional picture, the star formation rate is observed to increase with the passage of time. No physical explanation is available for that. In the accretion model, because of symmetry of the gas cloud, the FR is expected first to increase and then to decline with the passage of time. This is what is found in figure 16. Also the agreement between the theory and observation is found to be very good. It may be noted that although the mass functions are available the FR for the remaining clusters in group 2 could not be computed because of non-availability of data on deduced masses of single stars. However, since the mass functions of all the clusters in the group agree in a general way, as is evident from the diagram 15, and the FRs for two of these clusters (NGC 6811 and NGC 1245)

agree with the theoretical model we can argue in a qualitative way that the theory would also agree with the other clusters. It would however be of interest to see how it compares with observation of other clusters with reliable estimates of stellar masses.

From figure 17 and figure 18, it is clear that most of the stellar points lie within the predicted limiting region, indicating that the agreement between the theory and observation is quite good. There are however a number of points which have to be made. It is noted that most of the stars lying outside the region in fact lies below the main sequence. This is a problem in any theory. But the reason for this may be due to any error in observational data arising out of possible existence of circum stellar dust shells around some stars as suggested by Strom et al (1972). Secondly, very fewer numbers of stars are found near curve 1. This is probably because the region of highest density in the cloud is confined in a small volume near the centre. We would thus expect smaller number of stars in this region, which would evolve along curve 1 (corresponding to the highest density) or along any curve near to it. Moreover, although for simplicity we assumed that accretion terminates for all stars simultaneously, in reality it may be that accretion for some larger stars has terminated. These stars would then follow flatter constant mass curves in stead of following curve like 1. In that case the top end of the top curve is expected to be void of stellar points.

In conclusion, if the stars in a cluster form and evolve in the manner described by the model, then both the MF and FR, computed from the observational data, and the theoretical predictions are found to have good agreement with each other. The picture presented in the model is of course very simple in many respects. In our work we have not considered any rotational and magnetic effects. Nor any effect due to possible mass loss in any stage (T Tauri Stage) has been considered. In a detailed model, account must be taken of these. Account must also be taken of the manner in which accretion terminates for

individual stars. Bondi-Hoyle accretion model also needs to be modified due to the radiation pressure and the onset of a solar type wind. Also the evolution of PMS stars should be treated in more detailed manner following modern evolutionary model instead of the approximate method used. Nevertheless it is our contention that the proposed model predicts a MF and a FR that are in good agreement with observation, and so, it would be beneficial to produce higher order model based on the simple model of BW(1980).

iv. References

Bhattacharjee S. K. and Williams I. P., 1980, A&A, 91, 85

Bhattacharjee S. K. and Williams I. P., 1980a, MNRAS, 192, 841

Burke C. J., Gaudi B. S., Depoy D. L., Pogge R. W., and Pinsonneault M. H., 2004, preprint

Carraro G. and Patat F., 1994, AA, 289, 397-403

Chun M. Y. and Lee S. W., 1996, JKAS, 29, 137

D'Antona F. and Mazzitelli I., 1994, ApJS, 90, 467

Evans T. L., 1978, MNRAS, 184, 661-676

Flaccomio E., Micela G., Sciortino S., Favata F., Corbally C., and Tomaney A., 1999, A&A, 345, 521

Glushkova E. V., Batyrshinova V. M. and Ibragimov M. A., 1999, Astronomy Letters, 25, 2, 86-92

Hillenbrand L. A., 1997, AJ, 113, 1733

Iben I. Jr., 1967, ApJ, 147, 650

Maeder A., 1980, A&A, 92, 101

Mendoza E. E. and Teresa G., 1980, MNRAS, 190, 623-630

Piskunov A. E., 1997, VizieR On-line Data Catalog: V/19

Qian Z. Y. and Sagar R., 1994, MNRAS, 266, 114

Sagar R. and Joshi U., 1983, MNRAS, 205, 747-758

Schaller G., Schaerer D., Meynet G. and Maeder A., 1992, A&AS, 96, 269-331

Shevchenko V.S., Yakubov S.D., 1992, Soviet Astron. 36, 359

Shulov O.S., Kopatskaya G.N., Khudyakova T.N. , 1983, Trudy Astron. Obs. Leningrad, 38, 76

Siess L., Forestini M., and Bertout C., 1997, A&A, 326, 1001–1012

Strom S. E., Strom K. E., Brooke A. L., Bregman J. and Yost J., 1972, ApJ, 171, 2

Swenson F. J., Faulkner J., Rogers F. J., and Iglesias C. A., 1994, ApJ, 425, 286

Van Altena W. F., Lee J. F., Lu P. K., and Upgren A. R., 1988, AJ, 95, 1744

Van den Ancker M. E., The P. S. and Winter D. D., 2000, AA, 362, 580-584

Walker M. F., 1956, ApJS, 143, 111

Walker M. F., 1969, ApJ, 155, 447

Warren P. R. and Hesser J. E., 1977, ApJS, 34, 115

Wee S. O. and Lee M. G., 1996, JKAS, 29, 181-194